

Precipitation Depth-Duration-Frequency Analysis for the Nevada National Security Site and Surrounding Areas

Prepared by
Li Chen and Julianne J. Miller

Submitted to
Nevada Field Office
National Nuclear Security Administration
U.S. Department of Energy
Las Vegas, Nevada

August 2016

Publication No. 45269

Reference herein to any specific commercial product, process, or service by trade name, trademark, manufacturer, or otherwise, does not necessarily constitute or imply its endorsement, recommendation, or favoring by the United States Government or any agency thereof or its contractors or subcontractors.

Available for sale to the public from:

U.S. Department of Commerce
National Technical Information Service
5301 Shawnee Rd.
Alexandria, VA 22312
Phone: 800.553.6847
Fax: 703.605.6900
Email: orders@ntis.gov
Online ordering: <http://www.osti.gov/ordering.htm>

Available electronically at <http://www.osti.gov/bridge>.

Available for a processing fee to the U.S. Department of Energy and its contractors, in paper, from:

U.S. Department of Energy
Office of Scientific and Technical Information
P.O. Box 62
Oak Ridge, TN 37831-0062
Phone: 865.576.8401
Fax: 865.576.5728
Email: reports@adonis.osti.gov

Precipitation Depth-Duration-Frequency Analysis for the Nevada National Security Site and Surrounding Areas

Prepared by

Li Chen and Julianne J. Miller

Division of Hydrologic Sciences
Desert Research Institute
Nevada System of Higher Education

Publication No. 45269

Submitted to

Nevada Field Office
National Nuclear Security Administration
U.S. Department of Energy
Las Vegas, Nevada

August 2016

The work upon which this report is based was supported by the U.S. Department of Energy under Contract #DE-NA0000939. Approved for public release; further dissemination unlimited.

THIS PAGE INTENTIONALLY LEFT BLANK

EXECUTIVE SUMMARY

Accurate precipitation frequency data are important for Environmental Management Soils Activities on the Nevada National Security Site (NNSS). These data are important for environmental assessments performed for regulatory closure of Soils Corrective Action Unit (CAU) Sites, as well as engineering mitigation designs and post-closure monitoring strategies to assess and minimize potential contaminant migration from Soils CAU Sites. Although the National Oceanic and Atmospheric Administration (NOAA) Atlas 14 (Bonnin *et al.*, 2011) provides precipitation frequency data for the NNESS area, the NNESS-specific observed precipitation data were not consistent with the NOAA Atlas 14 predicted data. This is primarily due to the NOAA Atlas 14 products being produced from analyses without including the approximately 30 NNESS precipitation gage records, several of which approach or exceed 50 year of record. Therefore, a study of precipitation frequency that incorporated the NNESS precipitation gage records into the NOAA Atlas 14 dataset, was performed specifically for the NNESS to derive more accurate site-specific precipitation data products.

Precipitation frequency information, such as the depth-duration-frequency (DDF) relationships, are required to generate synthetic standard design storm hydrographs and assess actual precipitation events. In this study, the actual long-term NNESS precipitation gage records, some of which are the longest gage records in southern and central Nevada, were analyzed to allow for more accurate precipitation DDF estimates to be developed for the NNESS. Gridded maps of precipitation frequency for the NNESS and surrounding areas were then produced.

A standard statistical approach for precipitation frequency analysis was used to develop the DDF relationships for the NNESS precipitation gages. The long-term daily precipitation data records were then used to derive 2- and 100-year (yr), 24-hour (hr) duration precipitation depths. Analyses were performed for both the Annual Maximum Series (AMS) data and Partial Duration Series (PDS) data of the NNESS precipitation gage records. Although a log-normal (LogN) probability distribution was used to approximate the distribution of both precipitation series datasets, to be consistent with NOAA Atlas 14 analyses of AMS datasets, a Type I generalized extreme value (GEV) probability distribution (i.e., Gumbel distribution) was tested for the AMS data analysis. The GEV probability distribution (i.e., Gumbel distribution) was found to be the most appropriate for the AMS data for the NNESS. Additionally, because the NNESS location falls within an area with a generalized regional skew of zero (WRC, 1981), a Log Pearson Type III (LPIII) probability distribution of the PDS dataset was determined to be the most appropriate for the NNESS location.

The 1- and 6-hr precipitation depth data must be derived because the NNESS precipitation gage records are for a 24-hr period. The 2- and 100-yr, 6-hr precipitation depths were determined using spatial interpolation to calculate the ratio of 6- and 24-hr precipitation depths (i.e., $r = P6/P24$) for each of the NNESS precipitation gages. Once the 6- and 24-hr precipitation depths for the NNESS precipitation gages were known, an empirical relationship developed by the Clark County Regional Flood Control District (CCRFC, 1999) was used to calculate the 1-hr precipitation from 6- and 24-hr precipitation datasets, for both the 2- and 100-yr return intervals.

The NNSS precipitation frequency data (i.e., DDF data) developed in this study were then linked to the Mean Annual Maximum (MAM) grids of the Parameter-elevation Regressions on Independent Slopes Model (PRISM) dataset used by NOAA Atlas 14. Gridded maps (i.e., isopleth maps) of precipitation frequencies for the NNSS were produced by developing correlations between the specific NNSS precipitation gage DDF data and the PRISM MAM grid values. These gridded results were validated by comparing the AMS and PDS DDF values in the generated grids with the corresponding NOAA Atlas 14 values at five arbitrarily selected locations surrounding the NNSS. This comparison demonstrated the reliability of the results in this study for areas surrounding the NNSS, which provides confidence for the reliability of the results on the NNSS.

CONTENTS

EXECUTIVE SUMMARY	iii
LIST OF FIGURES	v
LIST OF TABLES	vii
LIST OF ACRONYMS	vii
INTRODUCTION	1
DATA	2
METHODS	4
Development of 2- and 100-year DDF data for 1-, 6-, and 24-hour durations for the NNSS Precipitation Gages	4
Development of Gridded Precipitation Frequencies for the NNSS	10
SUMMARY OF THE RESULTS AND FINDINGS	36
REFERENCES	38
APPENDIX A	A-1

LIST OF FIGURES

1. Study area (inclusive of Clark, Nye, Lincoln, Esmeralda, and Mineral counties, Nevada) and locations of NNSS and Off-Site precipitation gages used in this study	3
2. Differences between NOAA Atlas 14 and NNSS Precipitation Gage-generated 100-year, 6-hour DDF AMS values	9
3. Differences between NOAA Atlas 14 and NNSS Precipitation Gage-generated 100-year, 6-hour DDF PDS values	9
4A. AMS-based NNSS Precipitation Depth-Duration-Frequency Grid: 2-yr, 1-hr ..	11
4B. AMS-based NNSS Precipitation Depth-Duration-Frequency Grid for the focused area: 2-yr, 1-hr	12
5A. AMS-based NNSS Precipitation Depth-Duration-Frequency Grid: 2-yr, 6-hr	13
5B. AMS-based NNSS Precipitation Depth-Duration-Frequency Grid for the focused area: 2-yr, 6-hr	14
6A. AMS-based NNSS Precipitation Depth-Duration-Frequency Grid: 2-yr, 24-hr	15
6B. AMS-based NNSS Precipitation Depth-Duration-Frequency Grid for the focused area: 2-yr, 24-hr	16
7A. AMS-based NNSS Precipitation Depth-Duration-Frequency Grid: 100-yr, 1-hr	17

7B.	AMS-based NNSS Precipitation Depth-Duration-Frequency Grid for the focused area: 100-yr, 1-hr.....	18
8A.	AMS-based NNSS Precipitation Depth-Duration-Frequency Grid: 100-yr, 6-hr.....	19
8B.	AMS-based NNSS Precipitation Depth-Duration-Frequency Grid for the focused area: 100-yr, 6-hr.....	20
9A.	AMS-based NNSS Precipitation Depth-Duration-Frequency Grid: 100-yr, 24-hr.....	21
9B.	AMS-based NNSS Precipitation Depth-Duration-Frequency Grid for the focused area: 100-yr, 24-hr.....	22
10A.	PDS-based NNSS Precipitation Depth-Duration-Frequency Grid: 2-yr, 1-hr.....	23
10B.	PDS-based NNSS Precipitation Depth-Duration-Frequency Grid for the focused area: 2-yr, 1-hr.....	24
11A.	PDS-based NNSS Precipitation Depth-Duration-Frequency Grid: 2-yr, 6-hr.....	25
11B.	PDS-based NNSS Precipitation Depth-Duration-Frequency Grid for the focused area: 2-yr, 6-hr.....	26
12A.	PDS-based NNSS Precipitation Depth-Duration-Frequency Grid: 2-yr, 24-hr.....	27
12B.	PDS-based NNSS Precipitation Depth-Duration-Frequency Grid for the focused area: 2-yr, 24-hr.....	28
13A.	PDS-based NNSS Precipitation Depth-Duration-Frequency Grid: 100-yr, 1-hr.....	29
13B.	PDS-based NNSS Precipitation Depth-Duration-Frequency Grid for the focused area: 100-yr, 1-hr.....	30
14A.	PDS-based NNSS Precipitation Depth-Duration-Frequency Grid: 100-yr, 6-hr.....	31
14B.	PDS-based NNSS Precipitation Depth-Duration-Frequency Grid for the focused area: 100-yr, 6-hr.....	32
15A.	PDS-based NNSS Precipitation Depth-Duration-Frequency Grid: 100-yr, 24-hr.....	33
15B.	PDS-based NNSS Precipitation Depth-Duration-Frequency Grid for the focused area: 100-yr, 24-hr.....	34
16.	Selected off-NNSS locations used for validation.....	35

LIST OF TABLES

1.	NNSS precipitation gages used in this study.....	2
2.	Off-Site precipitation gages used in this study.....	4
3.	AMS-based NNSS precipitation gage DDF results using a GEV probability distribution (depth in inches), with the corresponding NOAA Atlas 14 values shown in italics.	6
4.	PDS-based NNSS precipitation gage DDF results using a LPIII probability distribution (depth in inches), with the corresponding NOAA Atlas 14 values shown in italics.	7

LIST OF ACRONYMS

AMS	Annual Maximum Series
ARL/SORD	Air Resources Laboratory/Special Operations and Research Division
CCRFCDF	Clark County Regional Flood Control District
DDF	depth-duration-frequency
GEV	generalized extreme value
HDSC	Hydrometeorological Design Studies Center
hr	hour
IDF	intensity-duration-frequency
IDW	inverse distance weighting
LogN	log-normal
LPIII	Log Pearson Type III
MAM	Mean Annual Maximum
NNSS	Nevada National Security Site
NOAA	National Oceanic and Atmospheric Administration
NWS	National Weather Service
PDS	Partial Duration Series
PRISM	Parameter-elevation Regressions on Independent Slopes Model
PFDS	Precipitation Frequency Data Server
yr	year

THIS PAGE INTENTIONALLY LEFT BLANK

INTRODUCTION

Accurate precipitation frequency data are important for Environmental Management Soils Activities on the Nevada National Security Site (NNSS), for environmental assessments performed for regulatory closure of Soils CAU Sites, and for both engineering mitigation designs and post-closure monitoring strategies to assess and minimize potential contaminant migration from Soils CAU Sites. Although point precipitation frequency data for the NNSS area are provided by the National Weather Service (NWS) Hydrometeorological Design Studies Center (HDSC) Precipitation Frequency Data Server (PFDS) National Oceanic and Atmospheric Administration (NOAA) Atlas 14 document (hereafter referred to as “NOAA Atlas 14”, which can be retrieved from http://hdsc.nws.noaa.gov/hdsc/pfds/pfds_map_cont.html?bkmrk=nv) (Bonnin *et al.*, 2011), the NNSS-specific reliability of this information was questioned because the observed NNSS precipitation data were not consistent with the NOAA Atlas 14 predicted data. This is most likely because the approximately 30 NNSS precipitation gage records, several of which approach or exceed 50 years of record, were not included in the analyses used to derive the NOAA Atlas 14 products. Therefore, a study of precipitation frequency, which incorporated the NNSS precipitation gage records into the NOAA Atlas 14 dataset, was performed specifically for the NNSS to derive more accurate site-specific precipitation data products.

Precipitation frequency information such as the relationships between depth-duration-frequency (DDF) and intensity-duration-frequency (IDF; not specifically included in this study) are required to generate synthetic standard design storm hydrographs and assess actual precipitation events, which are data that are needed for post-closure monitoring strategies at Soils CAU Sites to minimize potential contaminant migration, environmental assessments, engineering designs, and flood mitigation designs. These storms are associated with various return intervals such as the 100-year (yr) storm (on average, a 100-yr storm has a 1/100 chance of occurring in any given year, which corresponds to a frequency of 0.01) and the 2-yr storm (corresponding to a frequency of 0.5), with specified durations such as 1-, 6-, and 24-hour (hr). These DDF and IDF relationships are usually derived from measured historical precipitation data.

In this study, the DDF relationships for the NNSS were developed using NNSS precipitation gage records. Using the actual long-term NNSS precipitation gage records, which are some of the longest gage records in southern and central Nevada, allows for more accurate precipitation DDF estimates to be developed for use on the NNSS. The objectives of this study are to: 1) derive site-specific precipitation depths for 1-, 6-, and 24-hr durations for the 2- and 100-yr return intervals at each NNSS precipitation gage location; and 2) generate isopluvial maps for DDF relationships of various return intervals and durations across the NNSS by incorporating the NNSS data into the NOAA Atlas 14 datasets. These maps will allow the point precipitation DDF data from each of the NNSS precipitation gage location to be spatially extrapolated and appropriately spread across the entire NNSS, essentially creating isopleths of precipitation frequency data across the NNSS. Thus, revised DDF data, which incorporated the long-term NNSS precipitation gage datasets, would be available for any and all locations on the NNSS, regardless of proximity to a precipitation gage location. A summary of this work and resulting NNSS-specific revised DDF data are presented in the report body, with detailed technical information contained within the appendices.

DATA

Precipitation records from 27 NNESS precipitation gages (Table 1; Figure 1) were retrieved and used in the analysis. These gages only provide daily (i.e., 24 hr) precipitation data. The DDF estimates for other durations (i.e., 1- and 6-hr in this study) must be obtained by other means. Surrounding the NNESS area, thirteen precipitation gages (hereafter referred to as the “Off-Site precipitation gages”) were identified as having been used in the NOAA Atlas 14 analysis (Table 2; Figure 1). These gages provide supplemental data for precipitation frequency analysis to the NNESS and were used to develop the current DDF data in the NOAA Atlas 14 for use on the NNESS. Point precipitation frequency estimates of various durations and return intervals for these Off-Site precipitation gages were obtained from the NOAA Atlas 14 (http://hdsc.nws.noaa.gov/hdsc/pfds/pfds_map_cont.html?bkmrk=nv). These data, combined with the NNESS precipitation data, were subsequently used to develop the NNESS site-specific DDF estimates. (Where original NNESS gages were replaced with new gages at or very near the same location, these two records were merged, as evidenced by the gage names in Table 1.)

Table 1. NNESS precipitation gages used in this study.

GAGE	Latitude	Longitude	Elevation (ft)	Easting*	Northing*	Period of Record**(yr)
A12	37.1911	-116.2153	7490	569646.9	4116361.6	52
40MI	37.0492	-116.2875	4820	563355.1	4100564.0	52
M45_A01AA	37.0038	-116.0598	3990	583651.6	4095710.7	5
M17_A01AB	37.0629	-116.0537	4075	584127.8	4102264.5	5
M43_A06AEB	36.9375	-116.0378	3916	585683.4	4088374.6	5
M40_A12AA	37.1852	-116.2069	7525	570397	4115708.4	5
M14_A14AA	36.9676	-116.1814	4716	572870.9	4091586.3	5
M48_A15AA	37.2264	-116.0602	5112	583370.2	4120403.7	5
M7_A18AA	37.1514	-116.3956	5451	553669.6	4111834.5	5
M29_A20AB	37.3449	-116.5689	5585	538182.2	4133217.2	5
M47_A26AA	36.8122	-116.1614	4282	574800.2	4074363.8	4
BJY	37.0628	-116.0525	4070	584236.5	4102256.4	52
CS	36.8122	-116.0914	4000	581044	4074426.9	48
ETU	37.1917	-116.2011	6250	570903.8	4116433.8	20
M5_W5B	36.8019	-115.9653	3080	592305.2	4073401.1	52
M23_MERC	36.6608	-116.01	3770	588477.3	4057705.0	47
M26_4JA	36.7847	-116.2889	3422	563450.3	4071227.1	56
M28_A06	36.8994	-116.0344	3710	586025.5	4084152.7	19
MV	36.9725	-116.1719	4660	573704.4	4092142.0	48
M24_OYMAB	36.8394	-116.4686	4937	547380.4	4077187.2	5
PHS	37.2089	-116.0386	4565	585307.1	4118478.3	48
PM1	37.2489	-116.4375	6550	549885.7	4122631.2	48
RV	36.6853	-116.1922	3400	572168.7	4060264.1	49
TS2	37.0531	-116.1914	4980	571897.7	4101063.8	52
UCC	36.9564	-116.0475	3924	584799.2	4090458.3	53
DRA	36.6211	-116.0258	3250	587106.9	4053284.1	51
LF2	37.1181	-116.3039	5120	561841.7	4108195.5	36

* UTM Zone S11, NAD83; ** usable years of record

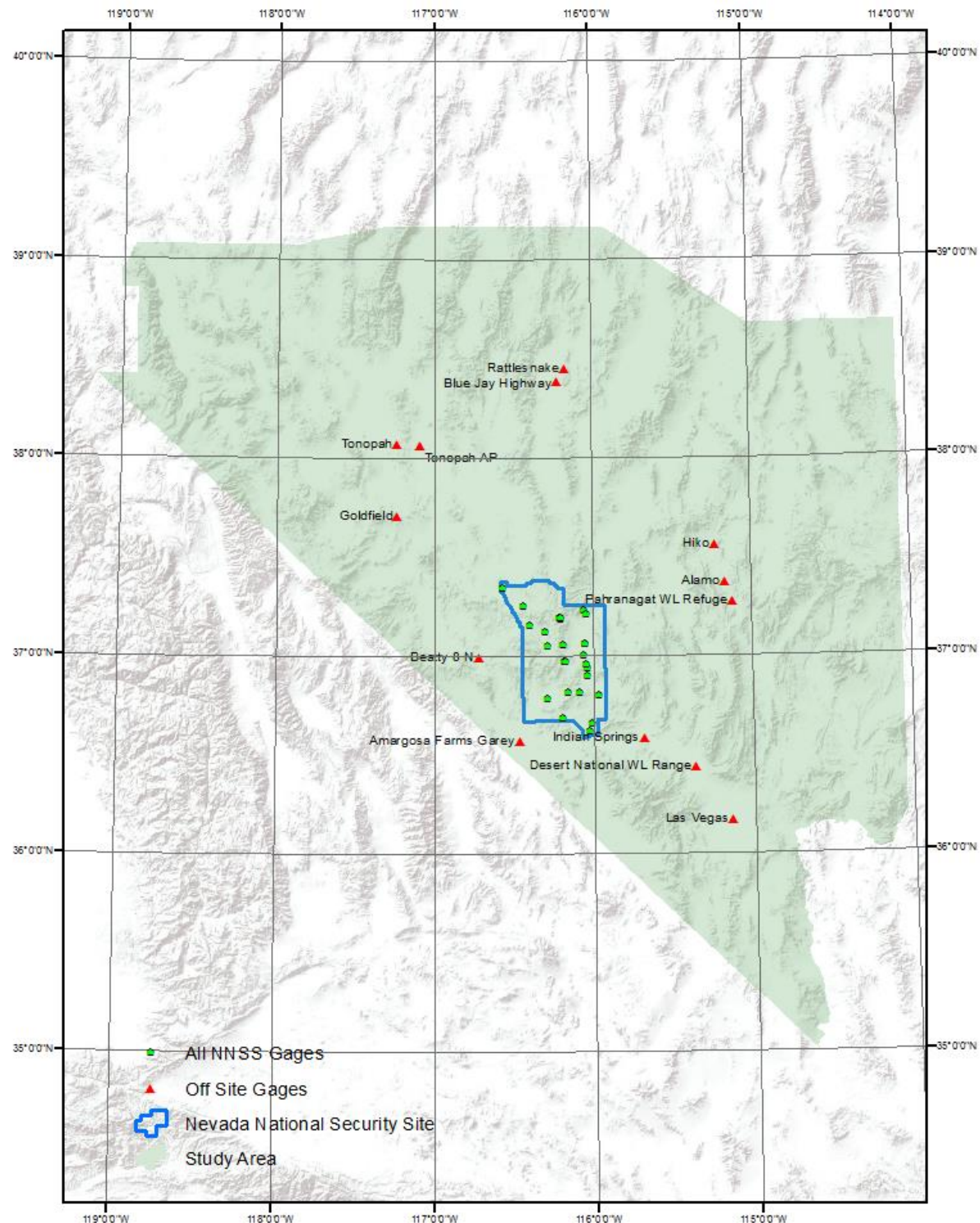


Figure 1. Study area (inclusive of Clark, Nye, Lincoln, Esmeralda, and Mineral counties, Nevada) and locations of NNSS and Off-Site precipitation gages used in this study.

Table 2. Off-Site precipitation gages used in this study.

GAGE	Latitude	Longitude	Elevation (ft)	Easting*	Northing*	Period of Record (yr)**
Amargosa Farms Garey	36.5717	-116.4619	2450	4047496.1	548145.4	33
Beatty 8 N	36.9950	-116.7183	3550	4094354.8	525066.2	29
Goldfield	37.7081	-117.2331	5690	4173454.5	479453.6	52
Tonopah	38.0667	-117.2333	6024	4213241.3	479535.4	32
Tonopah AP	38.0603	-117.0872	5430	4212509.1	492350.3	60
Blue Jay Highway	38.3833	-116.2167	5322	4248634.7	568412.6	7
Rattlesnake	38.4500	-116.1667	5915	4256074.2	572712.8	13
Hiko	37.5581	-115.2236	3900	4158270.0	656900.9	23
Alamo	37.3667	-115.1667	-999	4137129.4	662340.5	21
Pahranagat WL Refuge	37.2692	-115.1197	3400	4126393.2	666718.1	33
Las Vegas	36.1667	-115.1333	2011	4004052.5	667895.5	28
Desert National WL Range	36.4378	-115.3597	2920	4033758.8	647020.9	60
Indian Springs	36.5833	-115.6833	3123	4049454.9	617794.0	24

* UTM Zone S11, NAD83; ** usable years of record

METHODS

A comprehensive approach was used to derive the target DDF results (i.e., the 2- and 100-yr; 1-, 6-, and 24-hr precipitation depths) for the study area. The approach included: 1) deriving precipitation DDF relationships for each of the NNSS gages, and 2) producing gridded maps of precipitation frequency for the NNSS area.

Development of 2- and 100-year DDF data for 1-, 6-, and 24-hour durations for the NNSS Precipitation Gages

To perform the precipitation frequency analysis, the daily precipitation data records from the NNSS precipitation gages were retrieved from the NOAA Air Resources Laboratory/Special Operations and Research Division (ARL/SORD) website (www.sordx.nv.doe.gov/PrecipitationPage.php; last accessed on February 3, 2015). The Off-Site precipitation gage frequency data were retrieved from the NOAA NWS HDSC PFDS website (http://hdsc.nws.noaa.gov/hdsc/pfds/pfds_map_cont.html?bkmrk=nv). The procedures used to derive the DDF values for each NNSS precipitation gage location are summarized below and described in detail in Appendix A.

Using a standard statistical approach for precipitation frequency analysis (e.g., Chow *et al.* [1988]), the DDF relationships for the NNSS precipitation gages were analyzed using the long-term daily precipitation data records to derive 2- and 100-yr, 24-hr precipitation depths. Analyses were performed for both the Annual Maximum Series (AMS) data and the Partial Duration Series (PDS) data of the NNSS precipitation gage records. The AMS represents the dataset that consists of the single maximum daily precipitation value recorded in a specific year for each year of record at a specific gage. Thus, there is only one

gage-specific maximum precipitation value for each year that data were collected at each gage. The PDS dataset is obtained by determining the number of years of available records (years = n) at each specific gage, and then selecting the top n -ranking overall maximum daily precipitation events that occurred at that specific gage during the period of record. Therefore, if a specific precipitation gage collects data for n -years, then the PDS consists of the top n -ranking maximum daily precipitation values recorded during that period, regardless of specific year. The FreqPlot software (deRoulhac, 2007) was used to perform both the AMS and PDS statistical analyses.

Three statistical distributions were used to analyze the AMS and PDS datasets. A log-normal (LogN) probability distribution was used to approximate the distribution of both precipitation series datasets. However, to be consistent with NOAA Atlas 14 analyses of AMS datasets, a Type I generalized extreme value (GEV) probability distribution (i.e., Gumbel distribution) was tested for the AMS data analysis, and was found to be the most appropriate for the AMS data for the NNSS. Additionally, as the NNSS location falls within an area with a generalized regional skew of zero (WRC, 1981), a Log Pearson Type III (LPIII) probability distribution of the PDS dataset was determined to be the most appropriate for the NNSS location (Schmeltzer *et al.*, 1993), although the LPIII also can be approximated using a LogN distribution given the zero skew value. With a zero skew, if precipitation depth versus probability were plotted on log-probability paper, the flood frequency curve would plot as a LogN distribution (i.e., a straight line).

As the NNSS precipitation gage records are for a 24-hr period, the 6-hr precipitation depth data must be derived. The 2- and 100-yr, 6-hr precipitation depths were determined using spatial interpolation to calculate the ratio of 6- and 24-hr precipitation depths (i.e., $r = P6/P24$) for each of the NNSS precipitation gages. The P6/P24 ratio values for each NNSS precipitation gage were calculated using an inverse distance weighting (IDW) approach in conjunction with the P6/P24 ratios for the Off-Site precipitation gages by using the 6- and 24-hr precipitation depths for the Off-Site precipitation gages obtained from NOAA Atlas 14. The 6-hr NNSS precipitation depths were then calculated using both the P6/P24 ratio values from the Off-Site precipitation gages and the known 24-hr precipitation depths from the NNSS precipitation gages following the equation:

$$P6_{NNSS} = r_{NNSS}P24_{NNSS}$$

where r_{NNSS} is the P6/P24 ratio at a given NNSS gage, which is calculated by the IDW interpolation approach using all P6/P24 ratios; and $r_{Off-Site}$, for Off-Site precipitation gages is equal to:

$$r_{NNSS} = \sum w_i r_{Offsite,i}$$

in which w_i is the weight for the i th Off-Site precipitation gage. This analysis was performed for both the 2- and 100-yr return intervals for each NNSS precipitation gage, using both the AMS and PDS datasets.

Once the 6- and 24-hr precipitation depths for the NNSS precipitation gages were known, the Clark County Regional Flood Control District (CCRFCD, 1999) approach to determine the 1-hr duration datasets was used for both the 2- and 100-yr return intervals. The CCRFCD developed an empirical relationship that was used to calculate the 1-hr

precipitation depths from 6- and 24-hr precipitation values (see Appendix A, *Estimation of 1-hr Precipitation Depths for NNSS Gages*), which were assumed to be applicable to the NNSS based on the proximity to Clark County, Nevada (Schmeltzer *et al.*, 1993).

The DDF results for the NNSS gages are shown in Tables 3 and 4. Differences between the 100-yr, 6-hour DDF AMS and PDS values are shown in Figures 2 and 3. Additionally, spatial patterns of the 24-hr precipitation depths for the NNSS precipitation gages were compared with that of the Off-Site precipitation gages to examine the difference in precipitation between the NNSS and the surrounding areas, which also may show that a site-specific precipitation DDF study is necessary. Moreover, elevation effects on precipitation frequency were examined for the NNSS precipitation gages to determine if an elevation correction was needed. Although annual average precipitation has been shown to be correlated to elevation (French, 1983), it was determined in this study that an elevation correction was not necessary for the point DDF analysis of the AMS and PDS datasets used in this study (Appendix A, *Elevation Effects*).

Table 3. AMS-based NNSS precipitation gage DDF results using a GEV probability distribution (depth in inches), with the corresponding NOAA Atlas 14 values shown in italics.

GAGE (Years of Record**)	24-HR		6-HR		1-HR	
	2-yr	100-yr	2-yr	100-yr	2-yr	100-yr
A12 (52)	1.370 <i>1.690*</i>	3.737 <i>5.200</i>	0.942 <i>1.110</i>	2.776 <i>3.240</i>	0.599 <i>0.567</i>	2.050 <i>1.880</i>
40MI (52)	1.133 <i>1.250</i>	3.205 <i>3.900</i>	0.776 <i>0.836</i>	2.365 <i>2.570</i>	0.490 <i>0.454</i>	1.812 <i>1.600</i>
M45_A01AA (5)	0.832 <i>1.040</i>	3.338 <i>3.140</i>	0.588 <i>0.688</i>	2.538 <i>2.160</i>	0.380 <i>0.418</i>	1.952 <i>1.530</i>
M17_A01AB (5)	0.920 <i>1.470</i>	3.947 <i>3.980</i>	0.647 <i>0.747</i>	2.992 <i>1.990</i>	0.418 <i>0.369</i>	2.206 <i>1.340</i>
M43_A06AEB (5)	1.049 <i>1.030</i>	4.734 <i>3.100</i>	0.749 <i>0.686</i>	3.631 <i>2.160</i>	0.493 <i>0.414</i>	2.597 <i>1.520</i>
M40_A12AA (5)	1.071 <i>1.680</i>	3.556 <i>5.140</i>	0.737 <i>1.090</i>	2.643 <i>3.210</i>	0.466 <i>0.562</i>	1.977 <i>1.860</i>
M14_A14AA (5)	0.853 <i>1.240</i>	3.269 <i>3.850</i>	0.595 <i>0.820</i>	2.448 <i>2.530</i>	0.380 <i>0.456</i>	1.878 <i>1.610</i>
M48_A15AA (5)	0.960 <i>1.280</i>	3.180 <i>3.800</i>	0.666 <i>0.784</i>	2.387 <i>2.380</i>	0.424 <i>0.482</i>	1.847 <i>1.680</i>
M7_A18AA (5)	0.737 <i>1.390</i>	2.408 <i>4.310</i>	0.498 <i>0.925</i>	1.760 <i>2.860</i>	0.306 <i>0.467</i>	1.465 <i>1.640</i>
M29_A20AB (5)	0.682 <i>1.230</i>	2.659 <i>3.700</i>	0.456 <i>0.801</i>	1.927 <i>2.440</i>	0.276 <i>0.428</i>	1.549 <i>1.520</i>
M47_A26AA (4)	1.180 <i>1.260</i>	3.990 <i>4.040</i>	0.833 <i>0.793</i>	3.000 <i>2.500</i>	0.542 <i>0.441</i>	2.197 <i>1.580</i>
BJY (52)	0.945 <i>1.090</i>	2.659 <i>3.270</i>	0.664 <i>0.713</i>	2.016 <i>2.210</i>	0.429 <i>0.440</i>	1.648 <i>1.590</i>
CS (48)	1.130 <i>1.060</i>	3.150 <i>3.270</i>	0.810 <i>0.693</i>	2.411 <i>2.210</i>	0.536 <i>0.416</i>	1.887 <i>1.520</i>

** Usable years of record

Table 3. AMS-based NNESS precipitation gage DDF results using a GEV probability distribution (depth in inches), with the corresponding NOAA Atlas 14 values shown in italics (continued).

GAGE (Years of Record**)	24-HR		6-HR		1-HR	
	2-yr	100-yr	2-yr	100-yr	2-yr	100-yr
ETU (20)	1.294 <i>1.650</i>	3.136 <i>5.050</i>	0.891 <i>1.070</i>	2.332 <i>3.140</i>	0.566 <i>0.556</i>	1.803 <i>1.850</i>
M5_W5B (52)	0.770 <i>0.925</i>	2.100 <i>2.750</i>	0.569 <i>0.668</i>	1.661 <i>2.130</i>	0.386 <i>0.395</i>	1.486 <i>1.480</i>
M23_MERC (47)	0.880 <i>1.030</i>	2.933 <i>3.120</i>	0.656 <i>0.684</i>	2.328 <i>2.240</i>	0.449 <i>0.421</i>	1.890 <i>1.520</i>
M26_4JA (56)	0.894 <i>0.992</i>	3.214 <i>3.190</i>	0.616 <i>0.631</i>	2.342 <i>2.100</i>	0.388 <i>0.405</i>	1.783 <i>1.490</i>
M28_A06 (19)	0.924 <i>1.010</i>	3.507 <i>3.050</i>	0.663 <i>0.683</i>	2.701 <i>2.160</i>	0.438 <i>0.411</i>	2.064 <i>1.520</i>
MV (48)	1.260 <i>1.220</i>	3.550 <i>3.800</i>	0.880 <i>0.811</i>	2.662 <i>2.500</i>	0.568 <i>0.457</i>	2.001 <i>1.610</i>
M24_OYMAB (5)	0.573 <i>1.020</i>	1.585 <i>3.320</i>	0.387 <i>0.651</i>	1.140 <i>2.140</i>	0.235 <i>0.420</i>	1.113 <i>1.520</i>
PHS (48)	1.040 <i>1.190</i>	2.680 <i>3.510</i>	0.723 <i>0.755</i>	2.016 <i>2.300</i>	0.463 <i>0.462</i>	1.639 <i>1.630</i>
PM1 (48)	1.001 <i>1.490</i>	2.945 <i>4.540</i>	0.675 <i>1.040</i>	2.149 <i>3.150</i>	0.418 <i>0.476</i>	1.679 <i>1.650</i>
RV (49)	1.028 <i>1.680</i>	3.376 <i>5.140</i>	0.720 <i>1.090</i>	2.497 <i>3.210</i>	0.464 <i>0.562</i>	1.888 <i>1.860</i>
TS2 (52)	1.210 <i>1.310</i>	3.580 <i>4.000</i>	0.839 <i>0.872</i>	2.672 <i>2.650</i>	0.537 <i>0.478</i>	2.000 <i>1.660</i>
UCC (53)	1.010 <i>1.030</i>	2.750 <i>3.100</i>	0.719 <i>0.684</i>	2.103 <i>2.150</i>	0.471 <i>0.412</i>	1.708 <i>1.520</i>
DRA (51)	0.890 <i>0.985</i>	2.918 <i>2.980</i>	0.662 <i>0.662</i>	2.308 <i>2.190</i>	0.452 <i>0.410</i>	1.872 <i>1.490</i>
LF2 (36)	1.060 <i>1.330</i>	3.000 <i>4.150</i>	0.724 <i>0.872</i>	2.211 <i>2.680</i>	0.454 <i>0.470</i>	1.724 <i>1.640</i>

** Usable years of record

Table 4. PDS-based NNESS precipitation gage DDF results using a LPIII probability distribution (depth in inches), with the corresponding NOAA Atlas 14 values shown in italics.

GAGE (Years of Record**)	24-HR		6-HR		1-HR	
	2-yr	100-yr	2-yr	100-yr	2-yr	100-yr
A12 (52)	1.680 <i>1.890*</i>	3.690 <i>5.200</i>	1.163 <i>1.230</i>	2.654 <i>3.240</i>	0.747 <i>0.631</i>	1.935 <i>1.880</i>
40MI (52)	1.330 <i>1.390</i>	3.370 <i>3.900</i>	0.918 <i>0.931</i>	2.400 <i>2.570</i>	0.586 <i>0.505</i>	1.785 <i>1.600</i>
M45_A01AA (5)	1.210 <i>1.160</i>	2.150 <i>3.140</i>	0.861 <i>0.766</i>	1.590 <i>2.160</i>	0.566 <i>0.465</i>	1.382 <i>1.530</i>
M17_A01AB (5)	1.260 <i>1.640</i>	2.890 <i>3.980</i>	0.892 <i>0.831</i>	2.130 <i>1.990</i>	0.584 <i>0.411</i>	1.679 <i>1.340</i>
M43_A06AEB (5)	1.120 <i>1.140</i>	5.720 <i>3.100</i>	0.805 <i>0.763</i>	4.271 <i>2.160</i>	0.535 <i>0.460</i>	2.902 <i>1.520</i>

** Usable years of record

Table 4. PDS-based NNSS precipitation gage DDF results using a LPIII probability distribution (depth in inches), with the corresponding NOAA Atlas 14 values shown in italics (continued).

GAGE (Years of Record**)	24-HR		6-HR		1-HR	
	2-yr	100-yr	2-yr	100-yr	2-yr	100-yr
M40_A12AA (5)	1.450 <i>1.860</i>	2.360 <i>5.140</i>	1.005 <i>1.220</i>	1.699 <i>3.210</i>	0.645 <i>0.626</i>	1.418 <i>1.860</i>
M14_A14AA (5)	1.230 <i>1.380</i>	2.150 <i>3.850</i>	0.865 <i>0.912</i>	1.561 <i>2.530</i>	0.562 <i>0.508</i>	1.350 <i>1.610</i>
M48_A15AA (5)	1.120 <i>1.420</i>	2.640 <i>3.800</i>	0.782 <i>0.872</i>	1.926 <i>2.380</i>	0.503 <i>0.536</i>	1.555 <i>1.680</i>
M7_A18AA (5)	1.109 <i>1.550</i>	1.404 <i>4.310</i>	0.755 <i>1.030</i>	0.986 <i>2.860</i>	0.474 <i>0.520</i>	1.017 <i>1.640</i>
M29_A20AB (5)	1.140 <i>1.370</i>	1.600 <i>3.700</i>	0.767 <i>0.891</i>	1.118 <i>2.440</i>	0.475 <i>0.476</i>	1.084 <i>1.520</i>
M47_A26AA (4)	1.090 <i>1.400</i>	1.700 <i>4.040</i>	0.776 <i>0.883</i>	1.244 <i>2.500</i>	0.509 <i>0.491</i>	1.181 <i>1.580</i>
BJY (52)	1.110 <i>1.210</i>	2.610 <i>3.270</i>	0.786 <i>0.794</i>	1.924 <i>2.210</i>	0.513 <i>0.490</i>	1.564 <i>1.590</i>
CS (48)	1.310 <i>1.180</i>	3.190 <i>3.270</i>	0.946 <i>0.771</i>	2.378 <i>2.210</i>	0.633 <i>0.464</i>	1.833 <i>1.520</i>
ETU (20)	1.480 <i>1.830</i>	2.920 <i>5.050</i>	1.026 <i>1.190</i>	2.104 <i>3.140</i>	0.658 <i>0.619</i>	1.638 <i>1.850</i>
M5_W5B (52)	0.880 <i>1.030</i>	2.250 <i>2.750</i>	0.655 <i>0.744</i>	1.738 <i>2.130</i>	0.448 <i>0.440</i>	1.508 <i>1.480</i>
M23_MERC (47)	0.990 <i>1.140</i>	3.250 <i>3.120</i>	0.743 <i>0.761</i>	2.522 <i>2.240</i>	0.514 <i>0.469</i>	1.971 <i>1.520</i>
M26_4JA (56)	1.080 <i>1.100</i>	3.590 <i>3.190</i>	0.751 <i>0.702</i>	2.541 <i>2.100</i>	0.481 <i>0.450</i>	1.852 <i>1.490</i>
M28_A06 (19)	1.130 <i>1.120</i>	3.640 <i>3.050</i>	0.817 <i>0.760</i>	2.730 <i>2.160</i>	0.546 <i>0.458</i>	2.040 <i>1.520</i>
MV (48)	1.570 <i>1.360</i>	3.330 <i>3.800</i>	1.105 <i>0.902</i>	2.422 <i>2.500</i>	0.721 <i>0.508</i>	1.824 <i>1.610</i>
M24_OYMAB (5)	0.740 <i>1.140</i>	1.280 <i>3.320</i>	0.504 <i>0.724</i>	0.887 <i>2.140</i>	0.313 <i>0.468</i>	0.958 <i>1.520</i>
PHS (48)	1.190 <i>1.320</i>	2.600 <i>3.510</i>	0.833 <i>0.840</i>	1.902 <i>2.300</i>	0.538 <i>0.514</i>	1.544 <i>1.630</i>
PM1 (48)	1.120 <i>1.660</i>	3.200 <i>4.540</i>	0.761 <i>1.150</i>	2.249 <i>3.150</i>	0.476 <i>0.530</i>	1.687 <i>1.650</i>
RV (49)	1.210 <i>1.860</i>	3.610 <i>5.140</i>	0.856 <i>1.220</i>	2.602 <i>3.210</i>	0.560 <i>0.626</i>	1.910 <i>1.860</i>
TS2 (52)	1.390 <i>1.460</i>	4.350 <i>4.000</i>	0.971 <i>0.970</i>	3.145 <i>2.650</i>	0.628 <i>0.532</i>	2.211 <i>1.660</i>
UCC (53)	1.210 <i>1.140</i>	2.750 <i>3.100</i>	0.867 <i>0.761</i>	2.046 <i>2.150</i>	0.574 <i>0.459</i>	1.643 <i>1.520</i>
DRA (51)	1.030 <i>1.100</i>	3.200 <i>2.980</i>	0.771 <i>0.737</i>	2.474 <i>2.190</i>	0.532 <i>0.456</i>	1.938 <i>1.490</i>
LF2 (36)	1.170 <i>1.480</i>	3.120 <i>4.150</i>	0.805 <i>0.971</i>	2.218 <i>2.680</i>	0.511 <i>0.523</i>	1.684 <i>1.640</i>

** Usable years of record

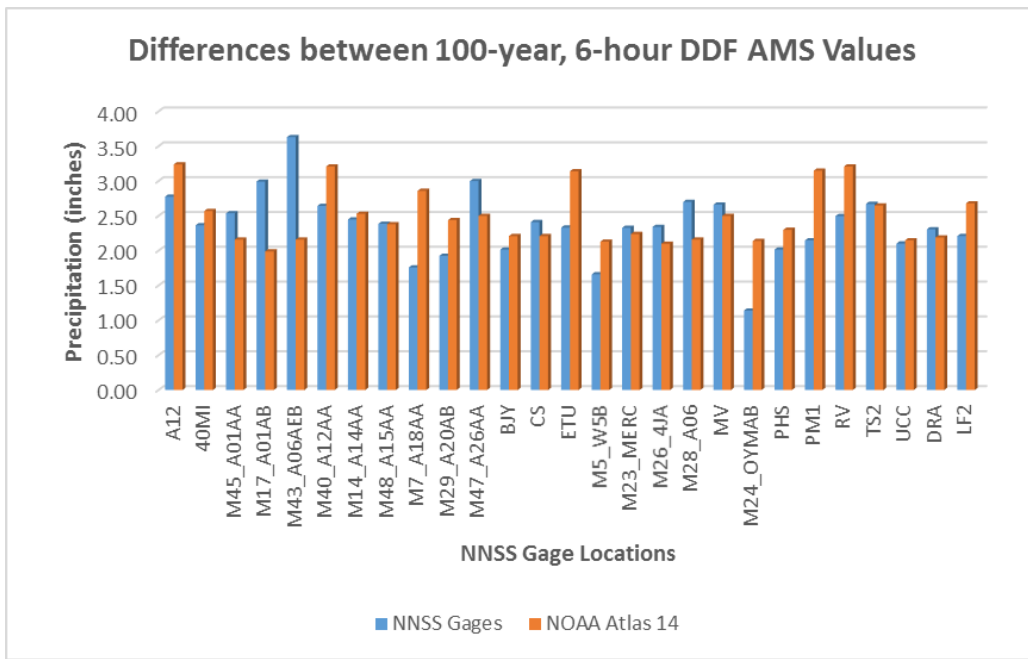


Figure 2. Differences between NOAA Atlas 14 and NNSS Precipitation Gage-generated 100-year, 6-hour DDF AMS values.

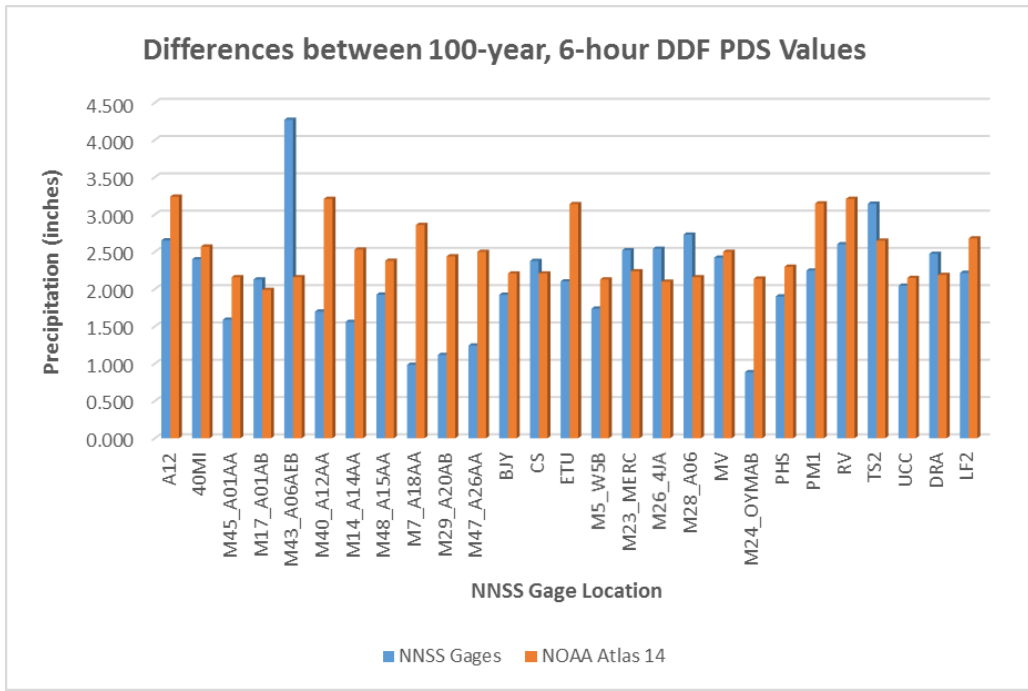


Figure 3. Differences between NOAA Atlas 14 and NNSS Precipitation Gage-generated 100-year, 6-hour DDF PDS values.

Development of Gridded Precipitation Frequencies for the NNSS

To develop gridded maps (i.e., isopleth maps) of precipitation frequencies for the NNSS, the NOAA Atlas 14 approach was used to produce precipitation frequency grids. This approach generates areal precipitation frequency results for the study area by linking the point frequency results developed in this analysis to other well-established areal precipitation products. In this case, the NNSS precipitation frequency data developed in this study were linked to the Mean Annual Maximum (MAM) grids of the Parameter-elevation Regressions on Independent Slopes Model (PRISM) dataset. As an unique knowledge-based system, PRISM uses point measurements of climatic variables, such as precipitation and temperature, to produce distributed, digital grid estimates of monthly, yearly, and event-based climatic parameters. The MAM grids (grid resolution of 800 m) were a special PRISM product developed for the NOAA Atlas 14 precipitation frequency analysis. The MAM grids used in this study were specifically requested from NOAA by DRI (personal communication, Pavlovic, 2015) for these analyses.

The NNSS precipitation frequency grids (Figures 4 through 15) were then produced by developing correlations between the specific NNSS precipitation-gage DDF data and the MAM grid values, which allowed for an initial grid across the NNSS to be estimated. This initial grid was further refined by using the residual values from the correlation analyses (Appendix A, *Creating Precipitation Frequency Grids for the NNSS*). Consistency checks were conducted to ensure the quality of the results. Analyses were performed using both the AMS and PDS datasets for the NNSS precipitation gages. Although this approach was directly applied to the AMS datasets, the approach was modified for the PDS datasets (as described in Appendix A) to better reflect the properties of these specific data.

To validate the gridded results, AMS and PDS DDF values in the generated grids at five arbitrarily selected locations surrounding the NNSS were compared with the corresponding NOAA Atlas 14 values (Figure 16). This comparison demonstrated the reliability of the generated results in this study for the Off-Site precipitation gage areas, which can serve as criteria to evaluate the reliability of the gridded precipitation results on the NNSS. A more detailed description of the approach that was used to develop the NNSS precipitation grids and the grid results are included in Appendix A, *Results Validation*.

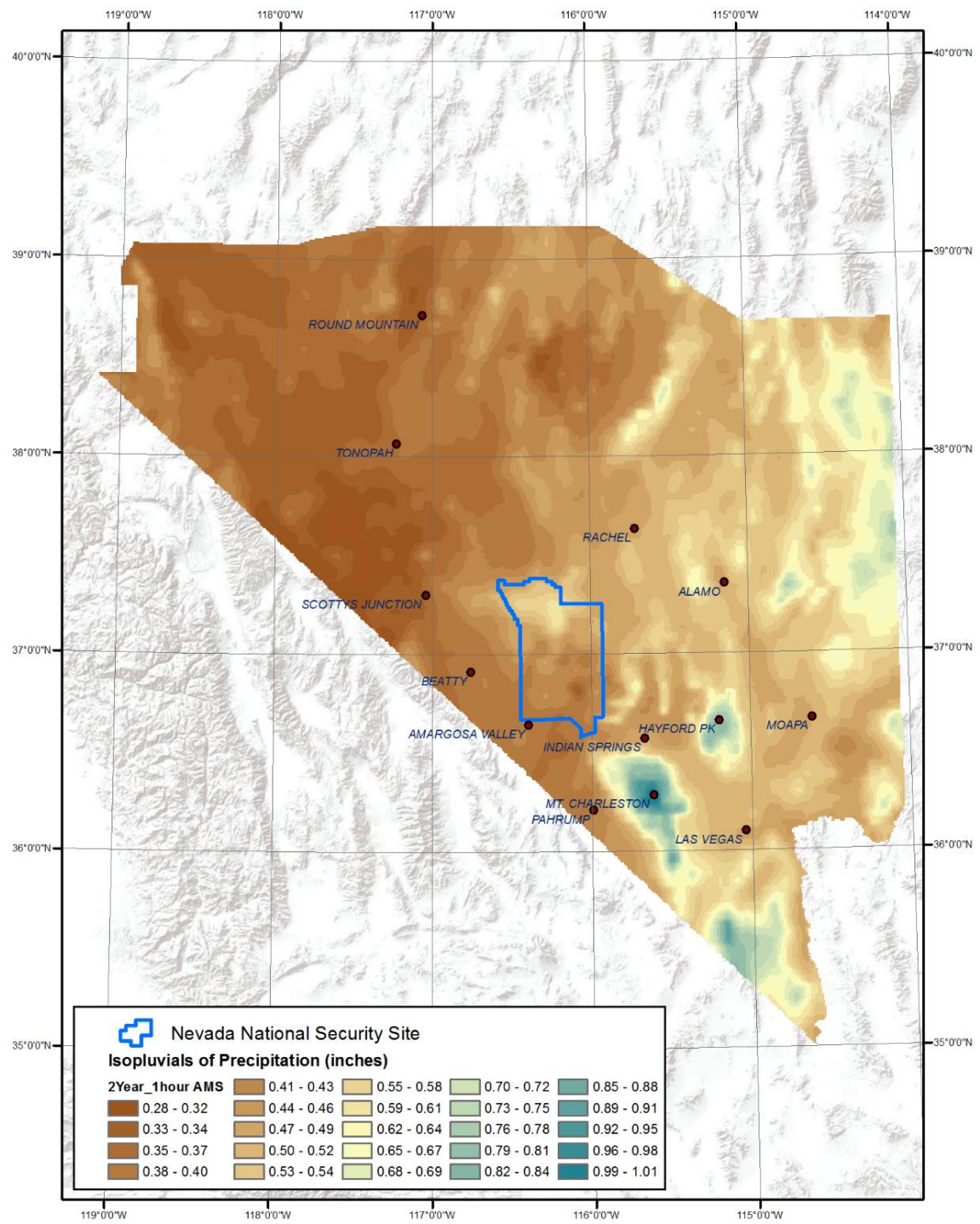


Figure 4A. AMS-based NNSS Precipitation Depth-Duration-Frequency Grid: 2-yr, 1-hr.

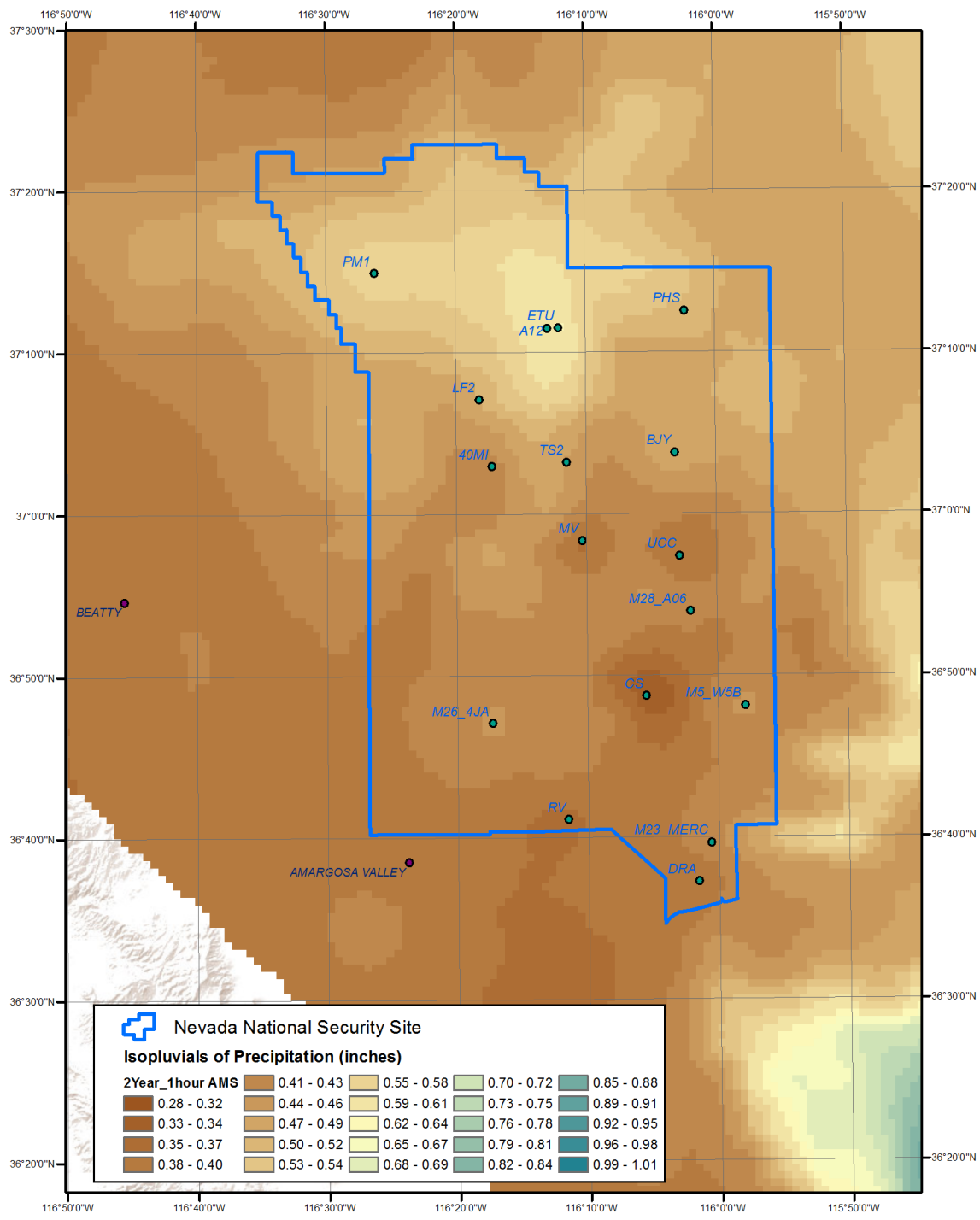


Figure 4B. AMS-based NNSS Precipitation Depth-Duration-Frequency Grid for the focused area: 2-yr, 1-hr.

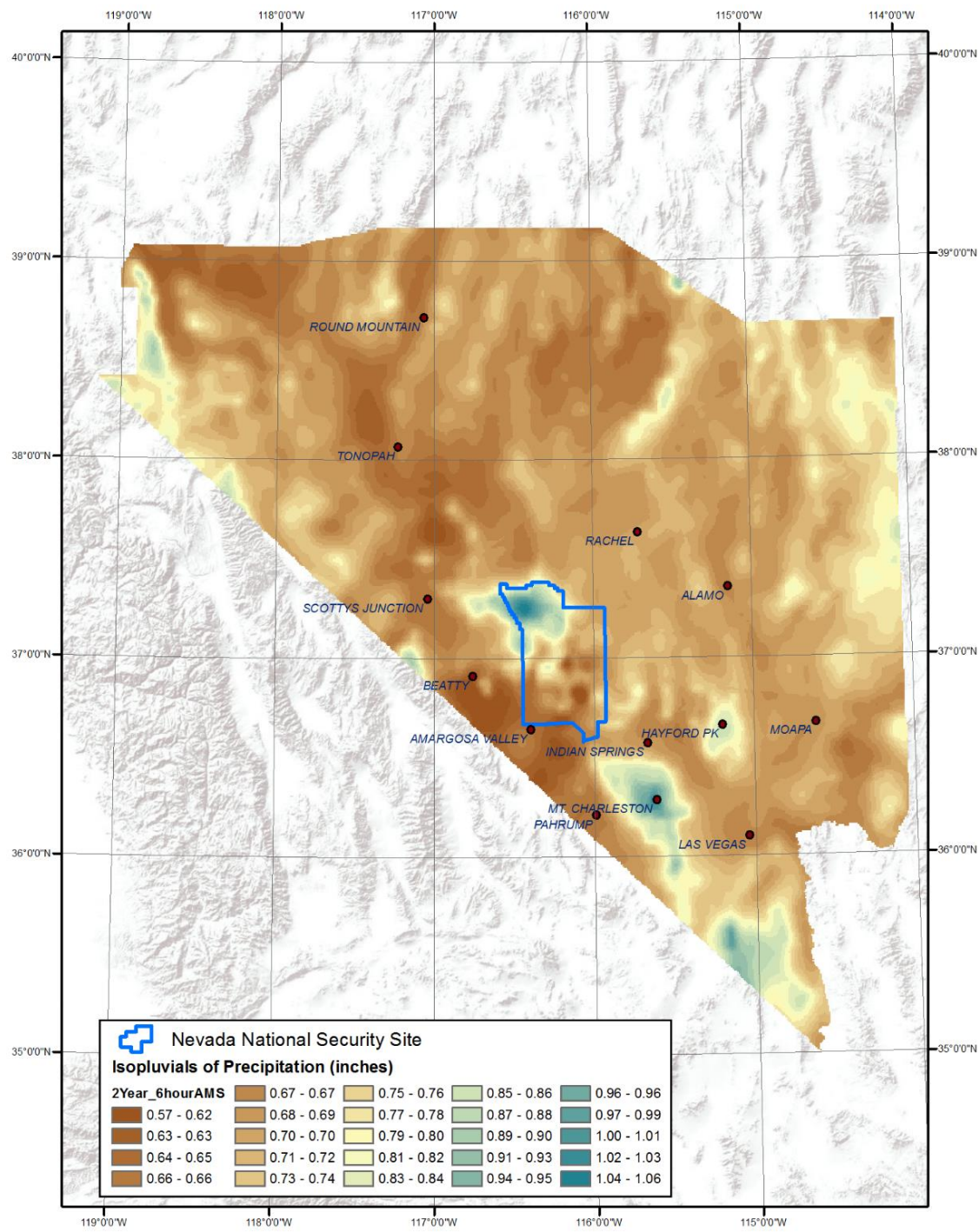


Figure 5A. AMS-based NNSS Precipitation Depth-Duration-Frequency Grid: 2-yr, 6-hr.

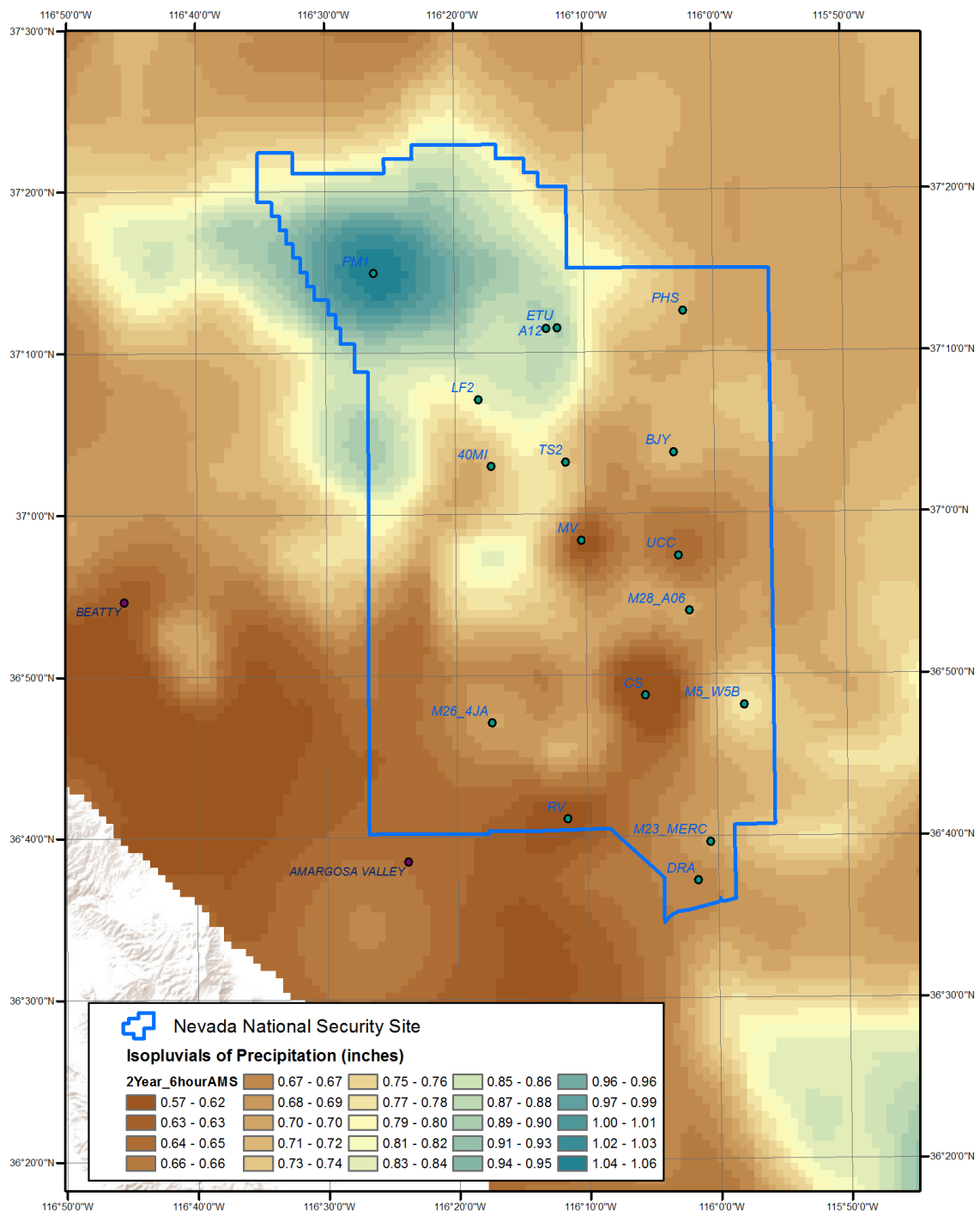


Figure 5B. AMS-based NNSS Precipitation Depth-Duration-Frequency Grid for the focused area: 2-yr, 6-hr.

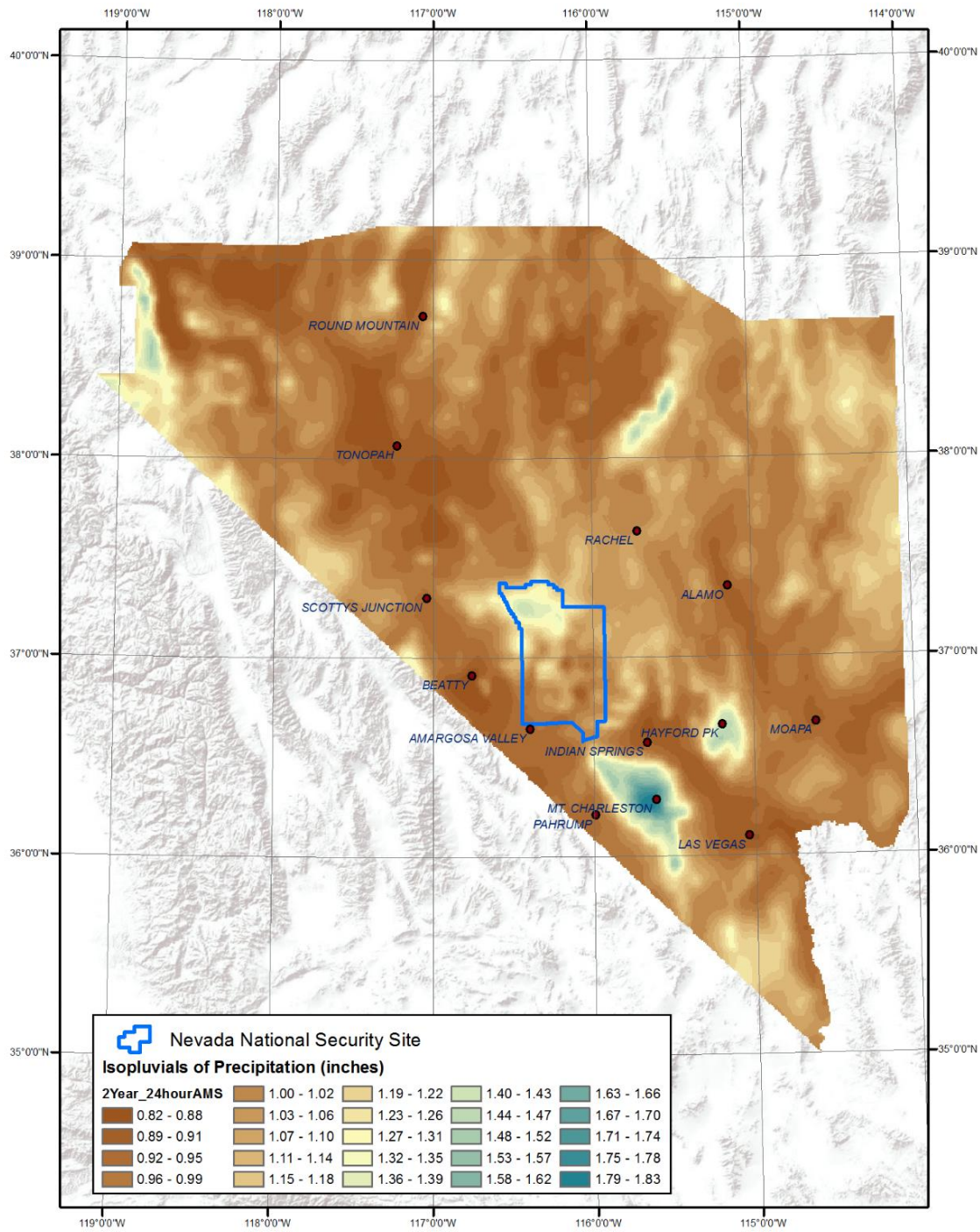


Figure 6A. AMS-based NNSS Precipitation Depth-Duration-Frequency Grid: 2-yr, 24-hr.

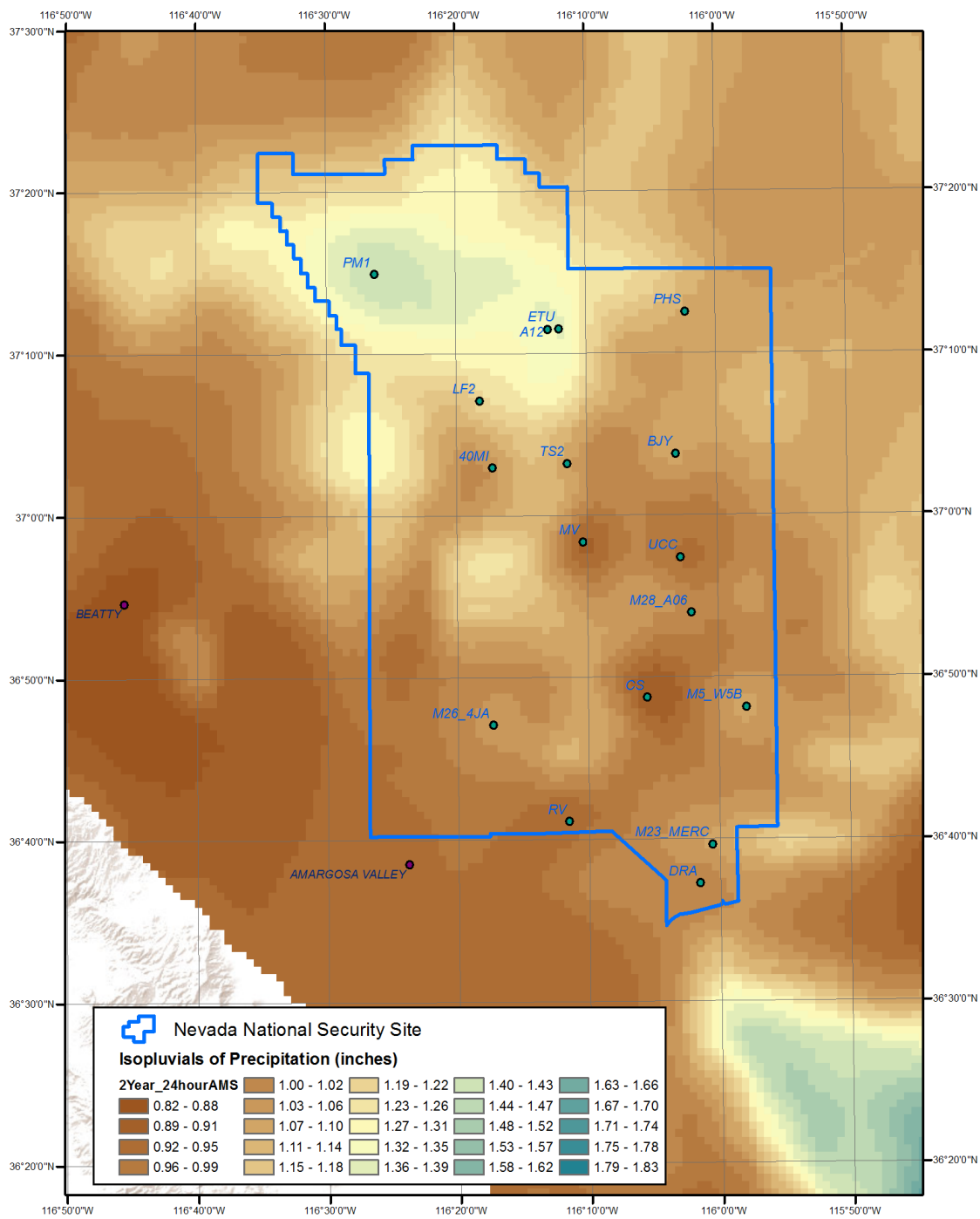


Figure 6B. AMS-based NNSS Precipitation Depth-Duration-Frequency Grid for the focused area: 2-yr, 24-hr.

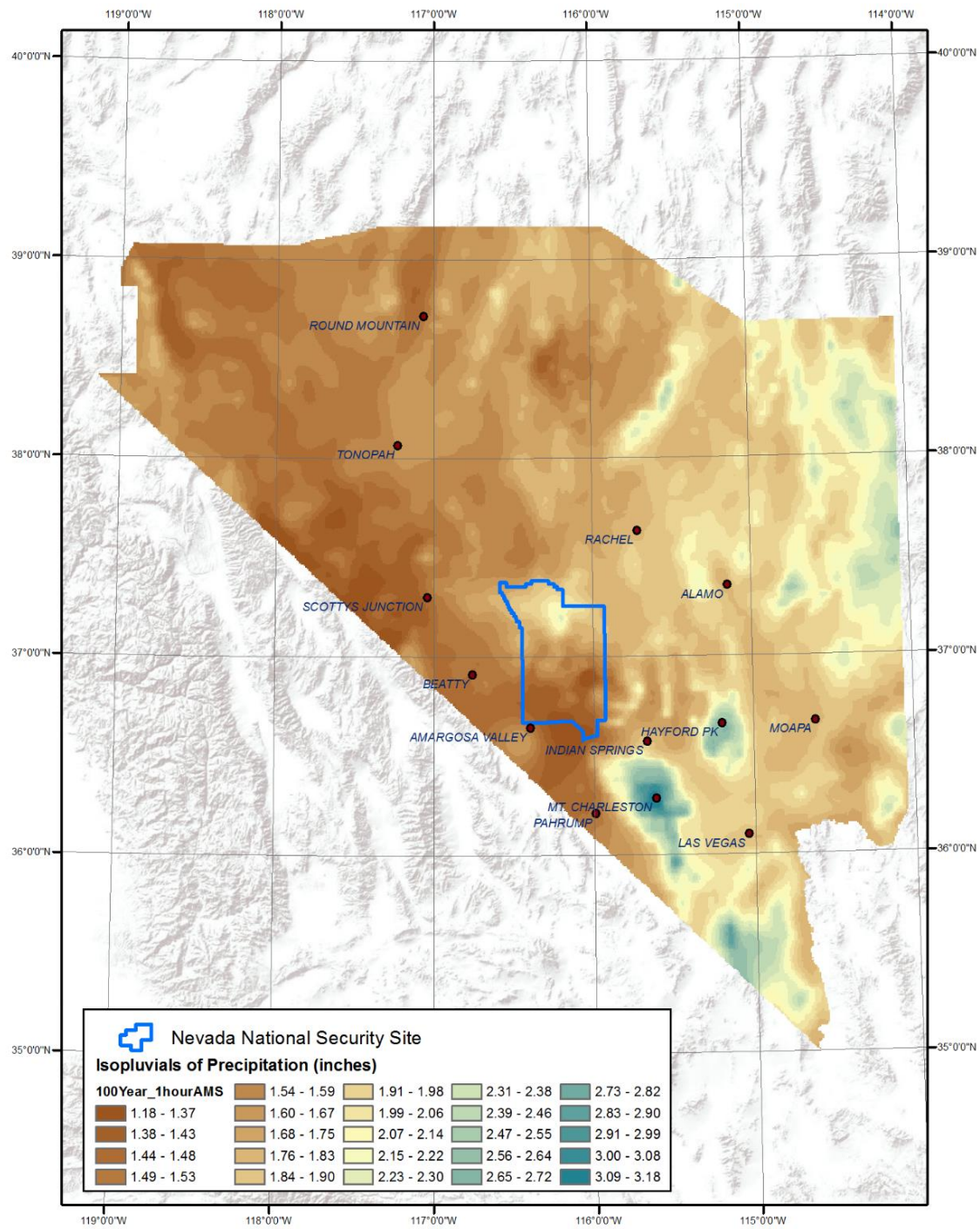


Figure 7A. AMS-based NNSS Precipitation Depth-Duration-Frequency Grid: 100-yr, 1-hr.

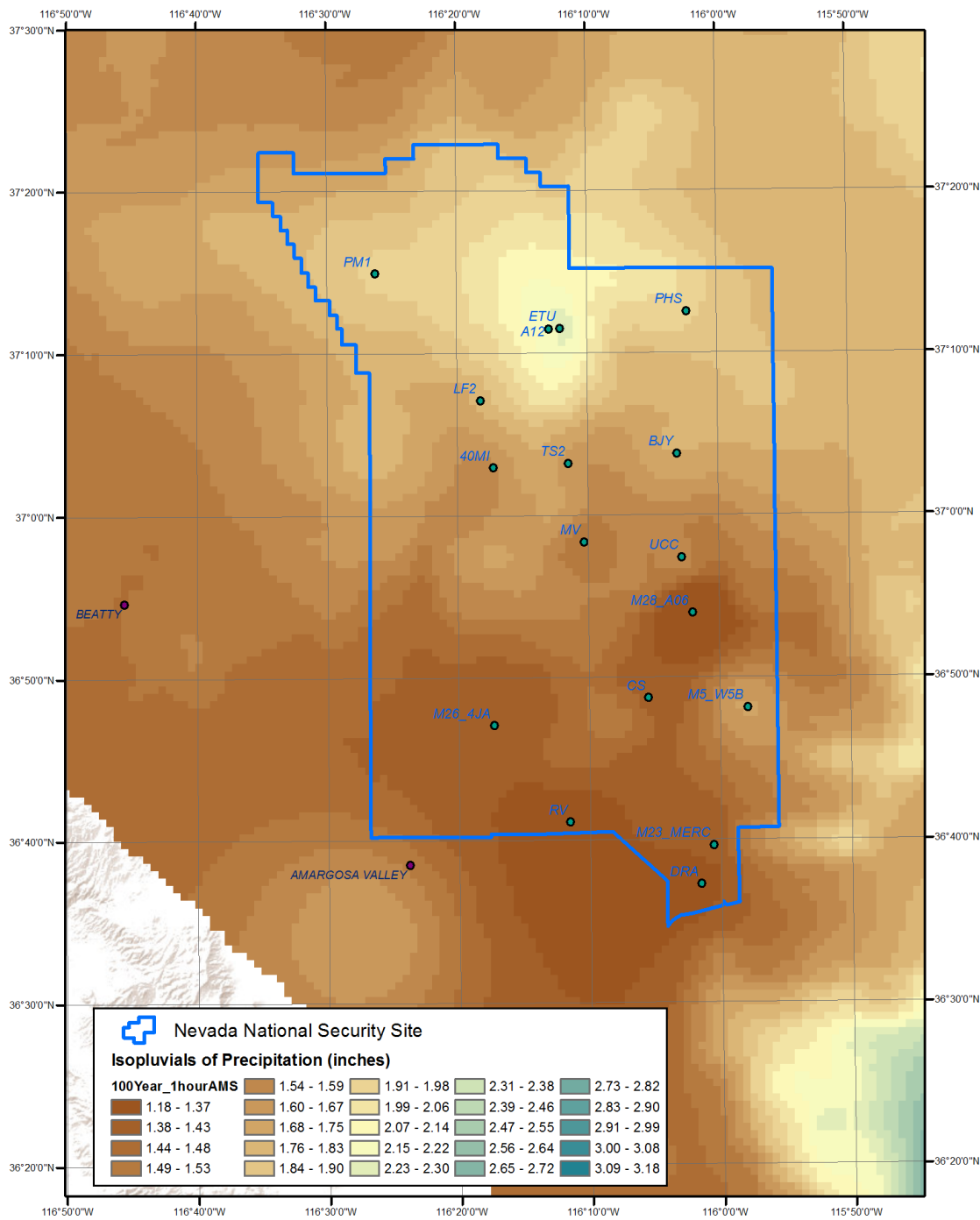


Figure 7B. AMS-based NNSS Precipitation Depth-Duration-Frequency Grid for the focused area: 100-yr, 1-hr.

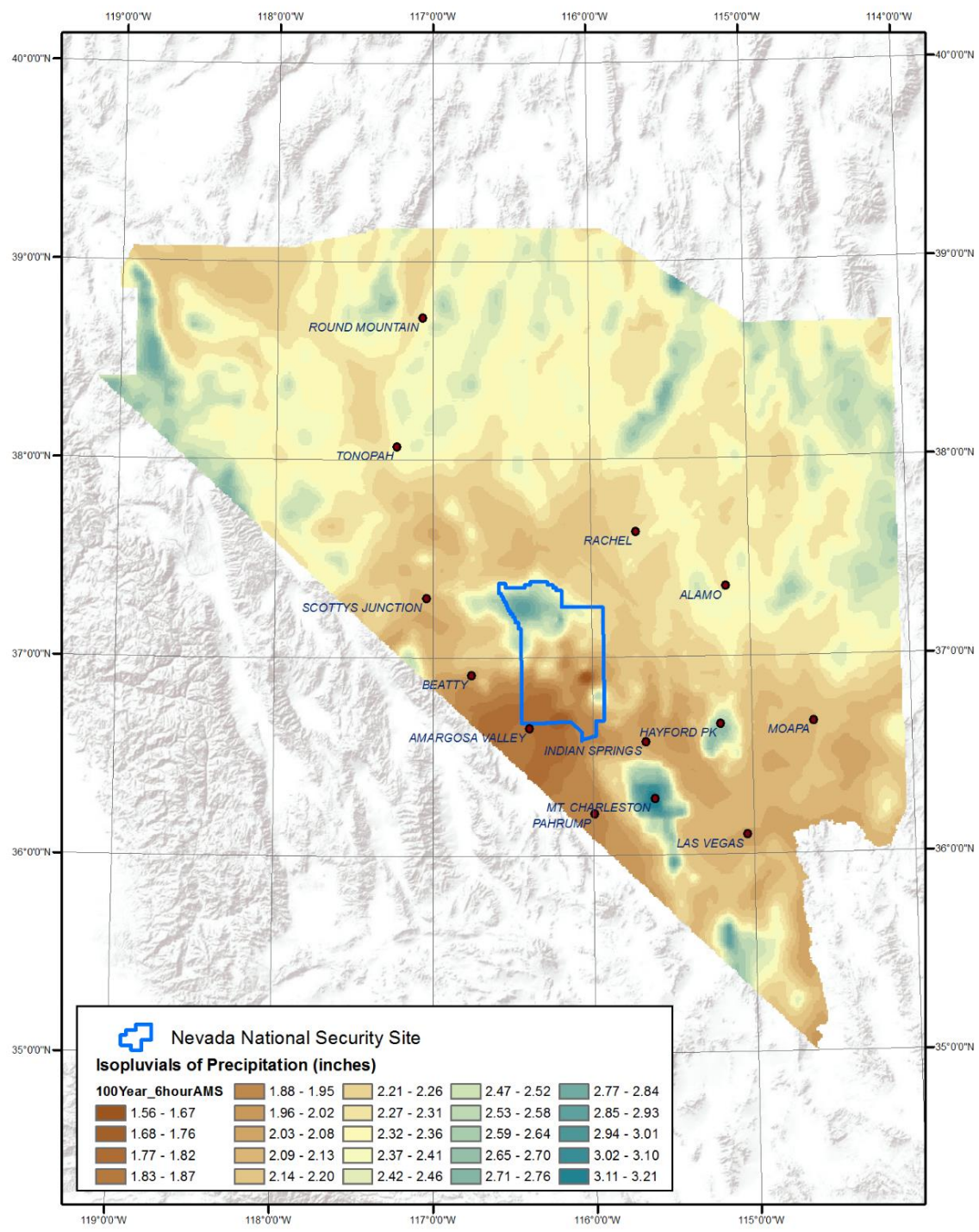


Figure 8A. AMS-based NNSS Precipitation Depth-Duration-Frequency Grid: 100-yr, 6-hr.

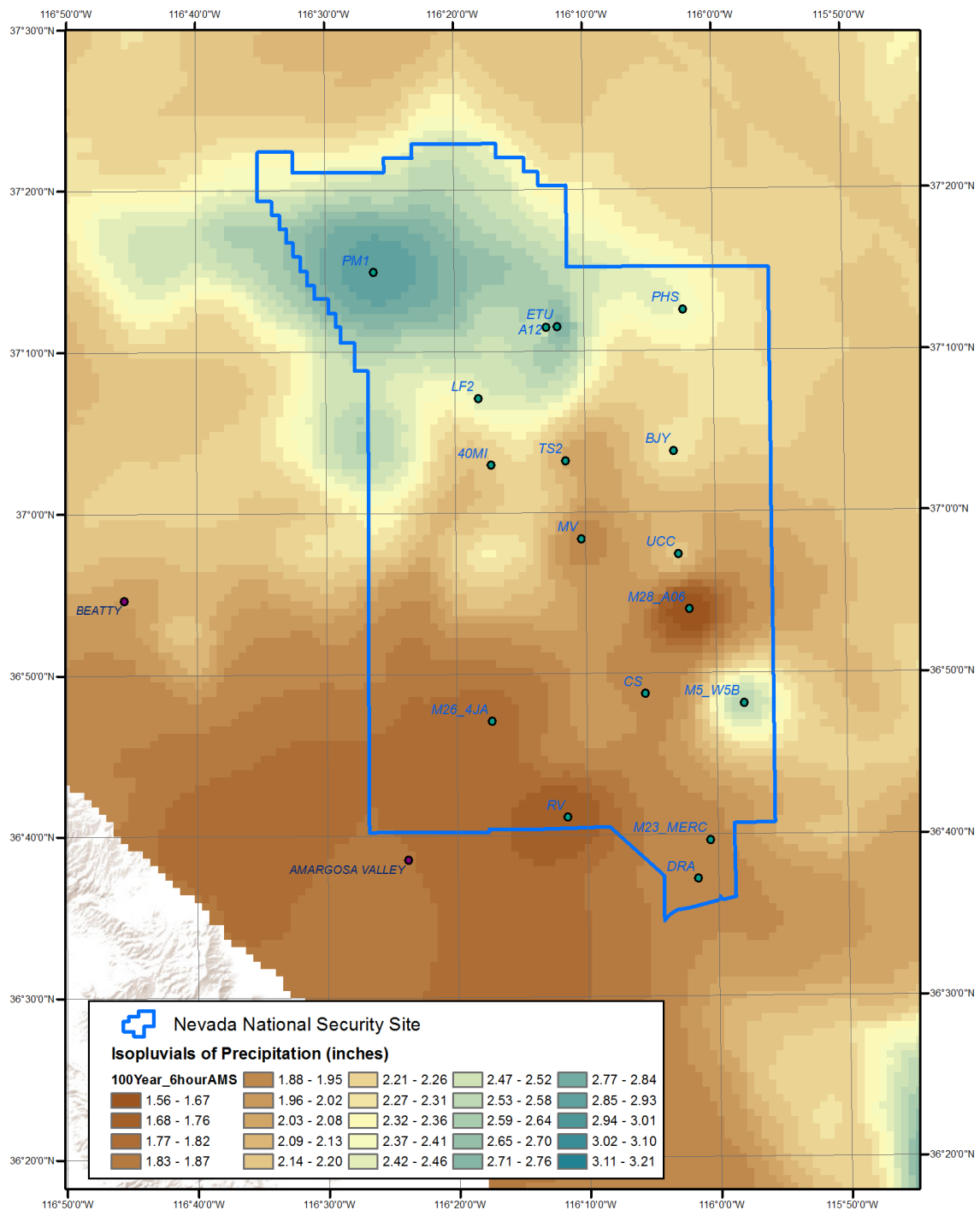


Figure 8B. AMS-based NNSS Precipitation Depth-Duration-Frequency Grid for the focused area: 100-yr, 6-hr.

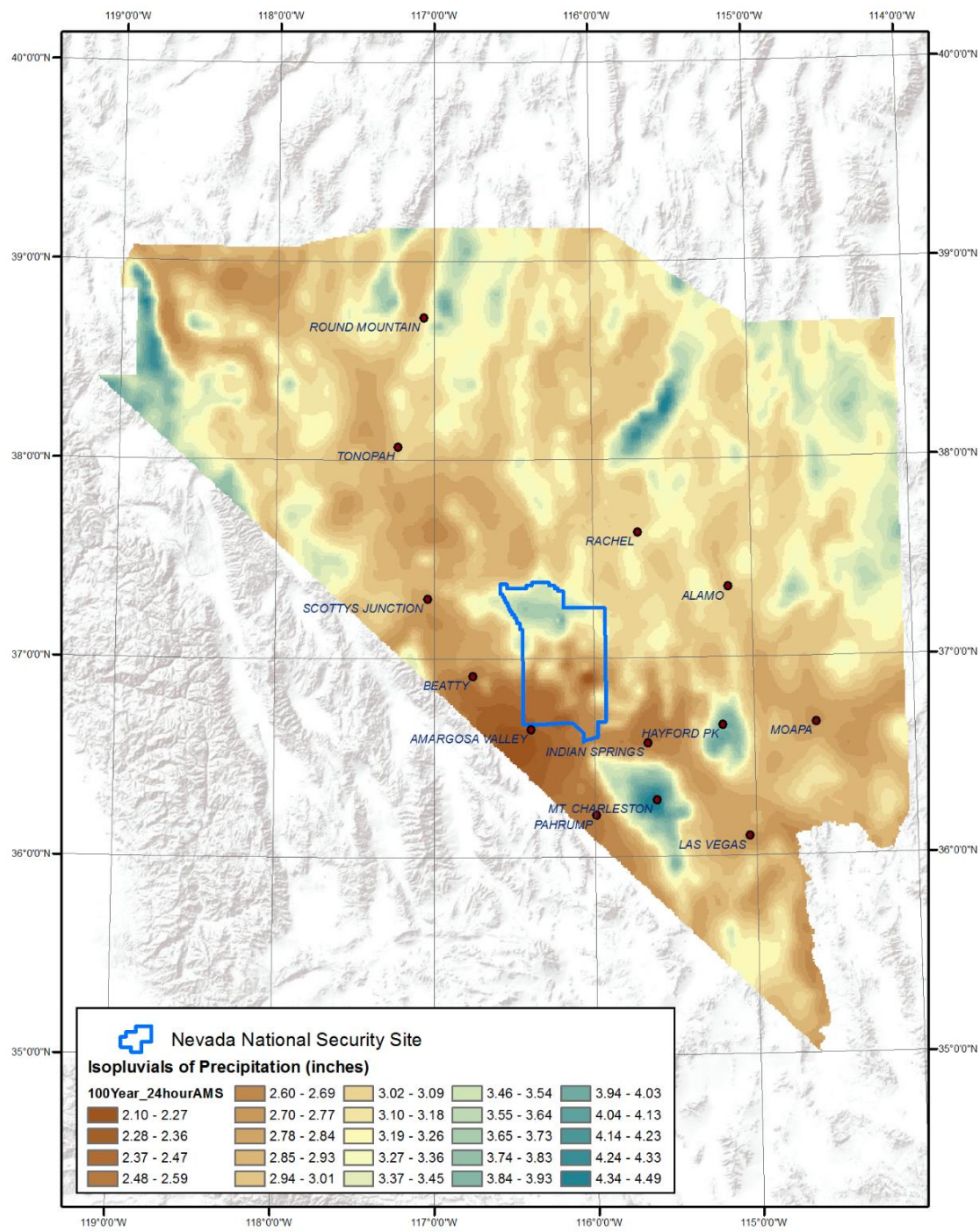


Figure 9A. AMS-based NNSS Precipitation Depth-Duration-Frequency Grid: 100-yr, 24-hr.

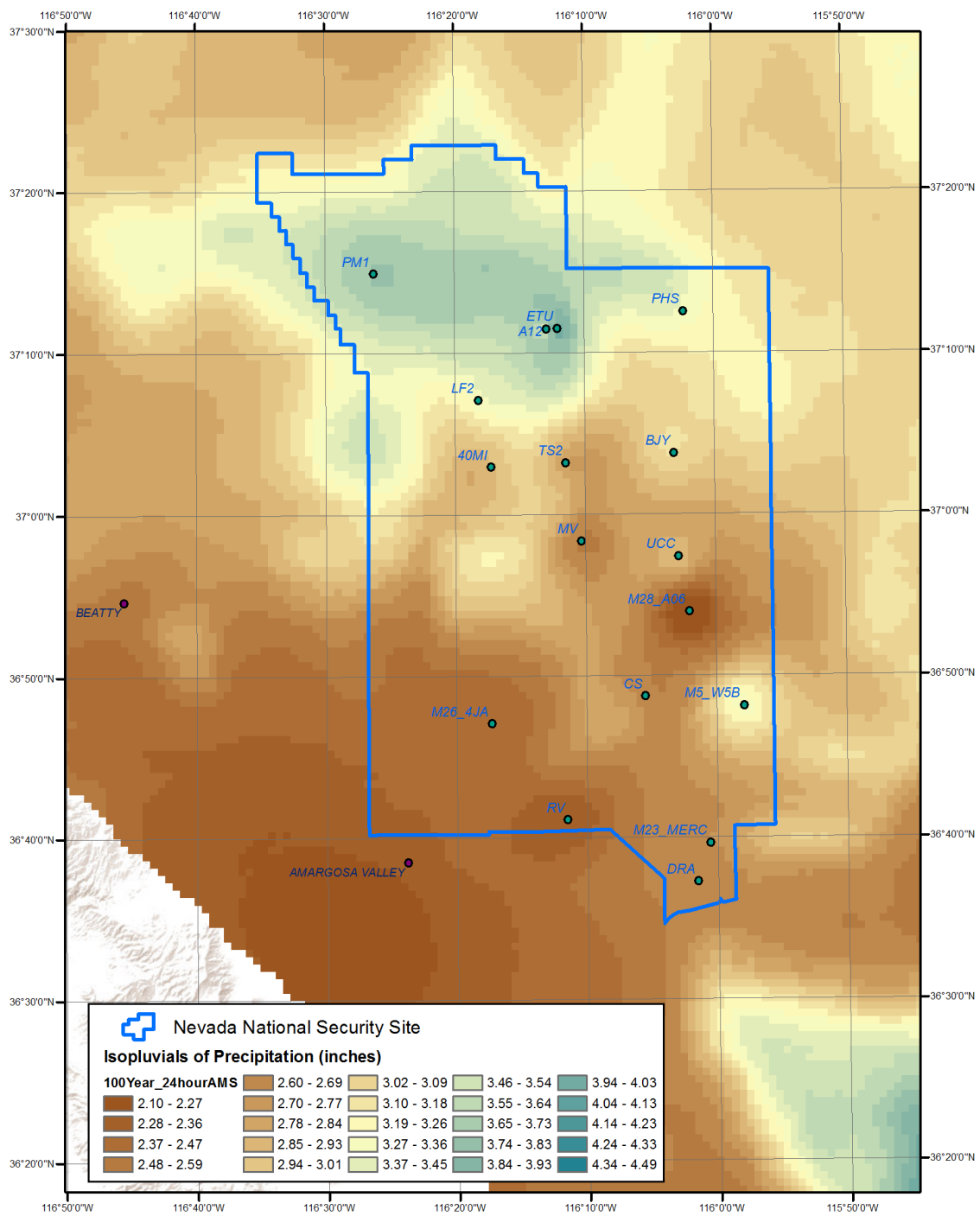


Figure 9B. AMS-based NNSS Precipitation Depth-Duration-Frequency Grid for the focused area: 100-yr, 24-hr.

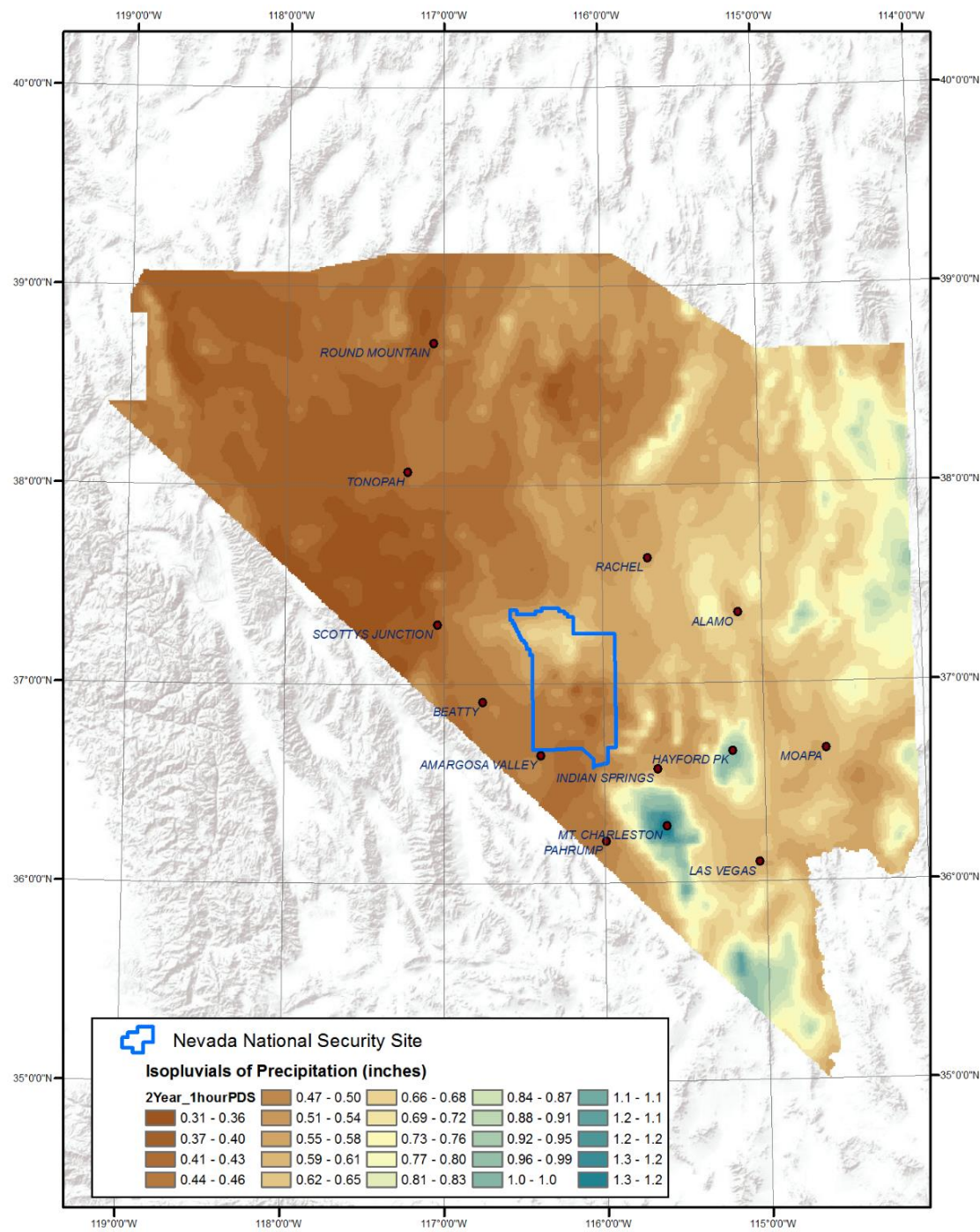


Figure 10A. PDS-based NNSS Precipitation Depth-Duration-Frequency Grid: 2-yr, 1-hr.

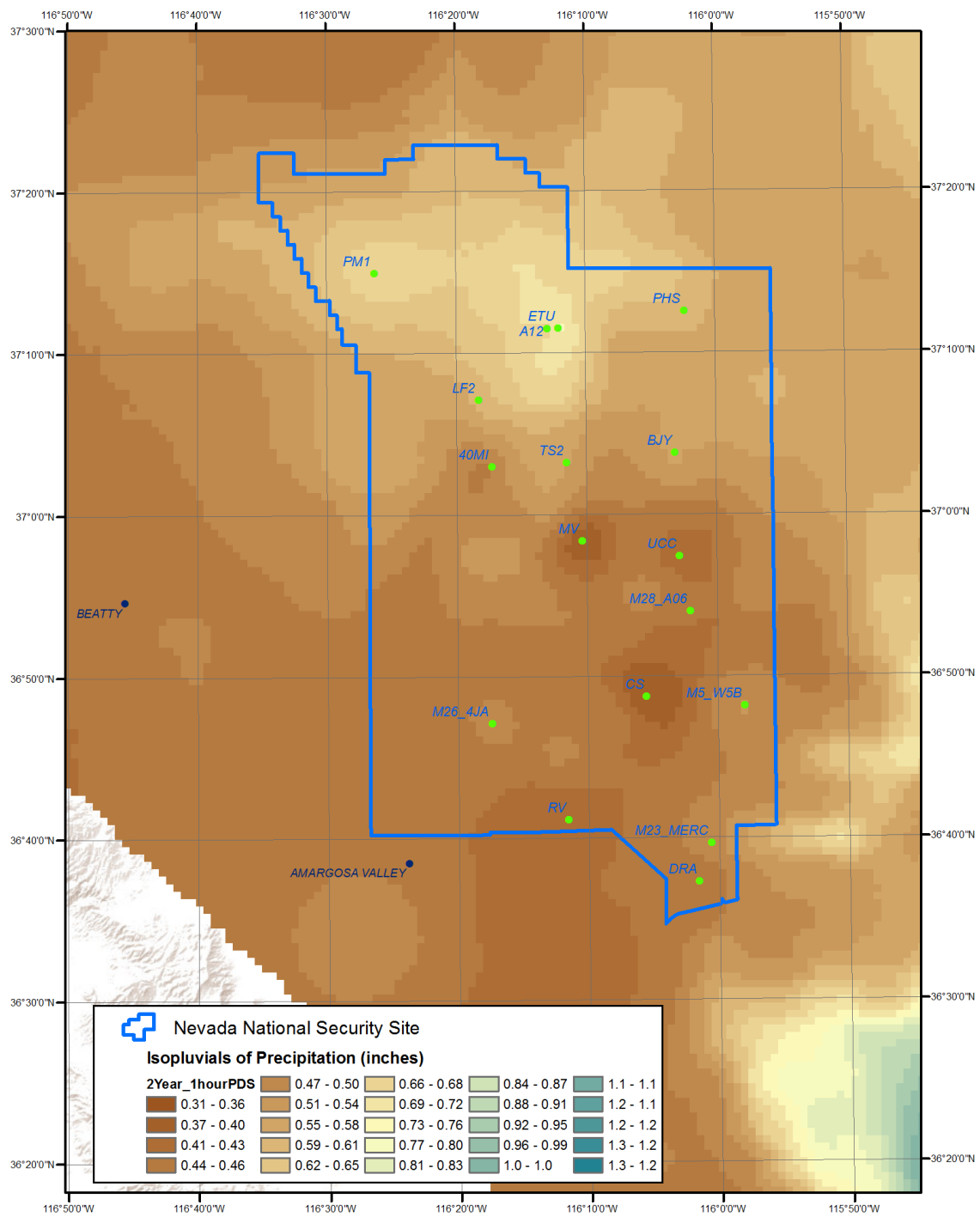


Figure 10B. PDS-based NNSS Precipitation Depth-Duration-Frequency Grid for the focused area: 2-yr, 1-hr.

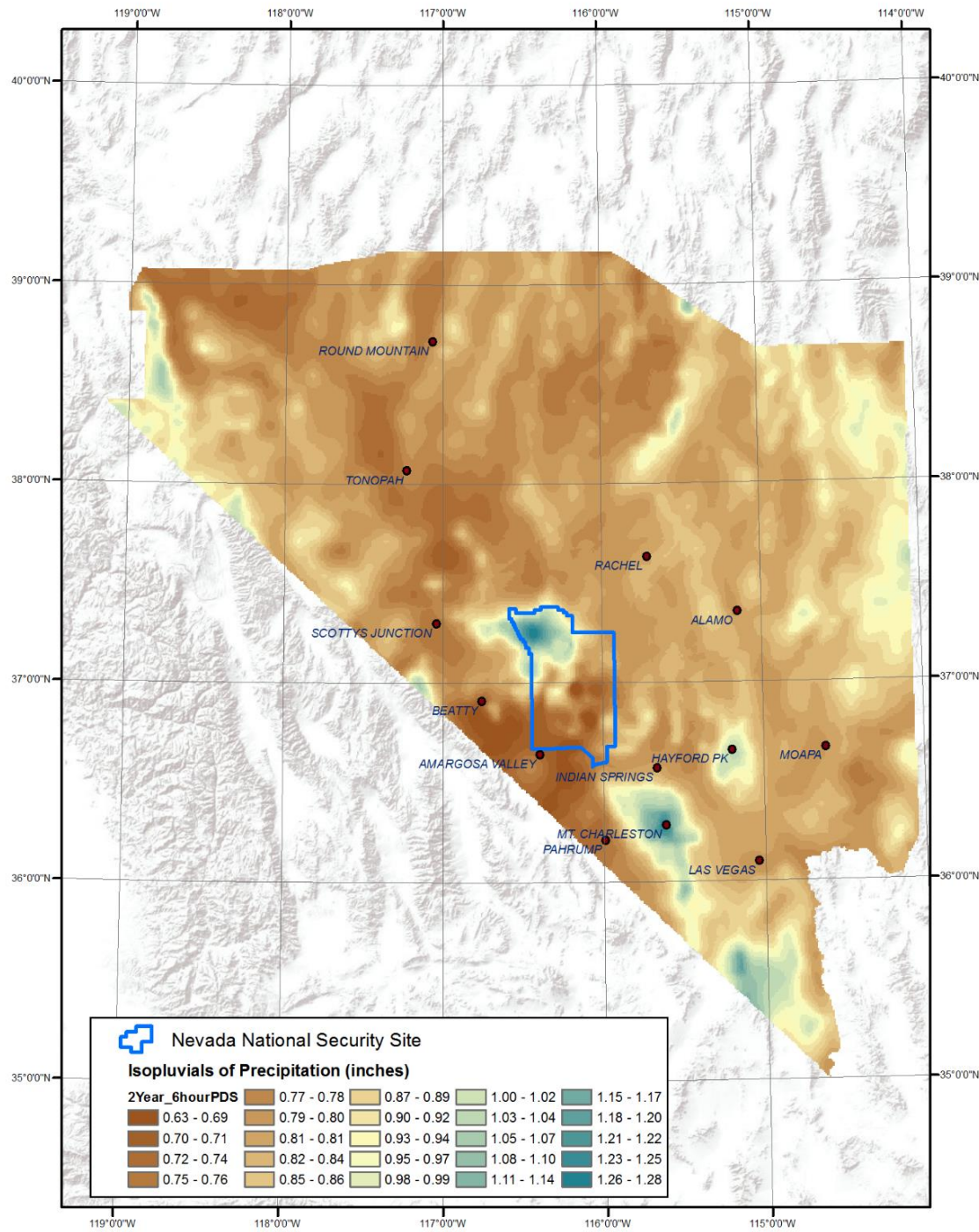


Figure 11A. PDS-based NNSS Precipitation Depth-Duration-Frequency Grid: 2-yr, 6-hr.

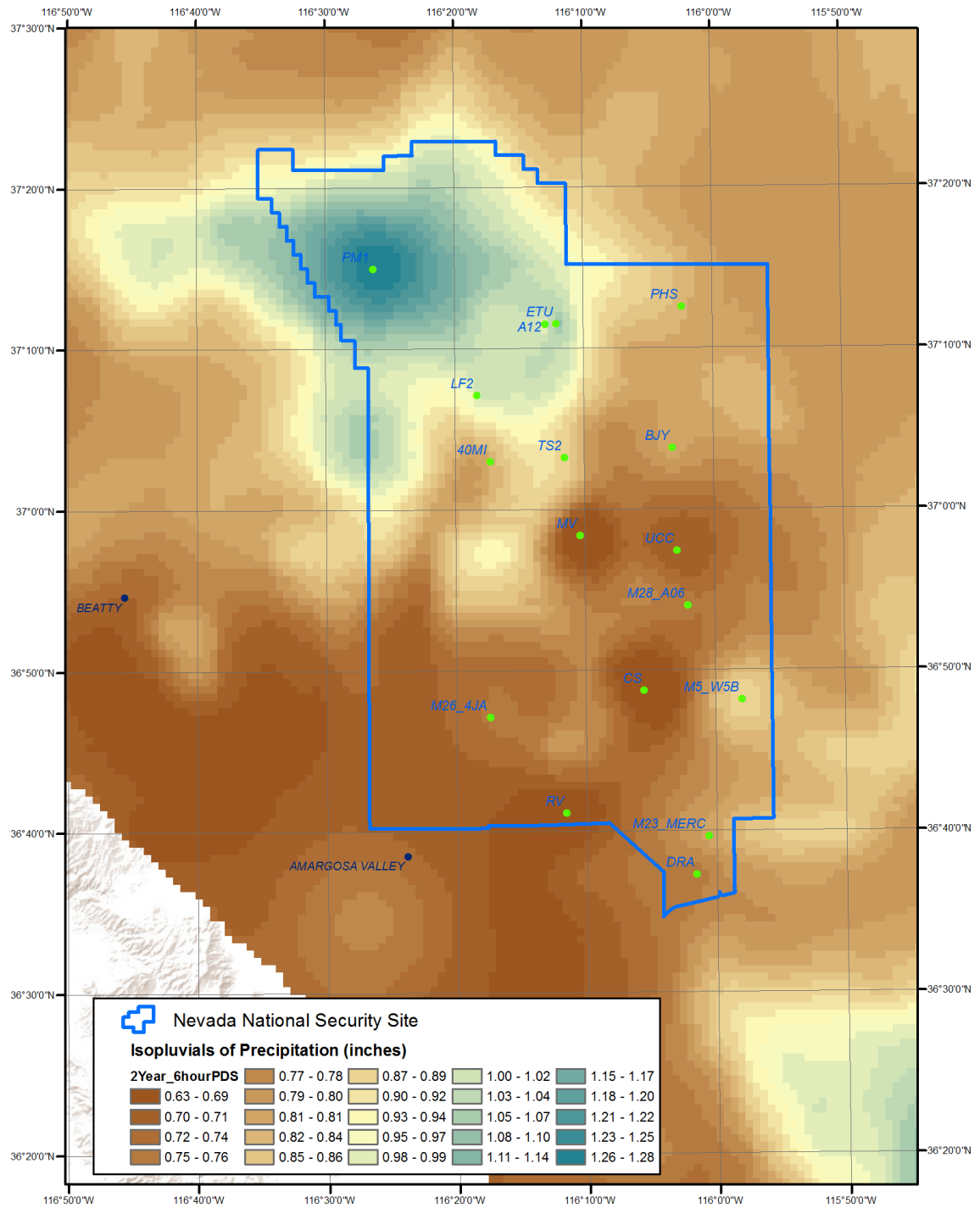


Figure 11B. PDS-based NNSS Precipitation Depth-Duration-Frequency Grid for the focused area: 2-yr, 6-hr.

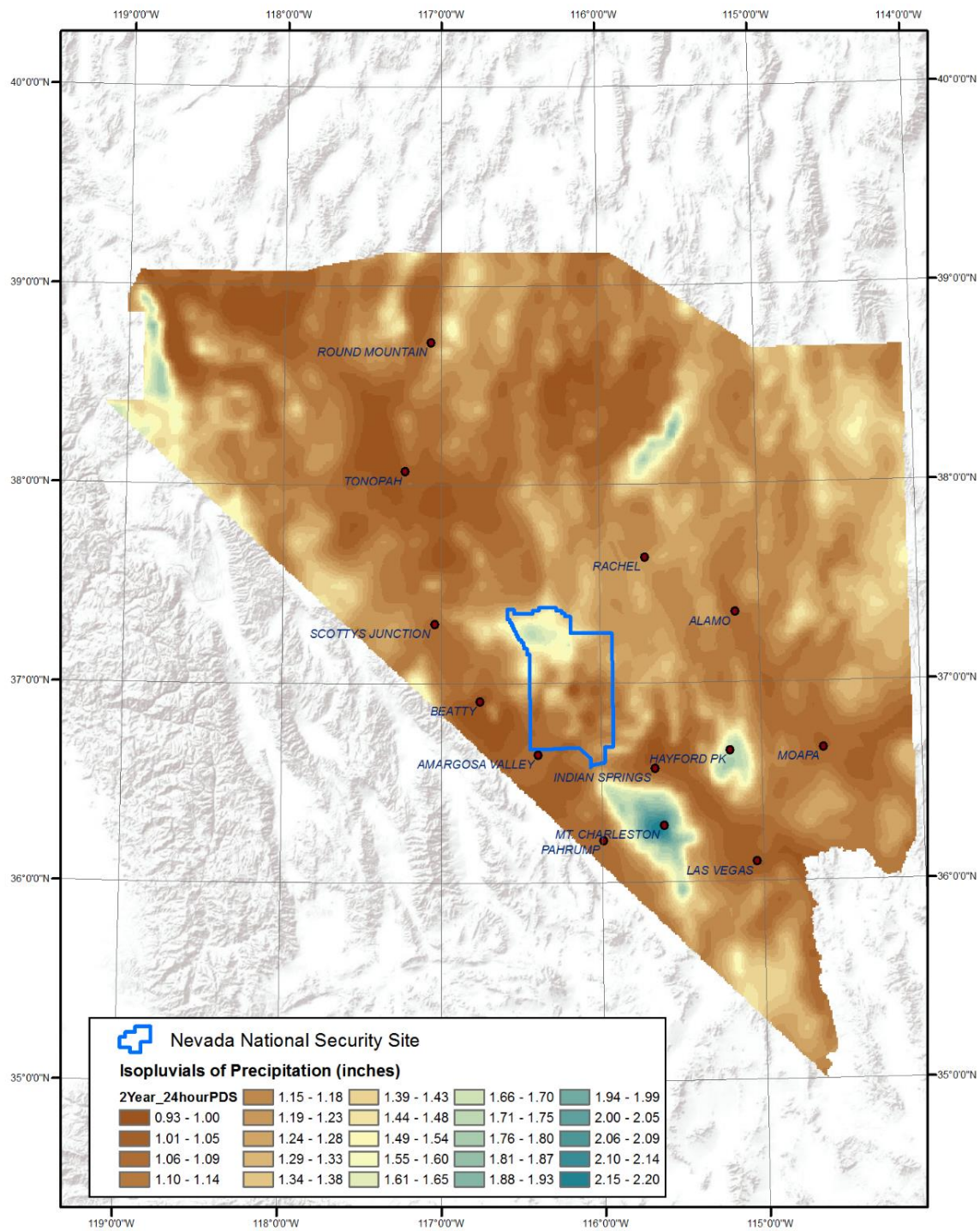


Figure 12A. PDS-based NNSS Precipitation Depth-Duration-Frequency Grid: 2-yr, 24-hr.

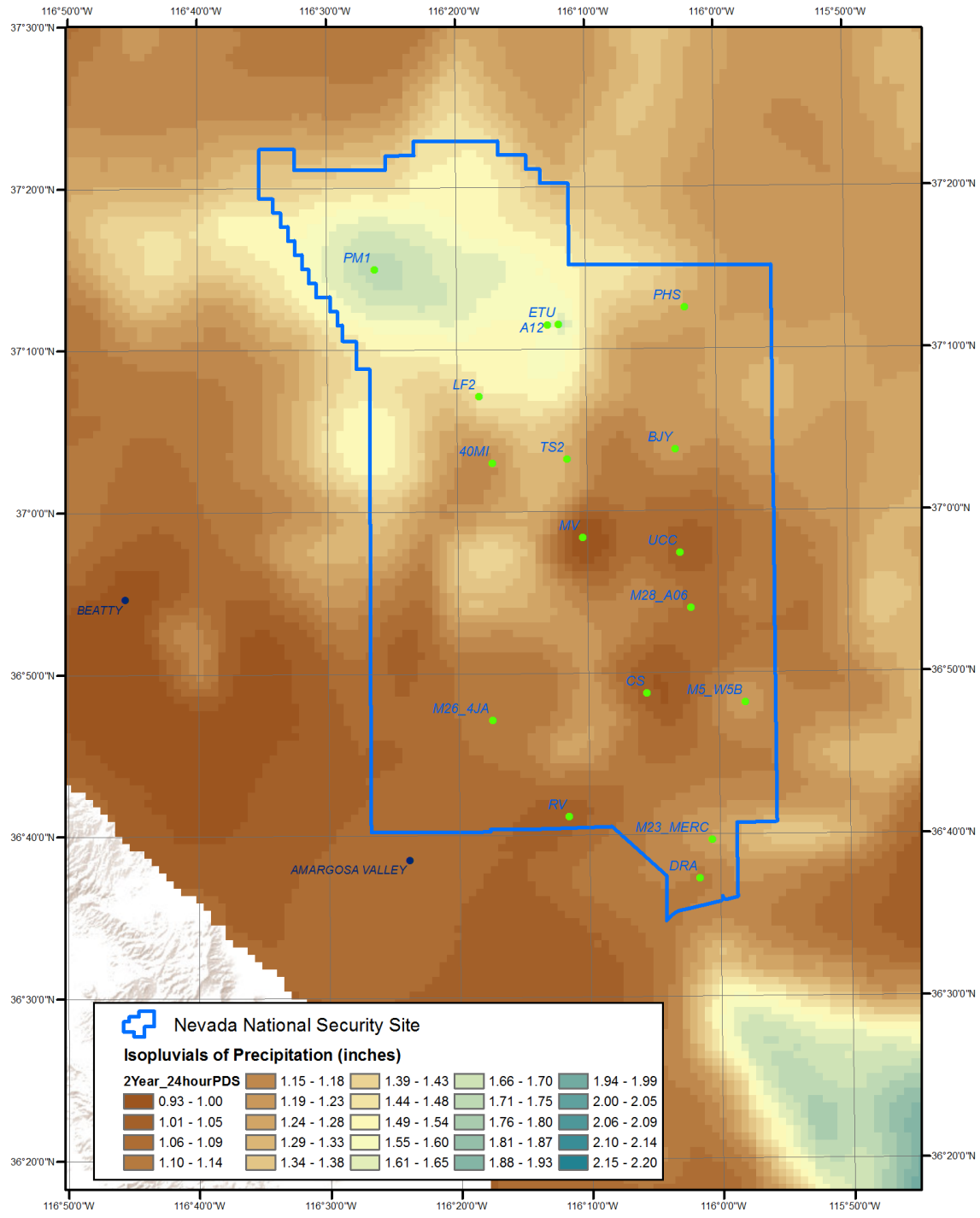


Figure 12B. PDS-based NNSS Precipitation Depth-Duration-Frequency Grid for the focused area: 2-yr, 24-hr.

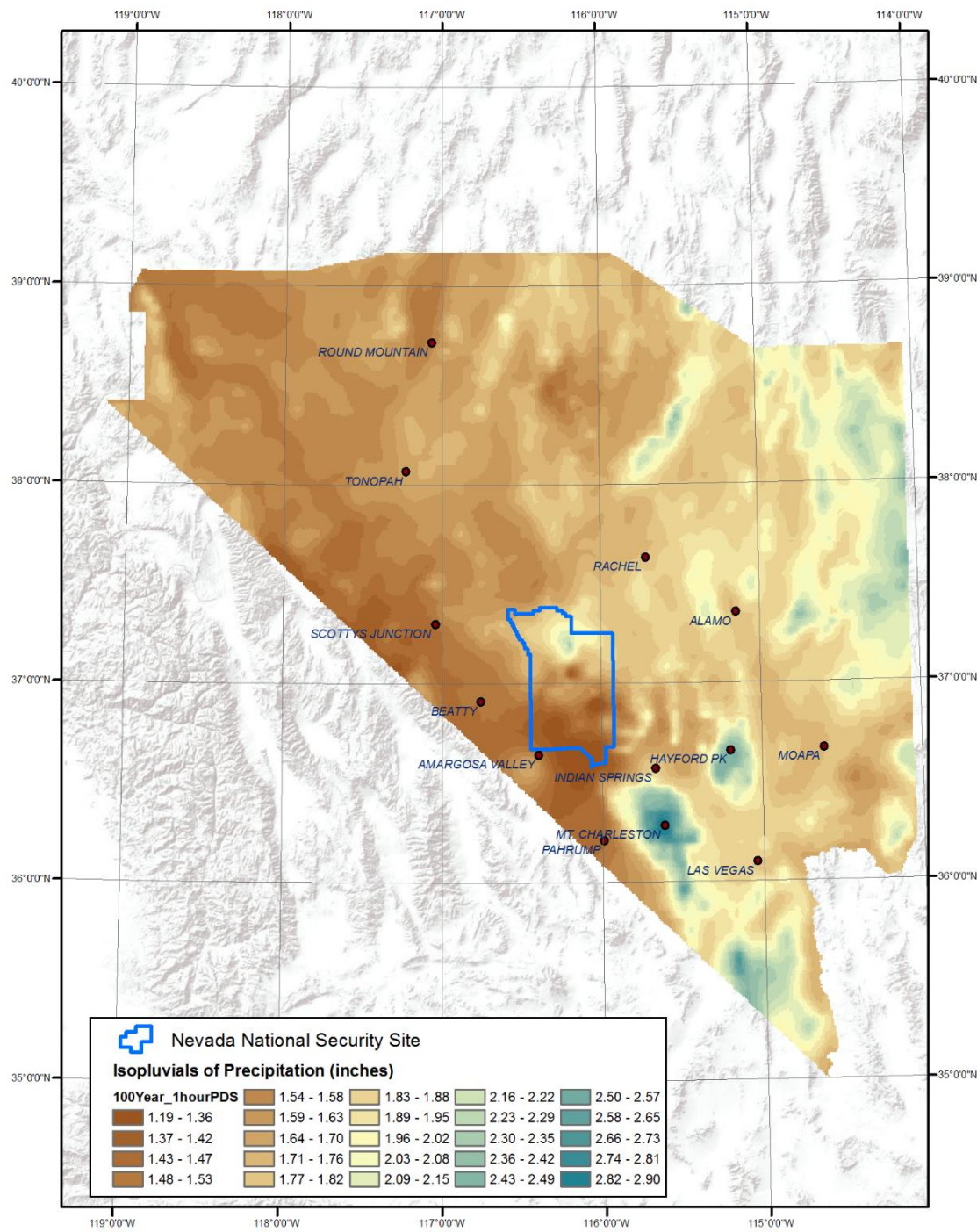


Figure 13A. PDS-based NNSS Precipitation Depth-Duration-Frequency Grid: 100-yr, 1-hr.

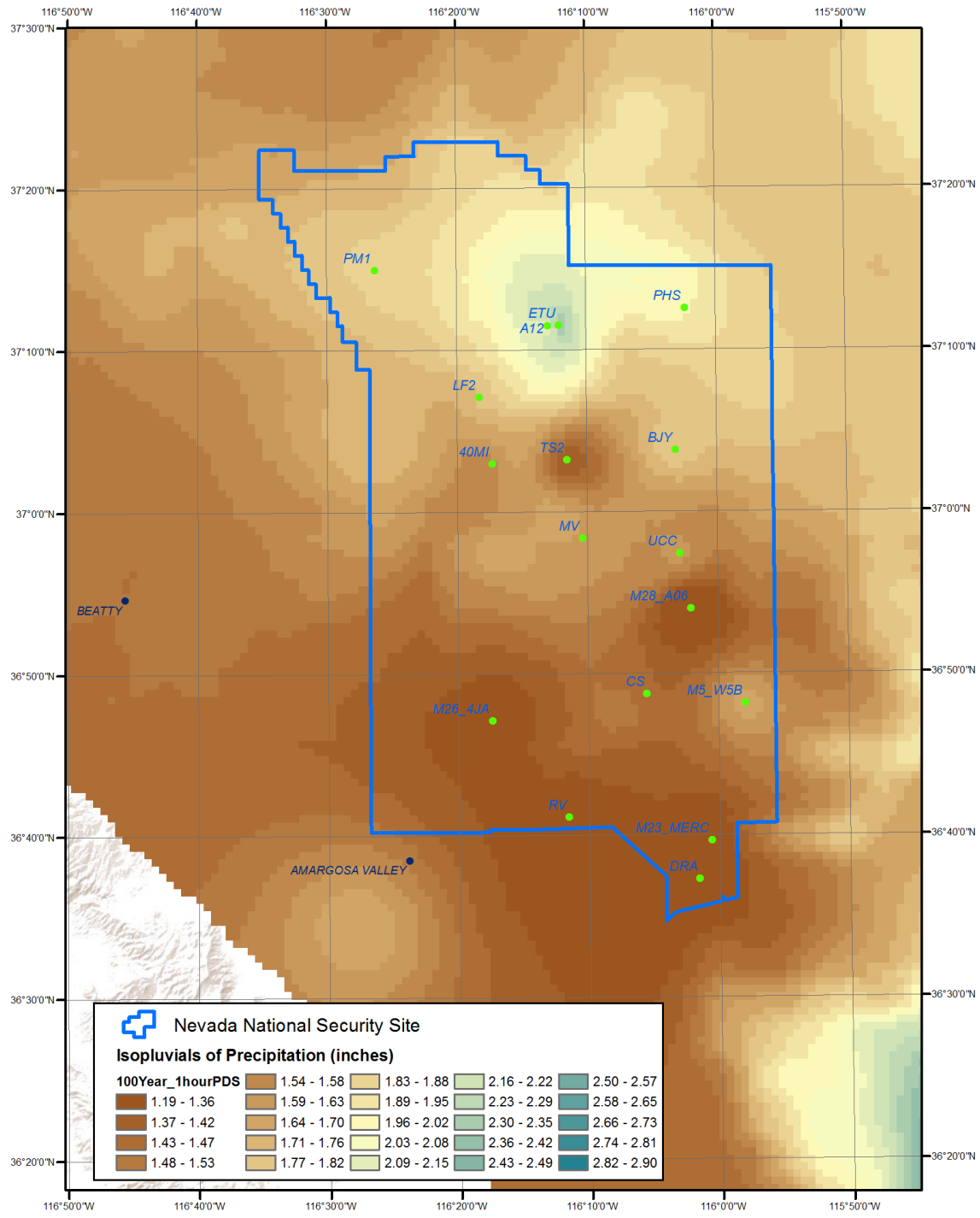


Figure 13B. PDS-based NNSS Precipitation Depth-Duration-Frequency Grid for the focused area: 100-yr, 1-hr.

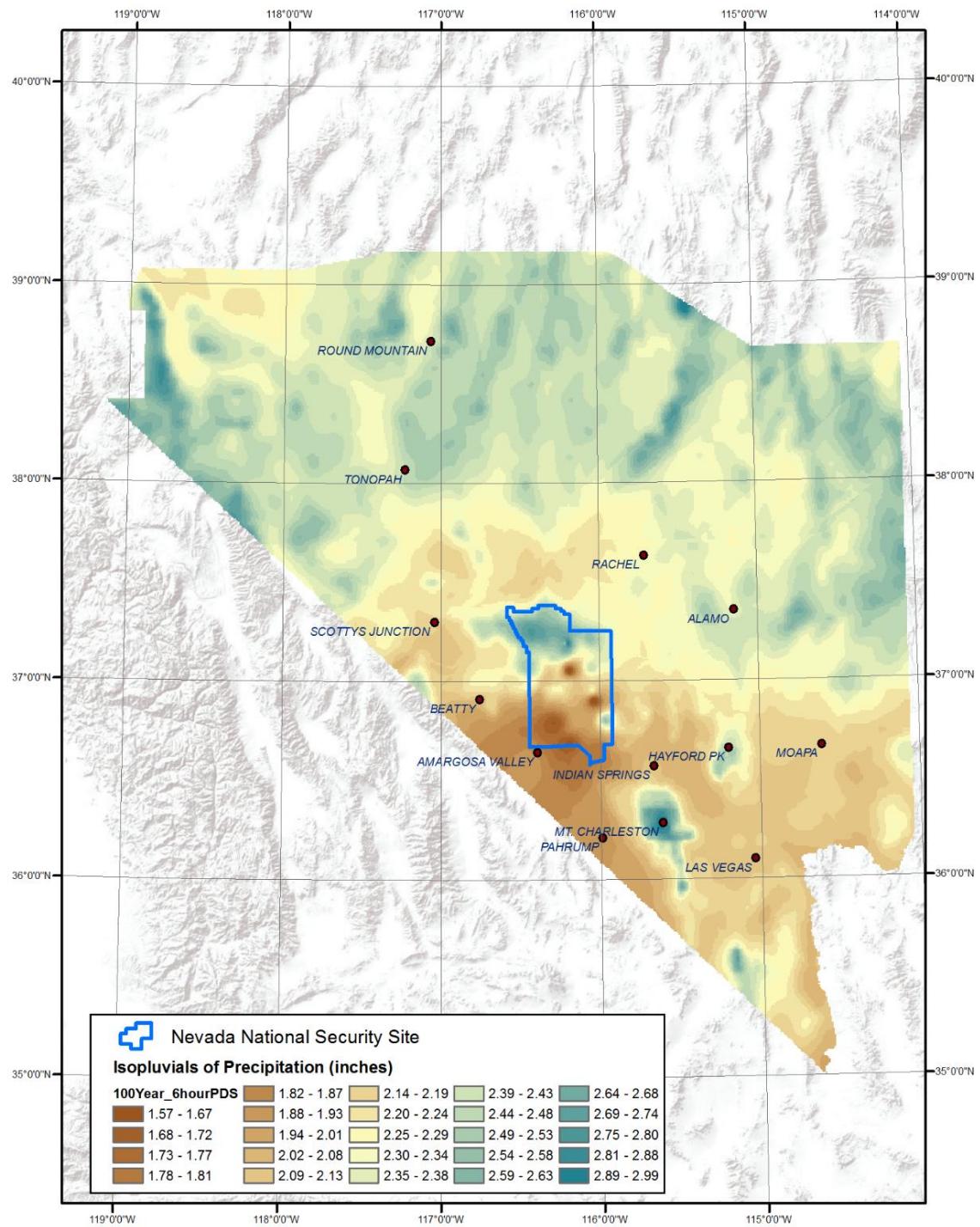


Figure 14A. PDS-based NNSS Precipitation Depth-Duration-Frequency Grid: 100-yr, 6-hr.

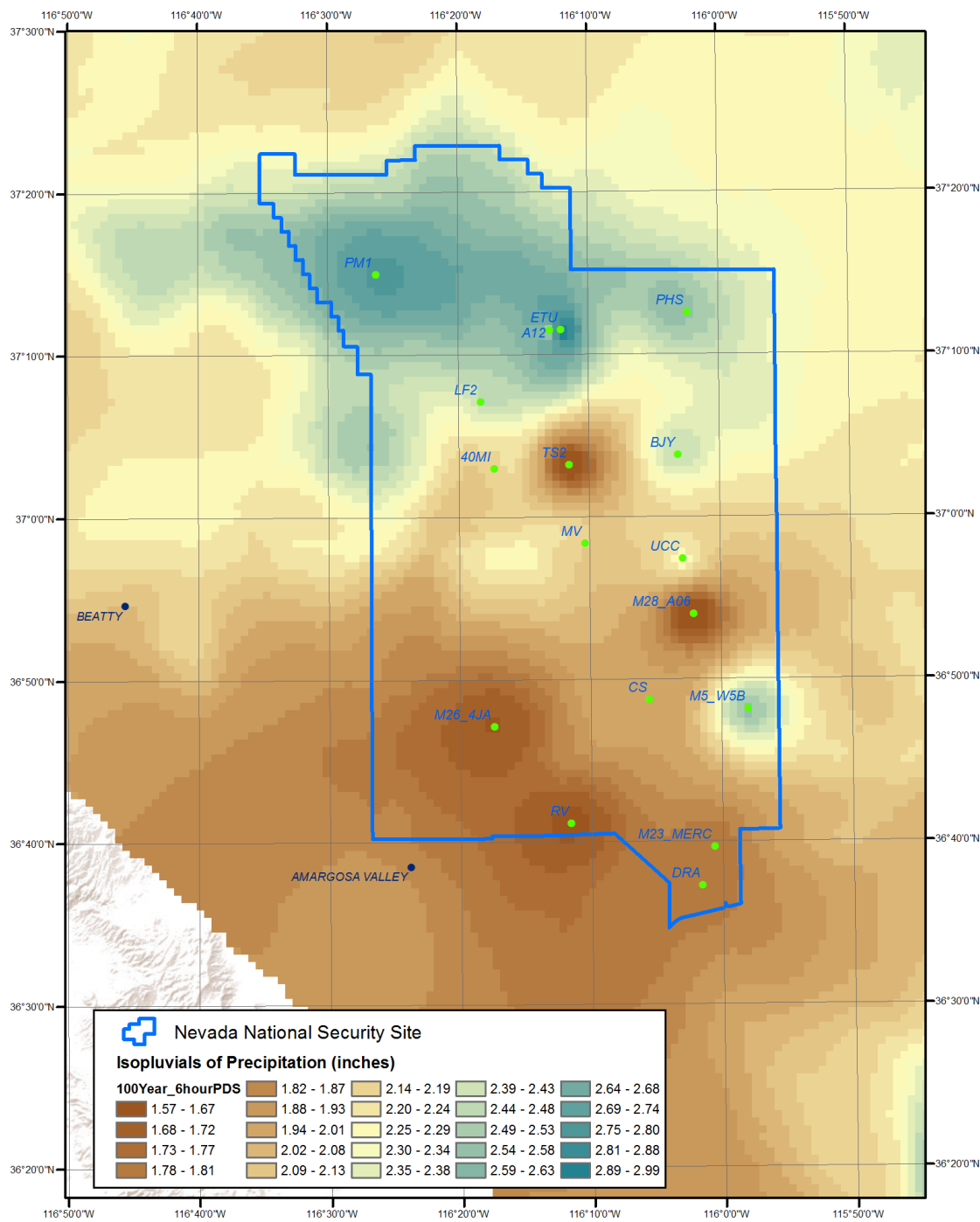


Figure 14B. PDS-based NNSS Precipitation Depth-Duration-Frequency Grid for the focused area: 100-yr, 6-hr.

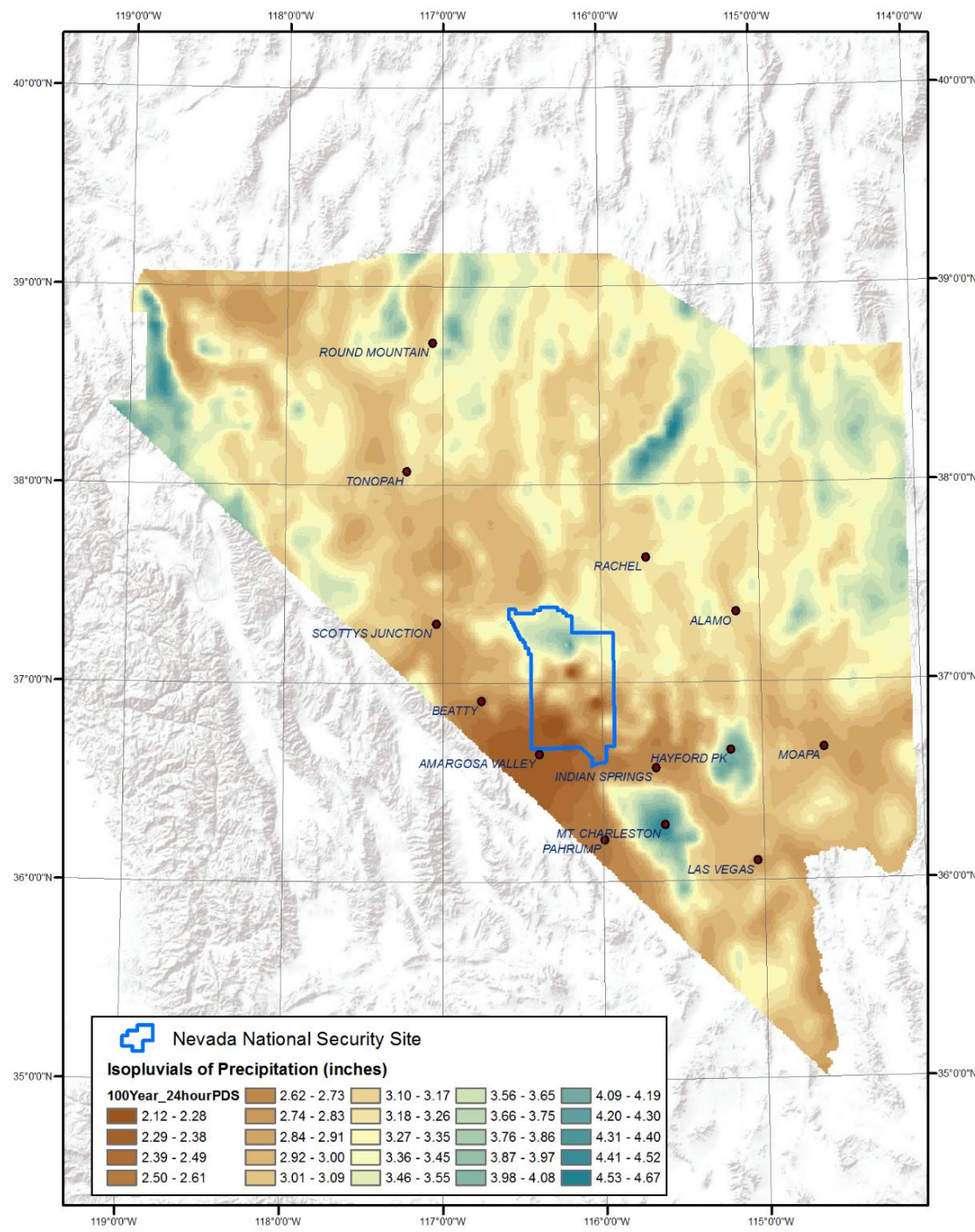


Figure 15A. PDS-based NNSS Precipitation Depth-Duration-Frequency Grid: 100-yr, 24-hr.

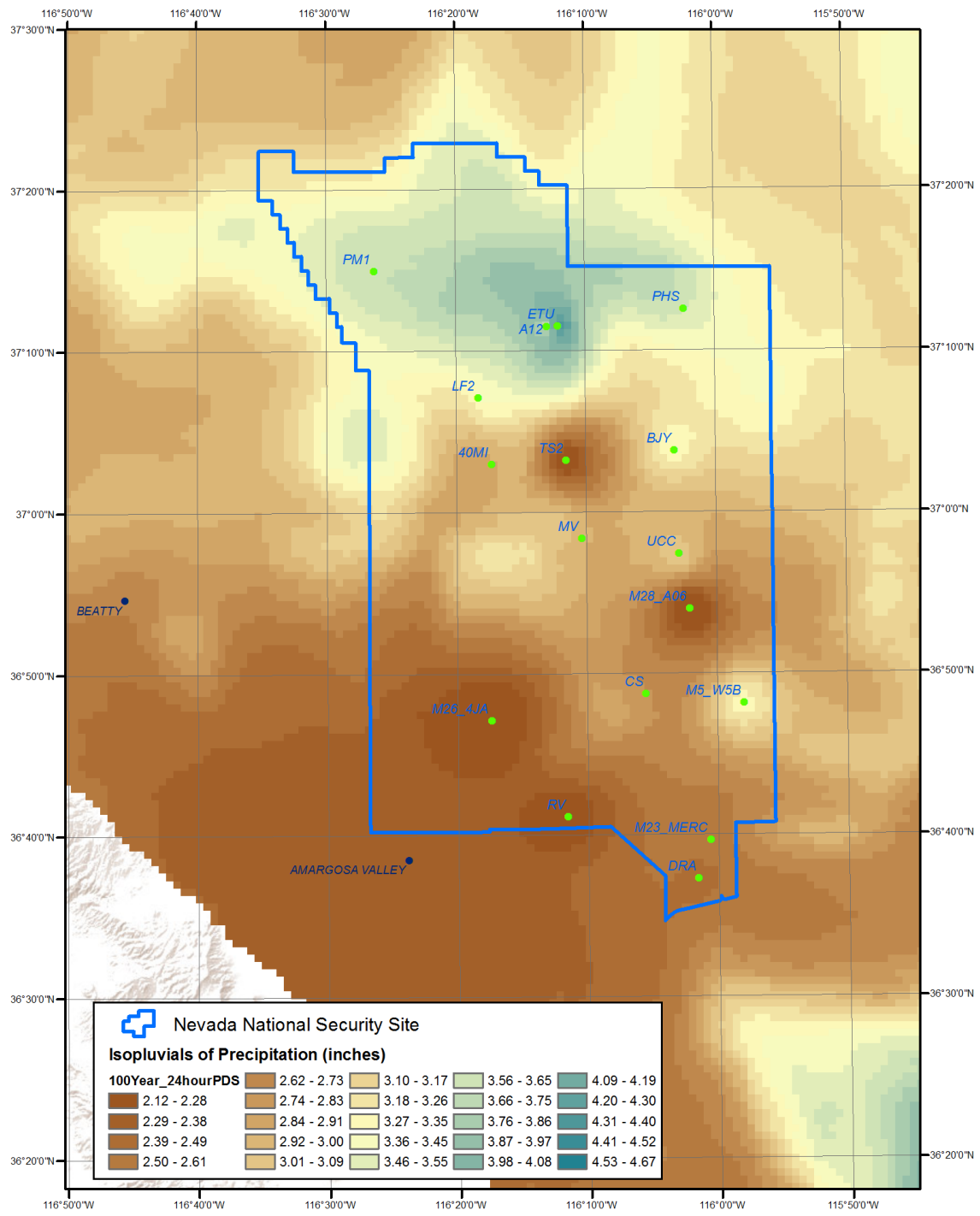


Figure 15B. PDS-based NNSS Precipitation Depth-Duration-Frequency Grid for the focused area: 100-yr, 24-hr.

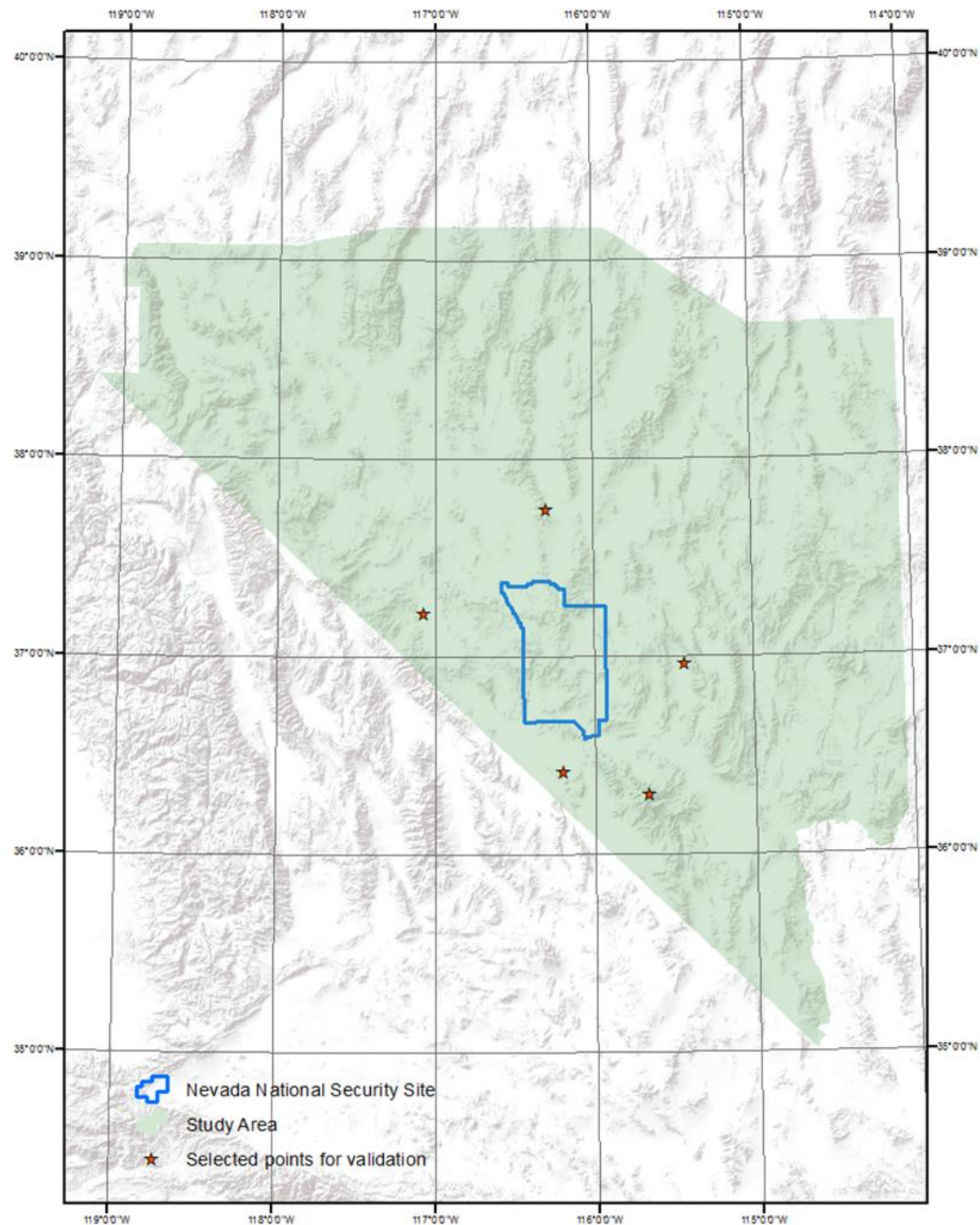


Figure 16. Selected off-NNSS locations used for validation.

SUMMARY OF THE RESULTS AND FINDINGS

This study produced the following results and findings. Supporting materials for the method and analysis can be found in the Appendix A.

1. The precipitation frequency (i.e., DDF) results for both the 2- and 100-yr return intervals for each of the 1-, 6-, and 24-hr durations were obtained for the NNSS precipitation gages through statistical analyses. The derived NNSS precipitation DDF values based on both the AMS and PDS datasets are included in Tables 3 and 4, respectively.
2. For the NNSS precipitation gages, the GEV and LogN probability distribution models were applied to the AMS datasets, whereas the LogN and LPIII probability distribution models were applied to the PDS datasets. These respective probability distributions were used to determine the 2- and 100-yr, 24-hr precipitation depths at each specific NNSS precipitation gage location. These precipitation depth results differed from those reported by the NOAA Atlas 14 (http://hdsc.nws.noaa.gov/hdsc/pfds/pfds_map_cont.html?bkmrk=nv) for the same locations, probably because the NNSS precipitation datasets were not incorporated into the NOAA Atlas 14 analyses; thus, the differences suggested that a site-specific analysis of the long-term NNSS precipitation gage records was necessary. The LogN distribution model was used to provide preliminary estimates for both the AMS and PDS datasets. However, it was found that using the GEV and LPIII probability distribution models for analyzing the AMS and PDS datasets, respectively, provided more reliable results.
3. Spatial patterns of the NNSS precipitation gage data are different from those of the Off-Site precipitation gage data, which reconfirmed the need to perform a site-specific study of precipitation frequency for the NNSS (Appendix A, *Spatial pattern of precipitation depths for both NNSS and Off-Site precipitation gage data*).
4. The effect of elevation on precipitation varies. On the NNSS, elevation is positively correlated to the annual average depth of precipitation, which is consistent with the findings of French (1983). However, there is basically no correlation between precipitation frequency (i.e., DDF data) and elevation on the NNSS when all NNSS precipitation gages were included in the analysis. When the dataset is pared to only precipitation gages with records longer than 15 years, a weak positive correlation was identified (Appendix A, *Elevation Effects*). In the areas surrounding the NNSS, there actually may be a negative trend between precipitation frequency and elevation, (i.e., precipitation depth of given durations and return intervals reduces with increasing elevation). Based on the varying trends across the study area, it was deemed that no corrections for elevation effects were necessary for the precipitation frequency analyses performed for the NNSS precipitation gages.
5. The 2- and 100-yr, 6-hr precipitation depths of the NNSS precipitation gages were obtained by applying the IDW interpolation method to both the NNSS precipitation gage 24-hr data and the Off-Site precipitation gage 6- and 24-hr data (Appendix A, *Estimation of 6-hr precipitation depths for NNSS gages*). Both AMS and PDS results were obtained and compared with the NOAA Atlas 14 estimates (Tables 3 and 4; Figures 2 and 3).

6. The 2- and 100-yr, 1-hr precipitation depths of the NNSS gages were obtained by applying the CCRFCD (1999) method, which calculates the 1-hr precipitation depth using the 6- and 24-hr data (Appendix A, *Estimation of 1-hr precipitation depths for NNSS gages*). Both AMS and PDS results were obtained and compared with the NOAA Atlas 14 estimates (Tables 3 and 4).
7. Grid maps (i.e., isopleth maps) of precipitation frequencies (2- and 100-yr return intervals; 1-, 6-, and 24-hr durations) for the NNSS area (Figures 4 through 15) were developed using the NOAA Atlas 14 approach for the AMS data and a modified approach for the PDS data. Only NNSS gages with 15 plus years of record were included in the final analysis (Appendix A, *Creating Precipitation Frequency Grids for the NNSS*).
8. To validate the gridded results, AMS and PDS precipitation frequency values in the grids at five arbitrarily selected locations surrounding the NNSS were compared with the corresponding NOAA Atlas 14 values (Figure 16). The difference between DDF values developed by this study and the NOAA Atlas 14 values were small, except for the large precipitation depths associated with 100-yr, 24-hr storms, for which the NOAA Atlas 14 predicted significantly larger values. These lower DDF values affected immediately adjacent areas when generating gridded data from point data (Appendix A, *Results Validation*).
9. At the majority of the NNSS precipitation gage locations, both the AMS and PDS 100-yr, 6-hr (typical design storm) DDF values from the NOAA Atlas 14 overestimate those values determined through site-specific analyses of the NNSS precipitation gage records (Figures 2 and 3).

REFERENCES

Bonnin, G.M., D. Martin, B. Lin, T. Parzybok, M. Yekta, and D. Riley, 2011. Precipitation-frequency atlas of the United States. NOAA atlas, 14, Volume 1, version 5.0.

Chow, V.T., D.R. Maidment, and L.W. Mays, 1988. Applied hydrology. McGraw-Hill, New York.

Clark County Regional Flood Control District, 1999. Hydrologic Criteria and Drainage Design Manual.

Daly, C., 2006. Guidelines for assessing the suitability of spatial climate data sets. *International journal of climatology*, 26(6), 707-721.

deRouhac, D., 2007. FreqPlot: Frequency Analysis Software.

French, R.H., 1983. A preliminary analysis of precipitation in southern Nevada. Water Resources Center, Desert Research Institute, University of Nevada System.

Pavlovic, S., 2015. PRISM MAM gridded data files (personal communication).

Schmeltzer, J.S., J.J. Miller, and D.L. Gustafson, 1993. Flood Assessment at a Low-Level Radioactive Waste Site in Southern Nevada. In *Engineering Hydrology* (proceedings), ed. C.Y. Kuo, American Society of Civil Engineers, San Francisco, California, July 25-30, 1993.

APPENDIX A

This appendix provides detailed descriptions of the approaches used in this study of the NNSS precipitation gage frequency analyses.

NNSS gage precipitation frequency analysis

This analysis was conducted using the observed daily (i.e., 24 hour) precipitation at 27 NNSS precipitation gages, the records of which were not included in the development of the National Oceanic and Atmospheric Administration (NOAA) Atlas 14 (Bonnin *et al.*, 2011) products. The daily precipitation data were analyzed based on a standard statistical approach for precipitation frequency analysis (Chow *et al.*, 1988) and the software FreqPlot (deRoulhac, 2007). Both Annual Maximum Series (AMS) and Partial Duration Series (PDS) were analyzed to derive the depth-duration-frequency (DDF) relationships for the 24-hr duration. Three probability distribution models were used in the frequency analysis to fit the precipitation data. The Generalized Extreme Value (GEV) model with a Gumbel distribution and Log-Normal (LogN) model were applied for the AMS, whereas the Log-Pearson Type III (LPIII) and LogN models were applied for the PDS dataset. Surrounding the NNSS area, thirteen precipitation gages (hereafter referred to as the “Off-Site precipitation gages”) were identified as having been used in the NOAA Atlas 14 analysis. These gages provided supplemental data for precipitation frequency analysis to the NNSS. These data, combined with the NNSS precipitation data, were subsequently used to develop the NNSS site-specific DDF estimates. Precipitation frequency data (both AMS-based and PDS-based) for Off-Site precipitation gages were obtained from the NOAA Atlas 14 (http://hdsc.nws.noaa.gov/hdsc/pfds/pfds_map_cont.html?bkmrk=nv, last accessed February 3, 2016). The NOAA Atlas 14 precipitation frequency data for the NNSS precipitation gage locations were also retrieved.

The 24-hr duration precipitation of 2-yr and 100-yr return intervals were compared in Figure A-1 and Figure A-2. For the 2-yr return interval AMS-based results of precipitation depth, the Off-Site precipitation gage values were comparable to the frequency analysis results of the NNSS precipitation gages using both the GEV and LogN probability distributions. For the NNSS precipitation gages where the GEV and LogN probability distributions produced much different results, the GEV values were closer to the Off-Site precipitation gage frequency results. However, the NOAA Atlas 14 values for the NNSS precipitation gages are much larger than that for the nearby Off-Site precipitation gages (Figure A-1a). For the 100-yr return interval AMS-based results, the NNSS precipitation gage values by both the GEV and LogN probability distributions are mostly larger than the Off-Site precipitation gage values, although the GEV values are relatively close to the Off-Site precipitation gage values. The Off-Site gage values are relatively homogeneous and the variance is comparable to the NNSS NOAA and GEV values, whereas the LogN values have much larger variance (Figure A-1b). A quantile comparison following the NOAA Atlas 14 approach (Bonnin *et al.*, 2011) shows that the GEV model better fits the observed data.

For the PDS-based results of 2-yr return interval, the NNSS gage values by all approaches are generally larger than the NOAA Atlas 14 estimates for the Off-Site precipitation gages. In many cases, the NOAA Atlas 14 estimates for the NNSS precipitation gages are larger than the values estimated by the LogN and LPIII models. For the PDS-based 100-yr results, the NNSS gage values obtained from the LogN and LPIII models are

comparable to the Off-Site precipitation gage values, whereas the NOAA Atlas 14 estimates for NNSS gages are significantly larger. In most cases, the LPIII model results for the NNSS precipitation gages are slightly larger than the LogN model results but the variance is larger than that of other results.

A quantile comparison following the NOAA Atlas 14 approach (Bonnin *et al.*, 2011) shows that the LogN model fitted the observed data slightly better than the other models. However, the LogN model resulted in larger inconsistency between the predicted PDS and AMS values. For the same return interval, PDS values are theoretically larger than the AMS values. However, as the LogN model predicted the opposite trend in all gages for the 100-year, 24-hr precipitation depths, the LPIII model for PDS values provided much more consistent results and thus is recommended for use.

According to the above analysis, the NOAA Atlas 14 estimates for the NNSS gages are likely not as accurate compared with the site-specific frequency analysis results based on the observed daily precipitation data. The GEV model is more suitable for the AMS data, whereas the LPIII model is more suitable for the PDS data. Therefore, the GEV and LPIII models were applied to the remaining AMS and PDS data analyses, respectively.

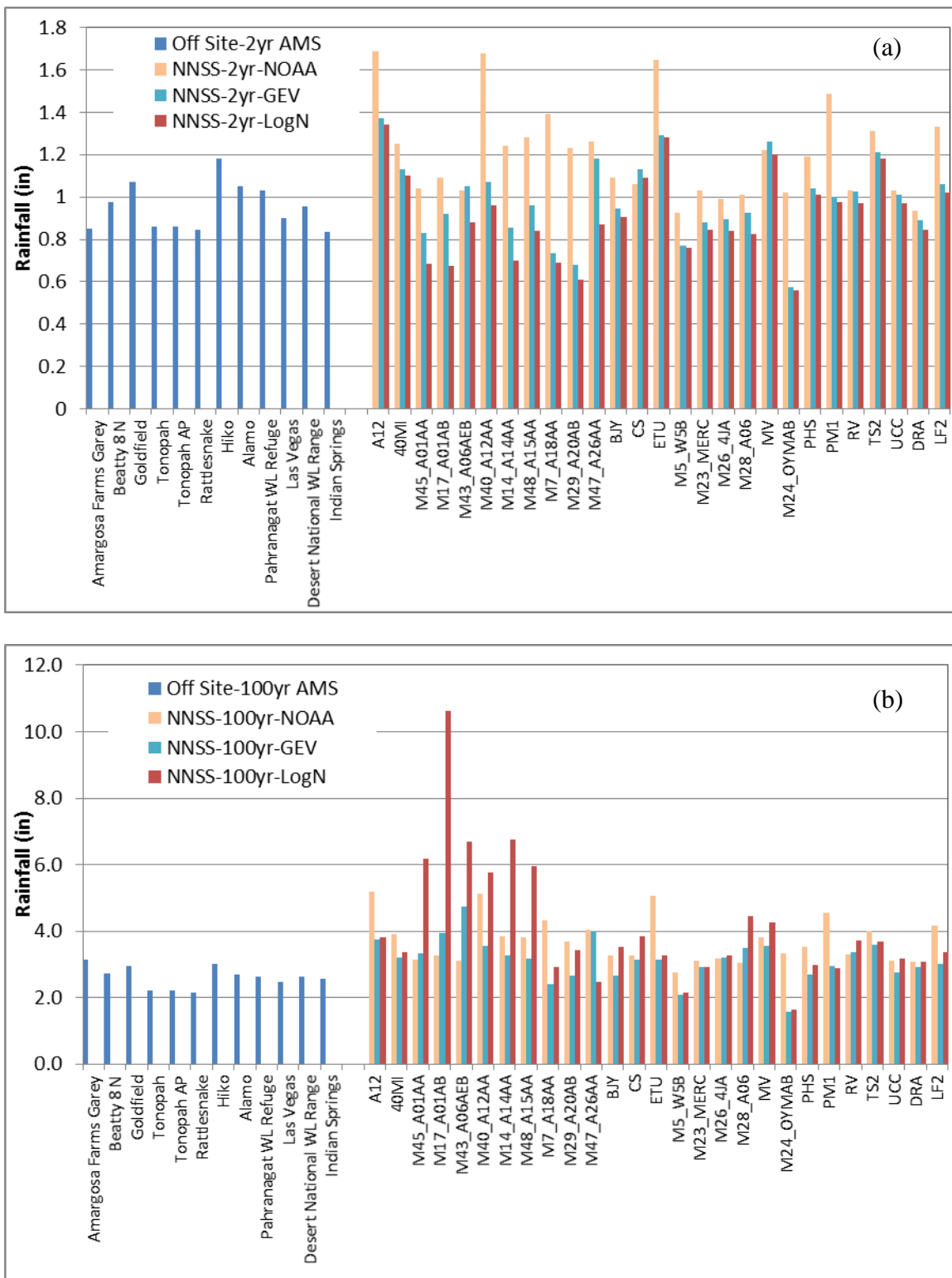


Figure A-1. Comparison of 24-hr duration AMS precipitation at NNSS gages and Off-Site gages: (a) 2-yr return interval; (b) 100-yr return interval.
(GEV = Generalized Extreme Value model; LogN = Log-Normal model)

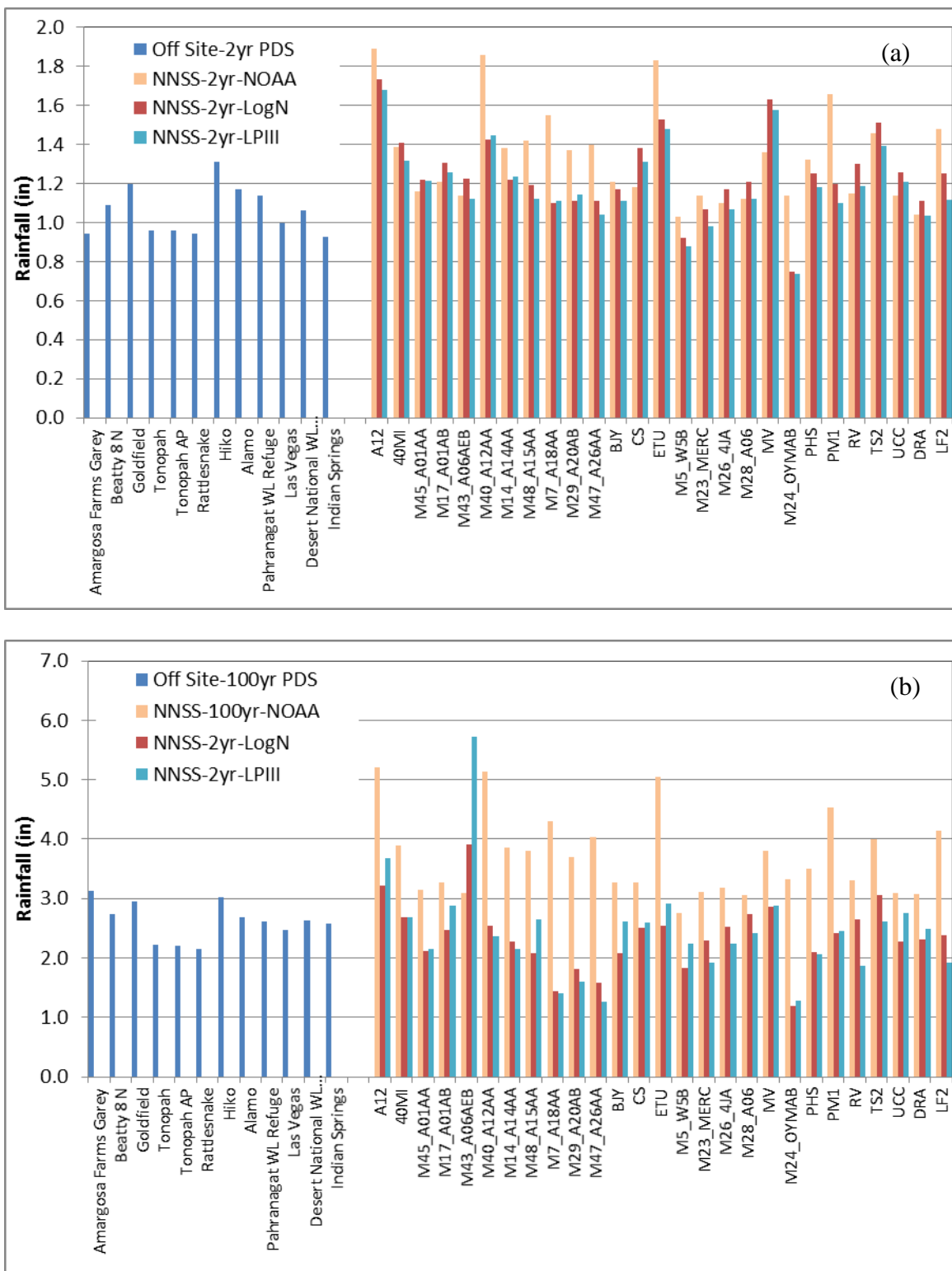


Figure A-2. Comparison of 24-hr duration PDS precipitation at NNSS and Off-Site precipitation gages: (a) 2-yr return interval; (b) 100-yr return interval
(LogN = Log-Normal model; LPIII = Log-Pearson Type III model)

Spatial pattern of precipitation depths for both NNSS and Off-Site precipitation gage data

To select better approaches for this study, the spatial patterns of the precipitation characteristics were analyzed for both the NNSS and Off-Site precipitation gage locations. The results of NNSS precipitation frequency analyses based on observed daily records from the NNSS precipitation gages (described above) and the NOAA Atlas 14 precipitation frequency values for the Off-Site precipitation gages were used in this analysis. Figures A-3a and A-3b show the spatial distributions of the AMS-based 24-hr precipitation depths of the Off-Site gages for 2- and 100-yr return intervals, respectively. In general, there is a positive gradient of precipitation depth from northwest to southeast in the area surrounded by the Off-Site gages. The spatial distributions of 24-hr AMS precipitation of the NNSS precipitation gages based on the GEV model are shown in Figure A-4a and A-4b. A comparison of the respective return interval graphics in Figures A-3 and A-4 shows different trends in precipitation between data recorded on the NNSS than at the surrounding Off-Site precipitation gages. Based on the NNSS precipitation gage records, the central area of the NNSS has higher AMS precipitation depths than the east and west zones of the NNSS, which is counter to the relationship between elevation and annual mean precipitation depth identified on the NNSS (French, 1983). Additionally, the NNSS precipitation gages have wider ranges of precipitation depths (lower minimum and higher maximum depths) than the ranges recorded at the Off-Site precipitation gages. These differences in the spatial patterns of precipitation both on and off of the NNSS indicates that producing precipitation frequency data for the NNSS from regional precipitation gage analysis without considering the actual NNSS precipitation gage data results in inaccuracies. Therefore, a site-specific analysis for NNSS precipitation frequency is necessary. These findings also need to be considered in the approach used to derive the 1-hr and 6-hr precipitation depths; however, a spatial interpolation using the 1-hr and 6-hr precipitation depths of Off-Site gages is not appropriate.

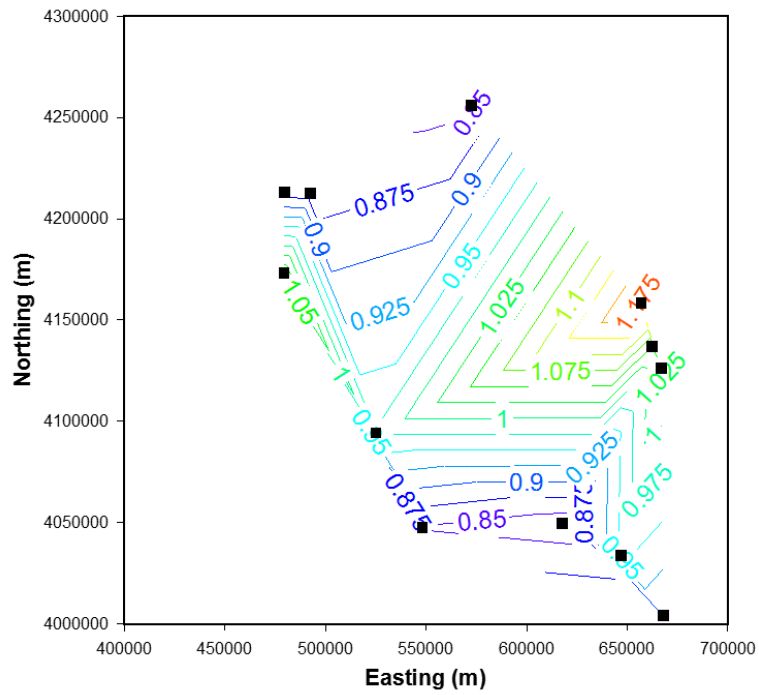


Figure A-3a. Spatial distribution of 2-yr, 24-hr AMS precipitation depths (inches) of Off-Site precipitation gages.

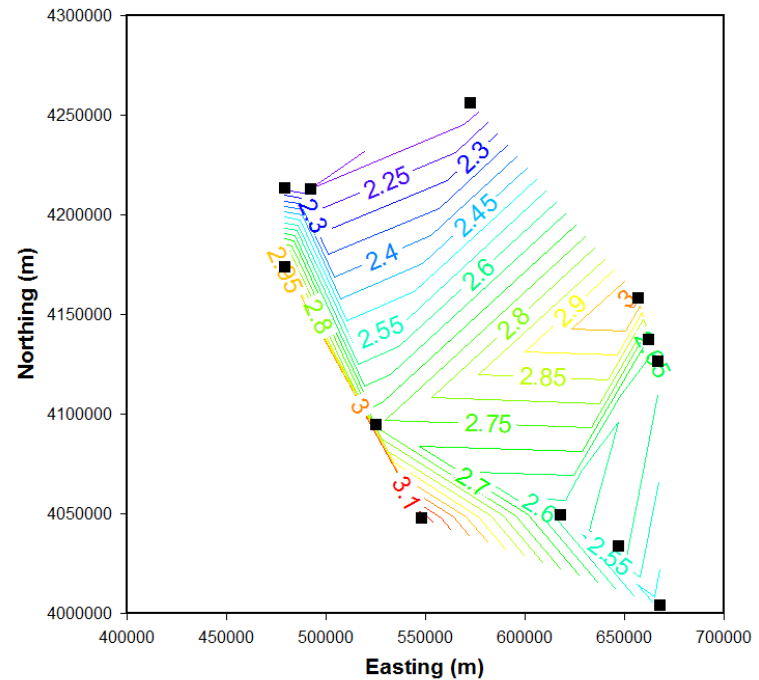


Figure A-3b. Spatial distribution of 100-yr, 24-hr AMS precipitation depths (inches) of Off-Site precipitation gages.

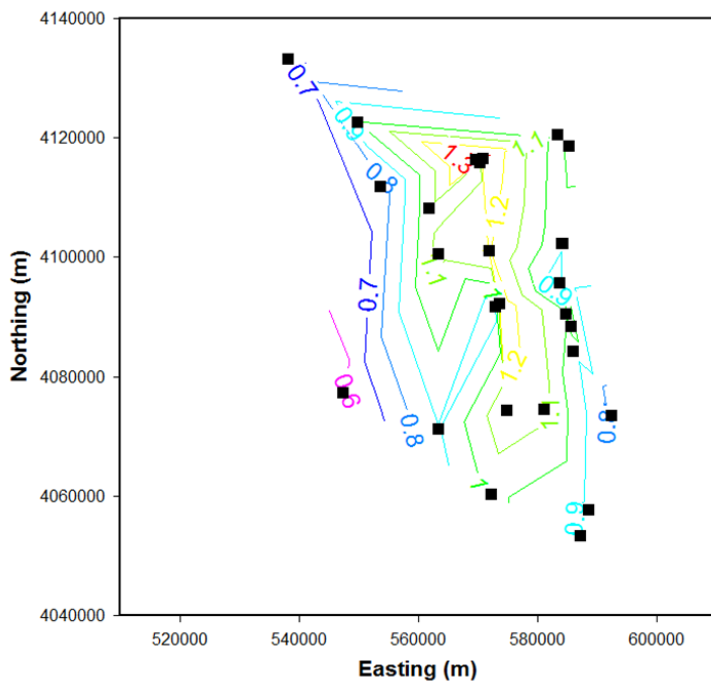


Figure A-4a. Spatial distribution of 2-yr, 24-hr AMS precipitation depths (inches) of the NNSS precipitation gages, based on the GEV model.

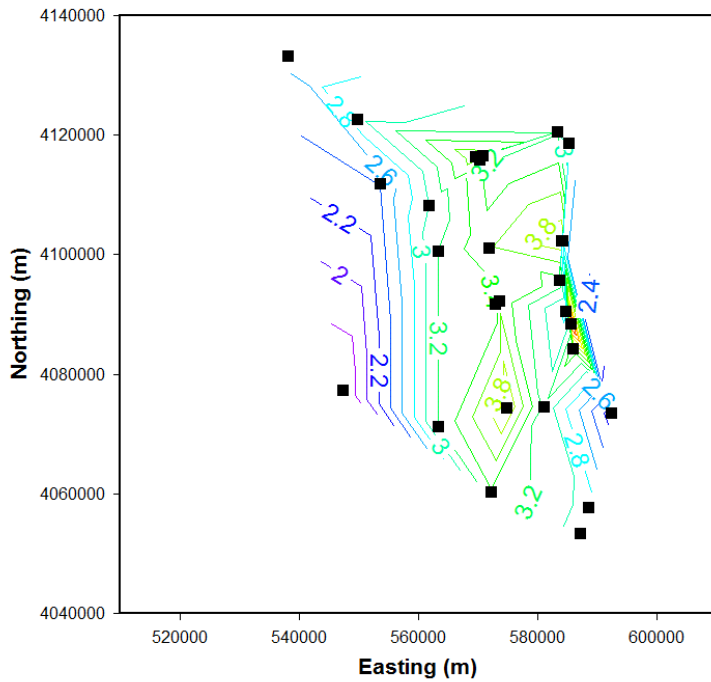


Figure A-4b. Spatial distribution of 100-yr, 24-hr AMS precipitation depths (inches) of the NNSS precipitation gages, based on the GEV model.

Elevation effects

It has been widely found that elevation can affect precipitation characteristics. To examine the elevation effect on the DDF relationships at the NNSS precipitation gages, correlations were made between the respective AMS and PDS precipitation depths and the elevations of both the Off-Site and NNSS precipitation gages. The results in Figures A-5a and A-5b show that in most cases, AMS precipitation depths and elevation are moderately correlated for Off-Site precipitation gages. The 100-yr AMS-based precipitation depths have a stronger negative correlation ($R^2=0.64$ with a p-value of 0.001 and $R^2=0.21$ with a p-value of 0.07 for 6- and 24-hr durations, respectively (Figures A-5a and A-5b) with gage elevation than the 2-yr AMS-based precipitation depths ($R^2=0.24$ with a p-value of 0.07 and $R^2=0.003$ with a p-value of 0.6 for 6- and 24-hr, respectively). Additionally, the 6-hr AMS precipitation depth has a stronger correlation with gage elevation than the 24-hr AMS precipitation depth. Only the 100-yr, 6-hr AMS precipitation depth has a strong correlation ($R^2=0.64$ and a p-value of 0.001) with elevation (Figure A-5a). The ratio of 6-hr AMS precipitation depth (P_6) and 24-hr AMS precipitation depth (P_{24}) for the Off-Site precipitation gages further illustrates this relationship. As shown in Figure A-5c, this ratio of both 100- and 2-yr return intervals is weakly correlated with elevation ($R^2 = 0.17$ with a p-value of 0.28 and $R^2 = 0.21$ with a p-value of 0.26, 100- and 2-yr, respectively), which indicates that the effect of elevation is not significant to the ratio, $r = P_6/P_{24}$. Additionally, the r trends (slopes of the regression functions) and r ranges (most values fall within 0.65-0.85) are similar for the 2- and 100-yr return intervals, which implies that the r ratio could be a useful parameter in further analysis for deriving the NNSS precipitation gage 1- and 6-hr precipitation depths.

For the NNSS precipitation gages, correlation between elevation and the 24-hr precipitation for both 2- and 100-yr return intervals were examined. The results (Figure A-5d) show that when all of the NNSS precipitation gages are included in the analysis, there is basically no correlation between elevation and 24-hr precipitation depths for the NNSS precipitation gages. Among the 27 NNSS precipitation gages analyzed, ten gages have less than 5 years of record, which are less likely to provide accurate statistics of long-term precipitation patterns, whereas the other seventeen NNSS precipitation gages have records longer than 15 years. Fifteen of these long-term precipitation gages on the NNSS have records longer than 30 years. If only the NNSS precipitation gages having records longer than 15 years are included, a weak to moderate correlation ($R^2 = 0.16$, with a p-value of 0.11) for 100-yr DDF can be found; however, a strong correlation ($R^2 = 0.57$, with a p-value of 0.0005) for 2-yr DDF can be found between precipitation frequency and elevation (Figure A-5e), similar to the annual average maximum precipitation values.

The elevation effect on annual average precipitation depth was also examined, which was found to be different from the elevation effect on precipitation frequencies. Figure A-6a shows a positive correlation ($R^2=0.55$, with a p-value of 1E-5) between the NNSS precipitation gage annual average precipitation depth and elevation (i.e., higher elevation areas receive more precipitation than lower elevation areas). This result is consistent with the conclusion of French (1983) for the NNSS. Figure A-6b also shows that the trend is more prominent (i.e., yielded higher correlation values: $R^2=0.73$, with a p-value of 1E-5) for the NNSS precipitation gages that have records longer than 15 years.

Based on the above analysis, the following points can be made. First, the elevation of a specific area affects the annual average precipitation (a measure of the total amount of precipitation). The higher the elevation, the greater the total average annual precipitation depth. Second, this effect does not extend to precipitation DDF. On the NNSS, the observed precipitation DDF is not sensitive to the variation of elevation (Figures A-5d and A-5e). And third, the data record length affects the analysis results. Data records from precipitation gages with shorter periods of record are not typically analyzed as the data are not representative of the long-term precipitation statistics of the area.

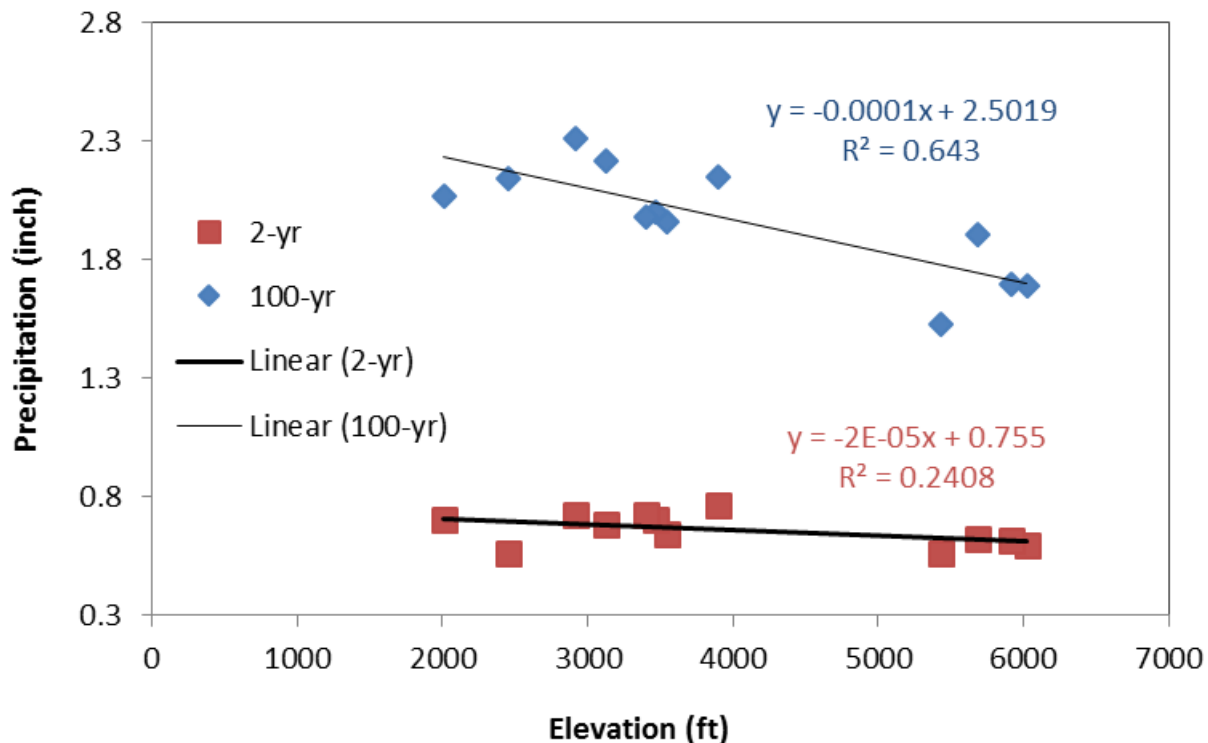


Figure A-5a. Precipitation-elevation correlation for the Off-Site precipitation gages: 6-hr AMS precipitation depths (inches).

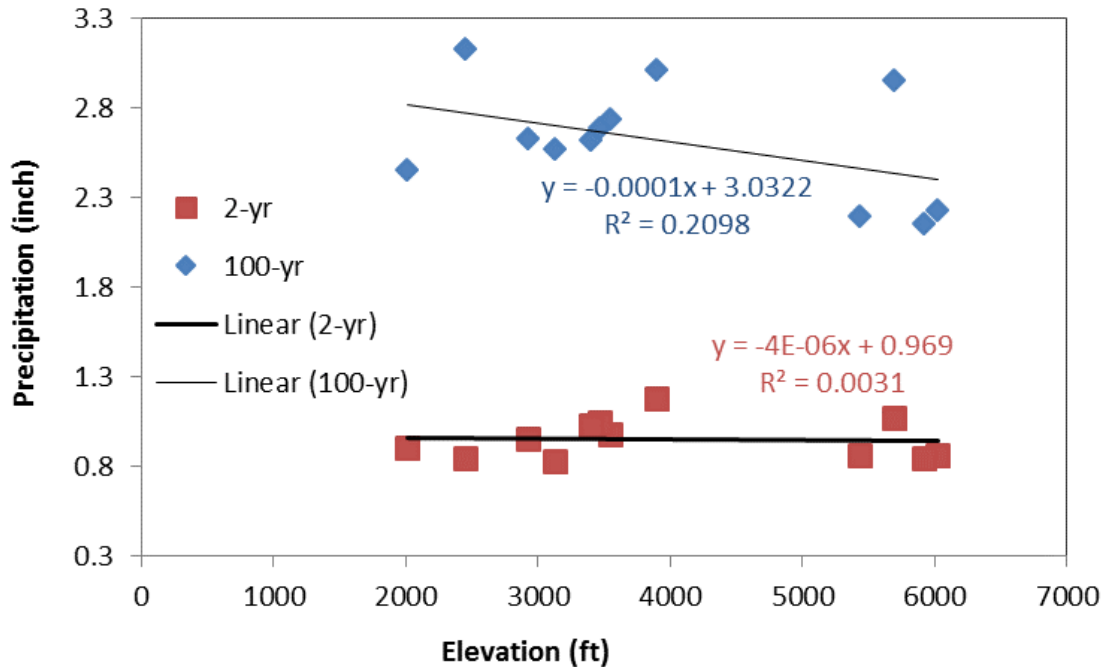


Figure A-5b. Precipitation-elevation correlation for the Off-Site precipitation gages: 24-hr AMS precipitation depths (inches).

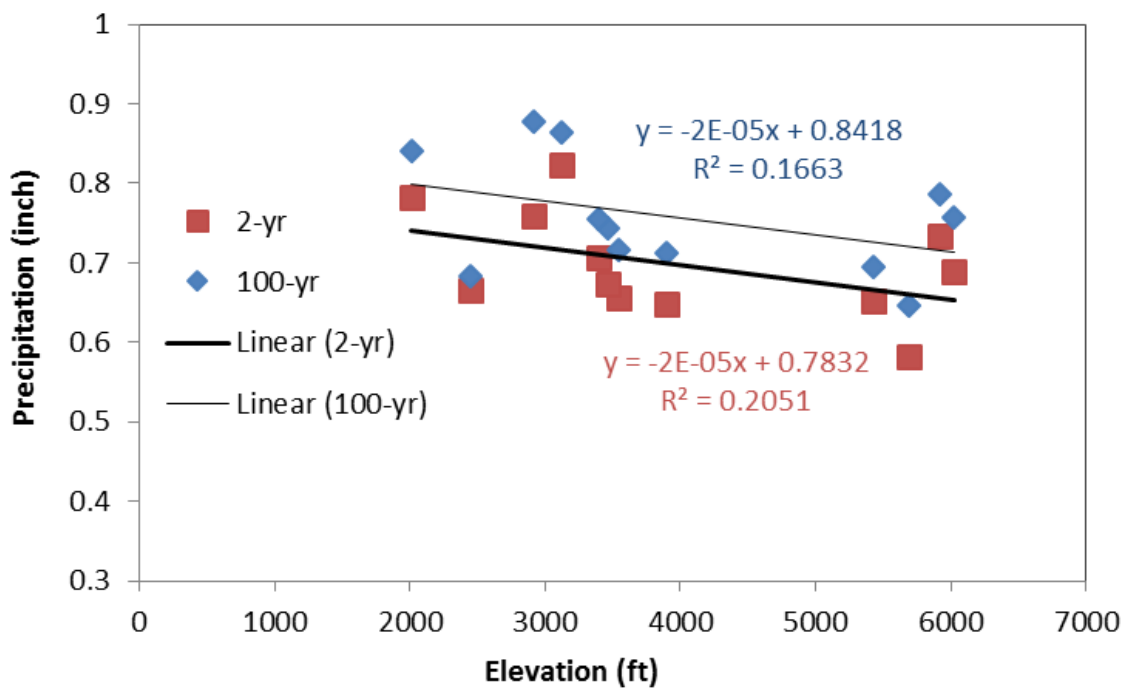


Figure A-5c. P6/P24 ratio-elevation correlation for the Off-Site precipitation gages: AMS precipitation depths (inches).

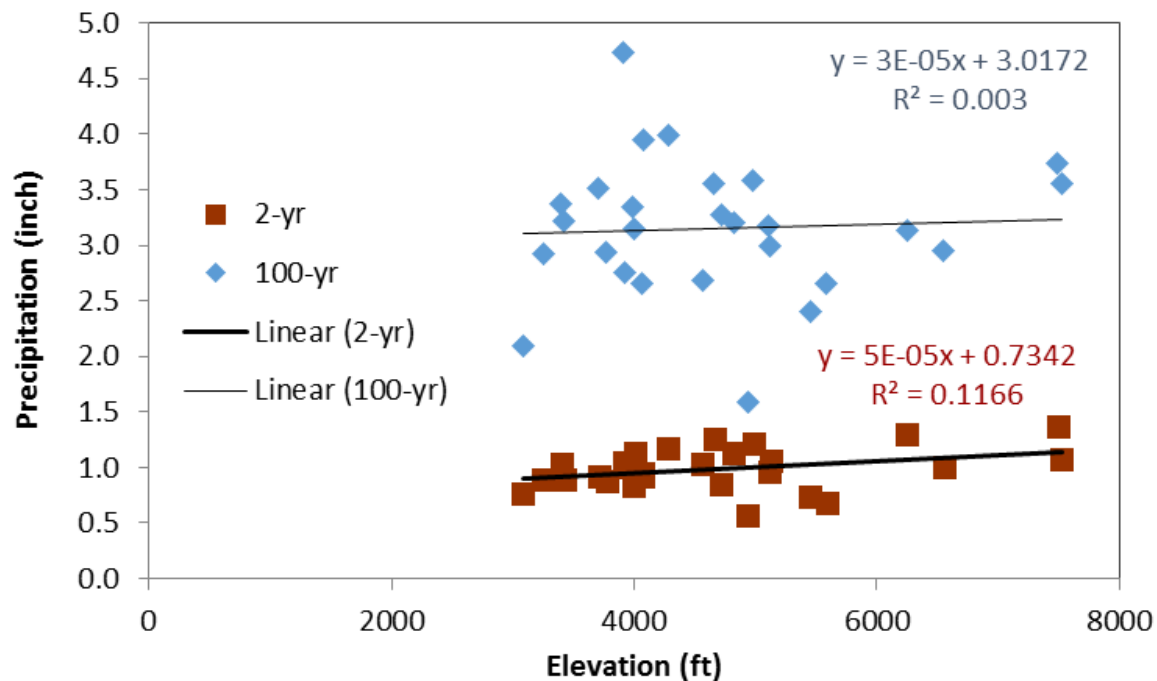


Figure A-5d. Precipitation-elevation correlation for the NNSS precipitation gages (all gages): 24-hr AMS precipitation depths (inches).

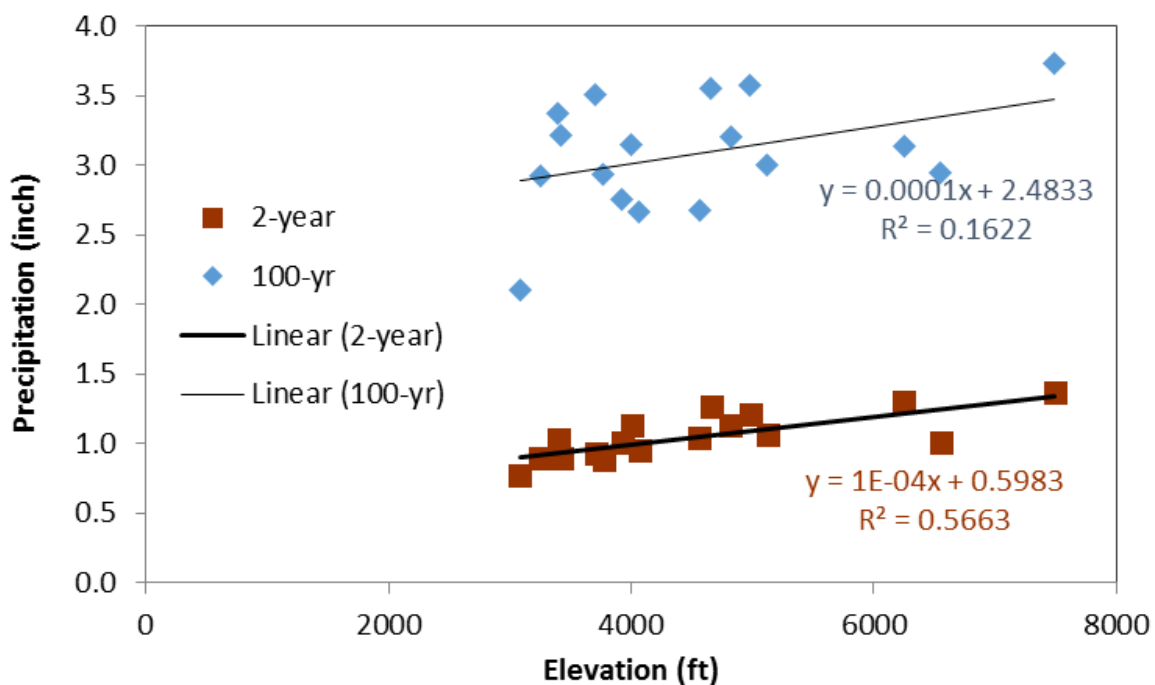


Figure A-5e. Precipitation-elevation correlation for the NNSS precipitation gages with 15+ years of records: 24-hr AMS precipitation depths (inches).

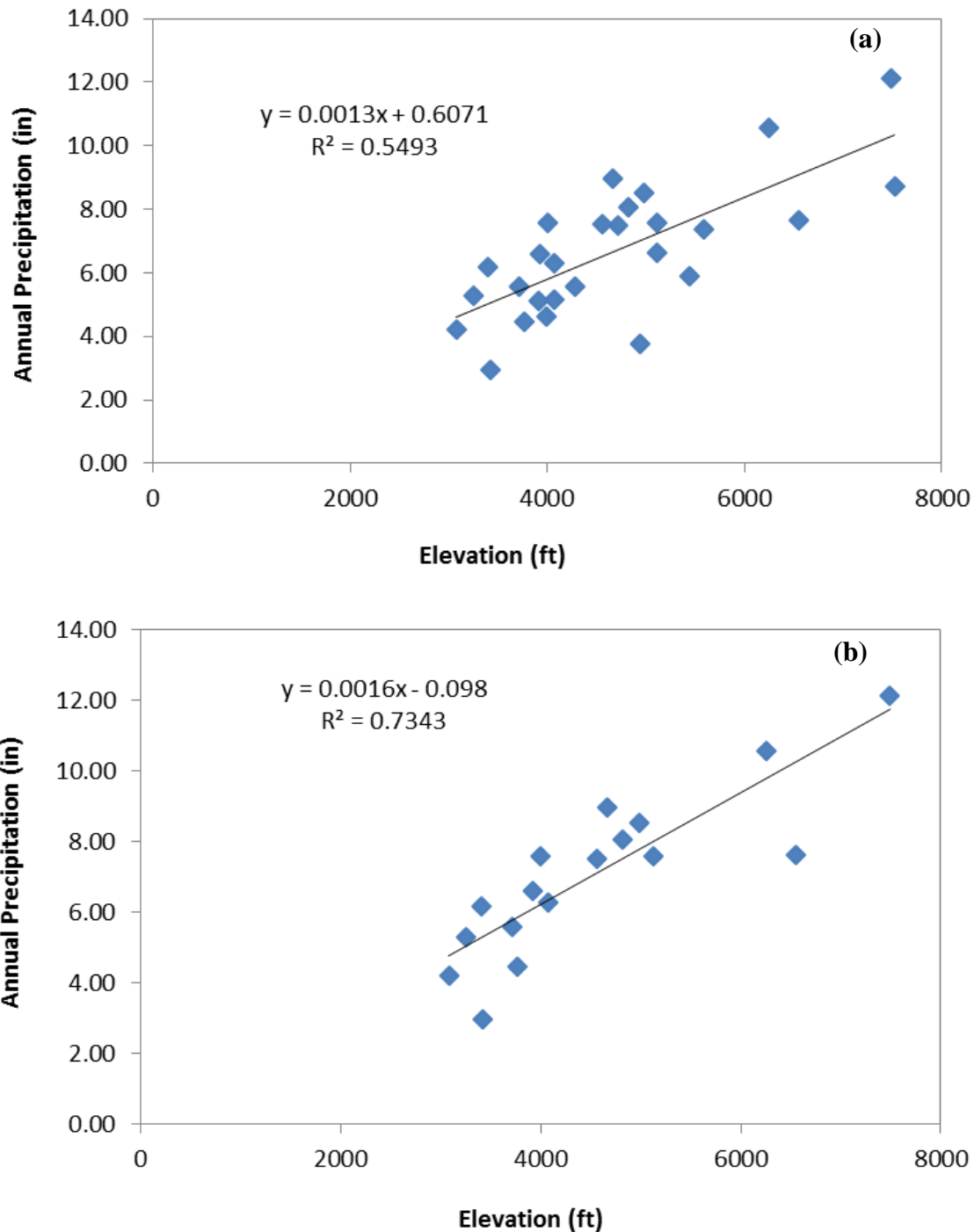


Figure A-6. NNSS annual mean precipitation-elevation correlation: (a) all NNSS precipitation gages; (b) NNSS precipitation gages with 15+ years of records.

Estimation of 6-hr precipitation depths for NNSS gages

To estimate the 6-hr precipitation of various return intervals for the NNSS gages for a given return interval, the ratio of 6- (P6) and 24-hr precipitation (P24) for the Off-Site precipitation gages was calculated. This ratio approach has been recognized to be useful, as the ratio of 1- or 6-hr values to corresponding 24-hr values for the same return period does not vary greatly over a small region and is therefore useful in smoothing the 1- and 6-hr isopluvials (CCRFC, 1999). Thus, it was assumed that the P6/P24 ratios for NNSS gages are spatially correlated to the Off-Site gages and therefore can be determined using spatial interpolation of the Off-Site precipitation gage P6/P24 ratios. The P6 values for the NNSS gages then can be calculated using the 24-hr precipitation depths obtained from analysis of the NNSS precipitation gage records in conjunction with the Off-Site precipitation gage P6/24 ratio values. The use of the P6/P24 ratio in the interpolation, rather than directly interpolating P6, mainly comes from the spatial patterns of the NNSS and Off-Site precipitation gage data. As the NNSS precipitation gage data have different spatial patterns and different minimum and maximum value ranges than the Off-Site precipitation gage data, directly interpolating P6 values for the NNSS precipitation gage from the 6-hr precipitation depths from the Off-Site precipitation gages would bias the intrinsic trend and narrow the value ranges of the NNSS precipitation gages. The resulting values are always within the range of interpolated values, and therefore interpolated 6-hr precipitation depths from the NNSS precipitation gages will definitely be located within the range of the Off-Site precipitation gage values. On the other hand, the P6/P24 ratio is always within the range of (0, 1) so that it will produce less bias. No correction for elevation is needed because the previous analysis showed that the ratio is not sensitive to elevation in the study area. Therefore, interpolating the ratio is a more reasonable choice for this study.

The P6/P24 ratio is calculated for both AMS and PDS data at the Off-Site precipitation gages. Spatial interpolation is implemented using the Inverse Distance Weighting (IDW) approach, which is described by the following equations:

$$u(\mathbf{x}) = \begin{cases} \frac{\sum_{i=1}^N w_i(\mathbf{x}) u_i}{\sum_{i=1}^N w_i(\mathbf{x})}, & \text{if } d(\mathbf{x}, \mathbf{x}_i) \neq 0 \text{ for all } i \\ u_i, & \text{if } d(\mathbf{x}, \mathbf{x}_i) = 0 \text{ for some } i \end{cases} \quad (1)$$

$$w_i(\mathbf{x}) = \frac{1}{d(\mathbf{x}, \mathbf{x}_i)^p} \quad w_i(\mathbf{x}) = \frac{1}{d(\mathbf{x}, \mathbf{x}_i)^p}$$

where $u(\mathbf{x})$ is the interpolation function for variable u ; u_i ($i = 1, N$) is the known value for variable u at point i ; \mathbf{x}_i denotes the coordinate of the interpolating point i ; \mathbf{x} is the spatial coordinate for an arbitrary (interpolated) point; $d(\mathbf{x}, \mathbf{x}_i)$ is the distance between \mathbf{x} and \mathbf{x}_i ; w_i is the weighting function for point i , based on distance d ; p is an exponent that determines the weighting function; $p = 2$ is Inverse Distance Square; $p = 1$ is Inverse Distance; and $p = 0$ represents the average of known points. A larger p value assigns greater influence to values closer to the interpolated point. For the case $p = 0$, p6/p24 ratios are equal for all interpolated gages.

The IDW interpolation of the P6/P24 ratio was conducted for $p = 2$, $= 1$, and $= 0$ at all of the NNSS precipitation gages using both the AMS and PDS precipitation data. For each p value, the weighting coefficients were calculated based on the distance between the interpolated NNSS precipitation gage and the Off-Site precipitation gage, according to Equation (1). These coefficients are the same for both the AMS and PDS datasets.

Estimation of 1-hr precipitation depths for NNSS gages

The 1-hr precipitation of 2- and 100-yr return intervals were calculated based on the following empirical equations developed by Clark County Regional Flood Control District (CCRFCD, 1999):

$$\begin{aligned} Y_2 &= -0.011 + 0.942[x_1 \cdot (x_1 / x_2)] \\ Y_{100} &= 0.494 + 0.755[x_3 \cdot (x_3 / x_4)] \end{aligned} \quad (2)$$

where Y_2 and Y_{100} are 1-hr precipitation values of 2- and 100-yr return intervals; x_1 is 2-yr, 6-hr precipitation; x_2 is 2-yr, 24-hr precipitation; x_3 is 100-yr, 6-hr precipitation; and x_4 is 100-yr, 24-hr precipitation.

The 1-hr precipitation for 2- and 100-yr return intervals were derived for all NNSS precipitation gages using both AMS and PDS data (Figure A-7). For different IDW interpolation approaches ($p = 2, 1, 0$), estimated 1-hr precipitation values are only slightly different. The maximum relative difference is 12 percent and most of the differences are less than 5 percent, which indicates that the result is not sensitive to the interpolation approaches. However, it is recommended that the result of inverse distance square ($p = 2$) interpolation approach is the most accurate and should be used. This is the most widely used approach and it better emphasizes the similarity of points at shorter distances.

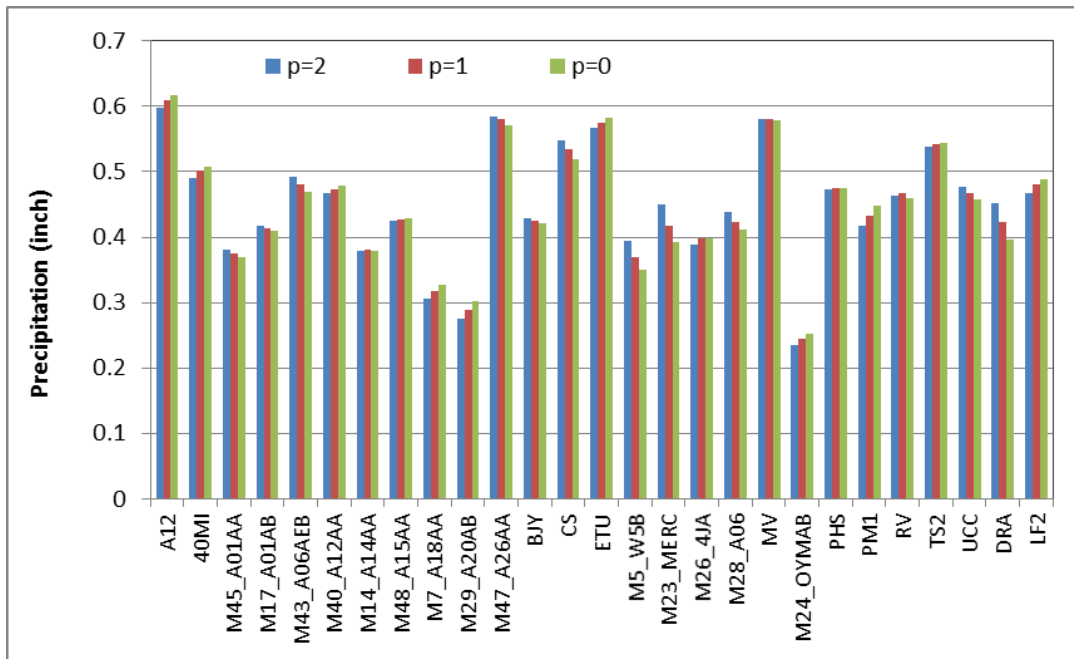


Figure A-7a. Calculated 2-yr, 1-hr AMS precipitation depths (inches) of NNSS precipitation gages, based on the GEV model results. The parameter p is the order of the IDW interpolation: $p = 2$ is Inverse Distance Square, $p = 1$ is Inverse Distance, and $p = 0$ is the average.

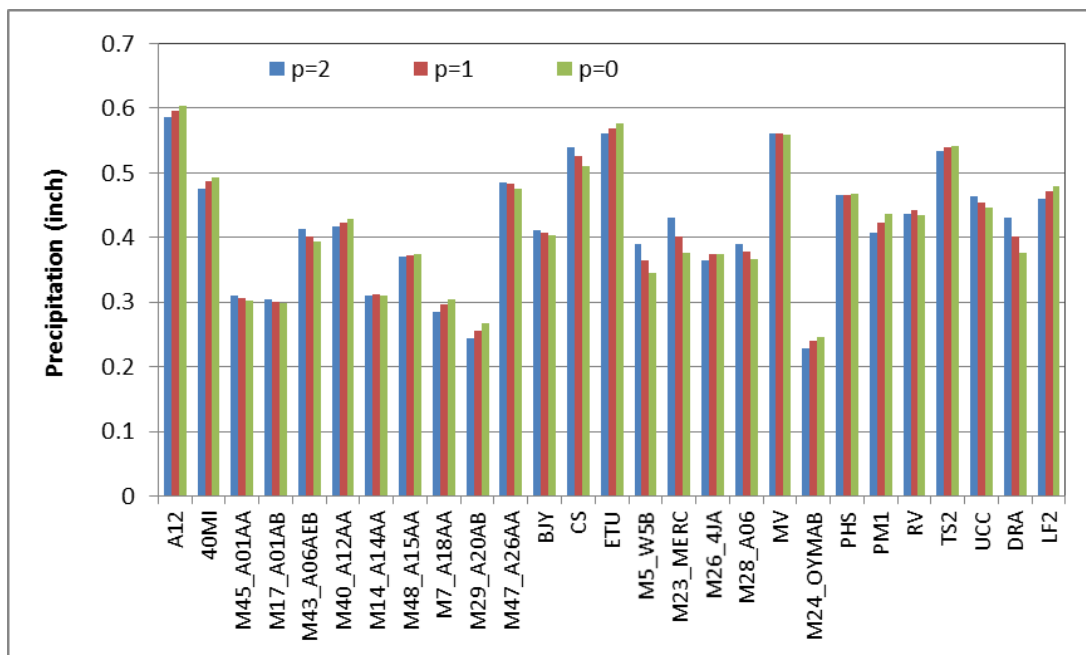


Figure A-7b. Calculated 2-yr, 1-hr AMS precipitation depths (inches) of NNSS precipitation gages, based on the LogN model results. The parameter p is the order of the IDW interpolation: $p = 2$ is Inverse Distance Square, $p = 1$ is Inverse Distance, and $p = 0$ is the average.

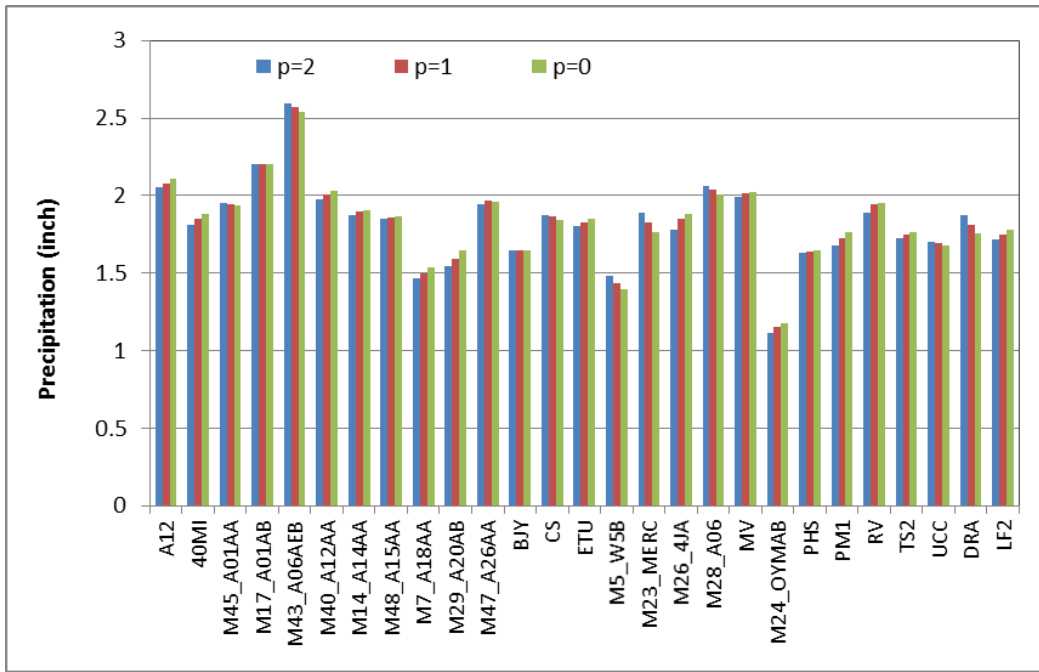


Figure A-7c. Calculated 100-yr, 1-hr AMS precipitation depths (inches) of NNSS precipitation gages based on the GEV model results. The parameter p is the order of the IDW interpolation: $p = 2$ is Inverse Distance Square, $p = 1$ is Inverse Distance, and $p = 0$ is the average.

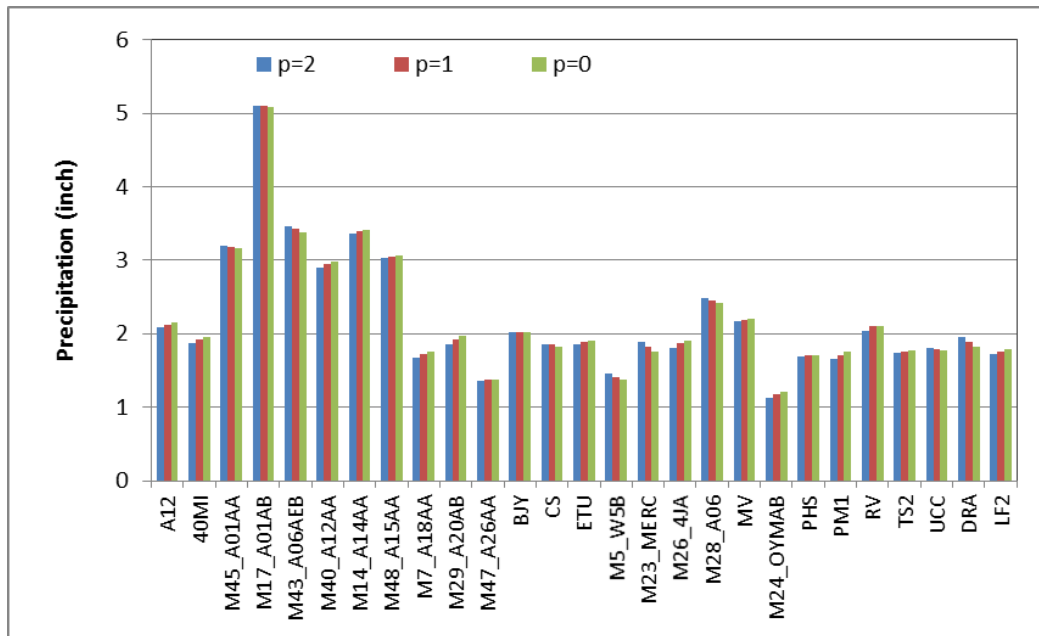


Figure A-7d. Calculated 100-yr, 1-hr AMS precipitation depths (inches) of NNSS precipitation gages based on the LogN model results. The parameter p is the order of the IDW interpolation: $p = 2$ is Inverse Distance Square, $p = 1$ is Inverse Distance, and $p = 0$ is the average.

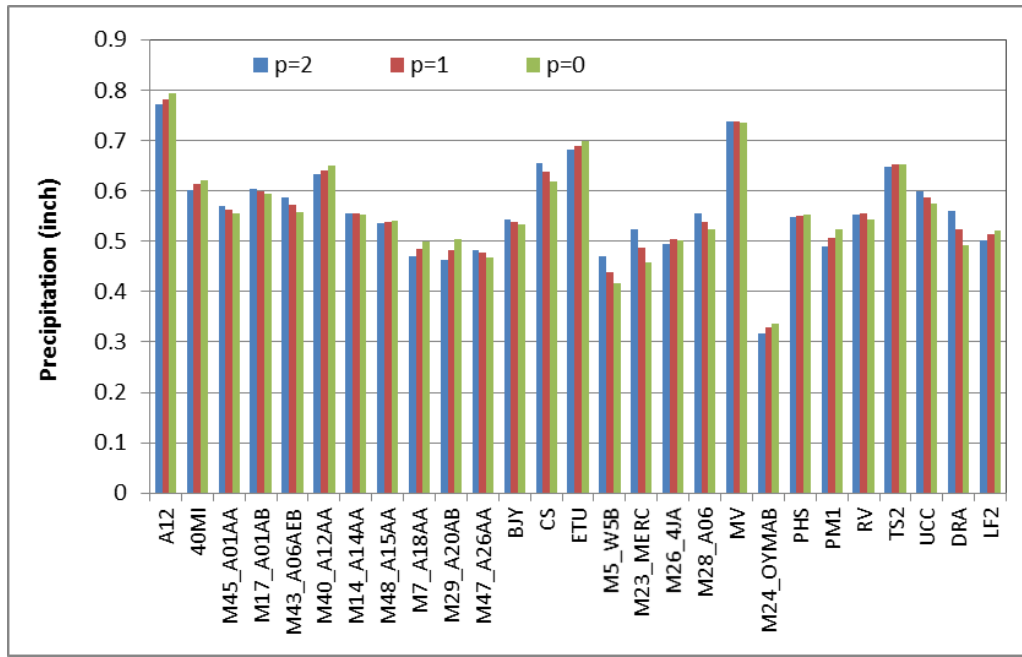


Figure A-7e. Calculated 2-yr, 1-hr PDS precipitation depths (inches) of the NNSS precipitation gages based on the LogN model results. The parameter p is the order of the IDW interpolation: $p = 2$ is Inverse Distance Square, $p = 1$ is Inverse Distance, and $p = 0$ is the average.

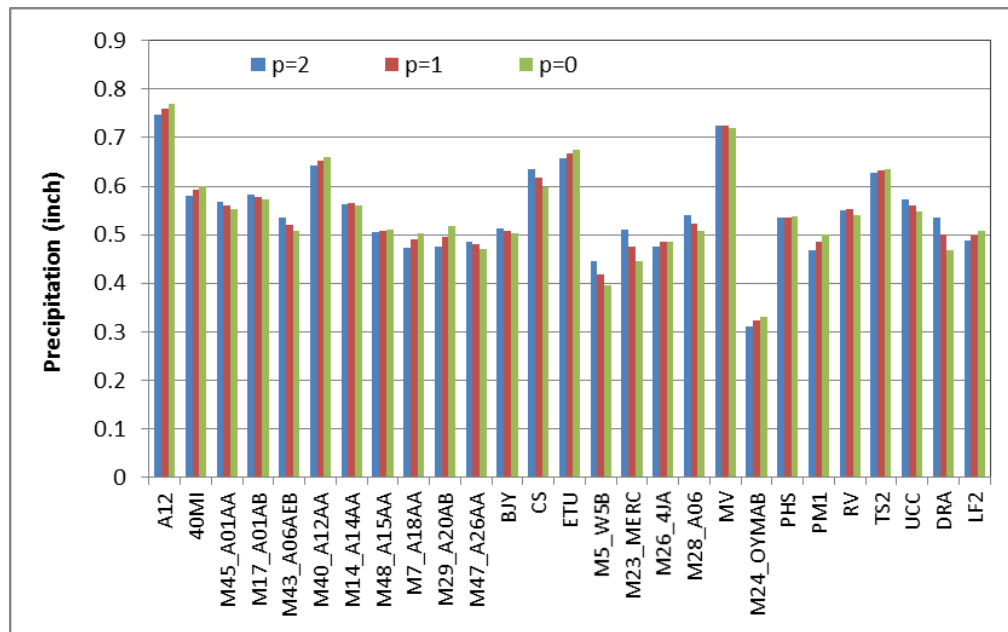


Figure A-7f. Calculated 2-yr, 1-hr PDS precipitation depths (inches) of the NNSS precipitation gages based on the LPIII model results. The parameter p is the order of the IDW interpolation: $p = 2$ is Inverse Distance Square, $p = 1$ is Inverse Distance, and $p = 0$ is the average.

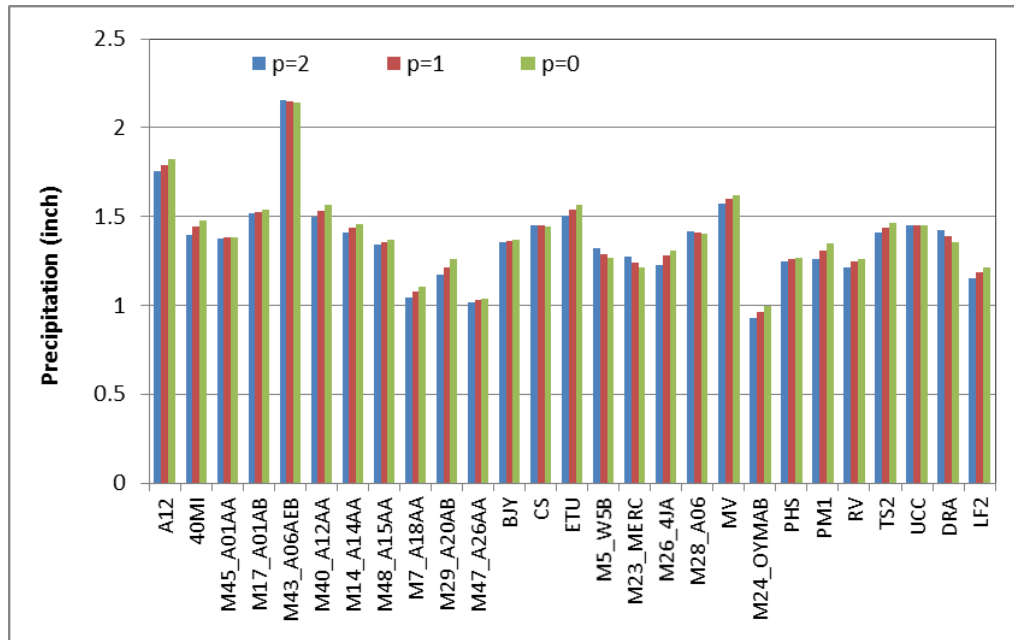


Figure A-7g. Calculated 100-yr, 1-hr PDS precipitation depths (inches) of the NNSS precipitation gages based on the LogN model results. The parameter p is the order of the IDW interpolation: $p = 2$ is Inverse Distance Square, $p = 1$ is Inverse Distance, and $p = 0$ is the average.

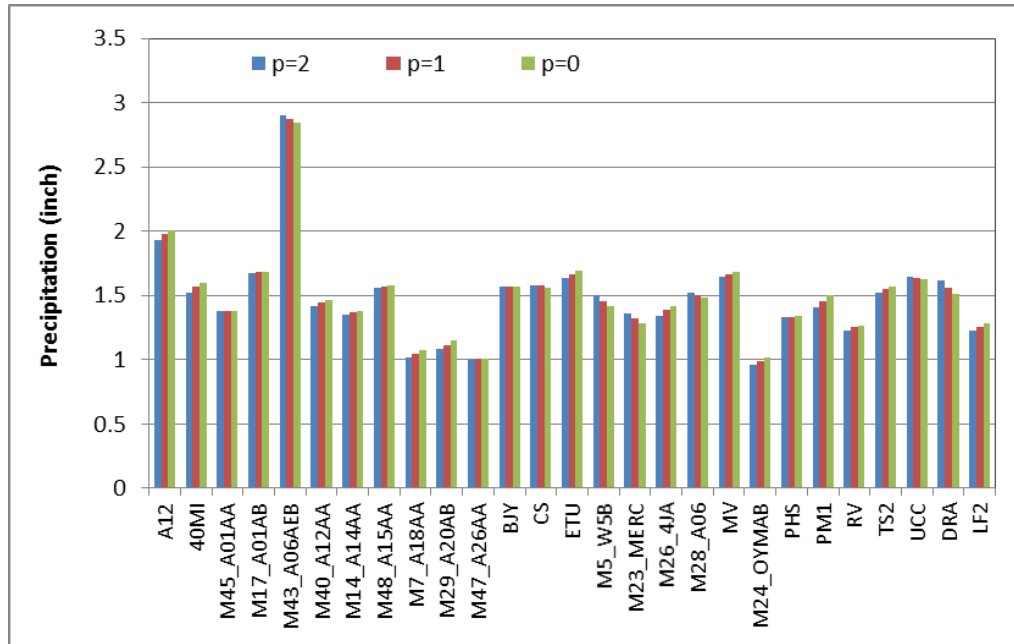


Figure A-7h. Calculated 100-yr, 1-hr PDS precipitation depths (inches) of the NNSS precipitation gages based on the LPIII model results. The parameter p is the order of the IDW interpolation: $p = 2$ is Inverse Distance Square, $p = 1$ is Inverse Distance, and $p = 0$ is the average.

Creating Precipitation Frequency Grids for the NNSS

A precipitation frequency grid can be produced by interpolating point precipitation frequency values into spatially continuous values. The NOAA Atlas 14 has presented a sophisticated approach for this purpose. The approach is based on the PRISM Mean Annual Maximum (MAM) precipitation grid that produced by the PRISM group (Daly, 2006) at a grid resolution of 800 m. By correlating the precipitation gage frequency values to MAM grid, the frequency grid can be generated. In this study, this approach was used to generate precipitation frequency grids for the NNSS (Figures A-8-1A through A-8-12B). The following procedures were applied to develop both the AMS and PDS grids:

1. Build area boundary
 - a. Use the lower five counties of Nevada to create the boundary of the study area covering the entire NNSS and all Off-Site precipitation gages that were used in this study
 - b. Clip the PRISM Mean Annual Maximum (MAM) grids provided by NOAA to the boundary of the concerned area
2. Extract point values from PRISM MAM grid
 - a. Extract values at the NNSS and Off-Site precipitation gage locations from the PRISM MAM 1-hr, 6-hr, and 24-hr grids using ArcGIS Toolbox
3. Build Initial grids
 - a. Use the frequency values derived from observed data at NNSS precipitation gages and PRISM MAM data at the same locations to develop correlations between frequencies and MAM (e.g., 24-hr, 100-yr precipitation and MAM relationship)
 - b. Build the Initial grid (e.g., 24-hr, 100-yr precipitation) based on the regression relationships
4. Build Residual Grids
 - a. Calculate the residual (actual minus predicted) frequency values at the precipitation gage locations
 - b. Normalize the residual by dividing by the MAM values
 - c. Create the normalized residual grid by spatially interpolating the normalized residual values using the inverse distance weighting
 - d. Multiply the normalized residual grid by the MAM grid to produce the actual residual grid
 - e. Add the actual residual grid to the initial grid to obtain the pre-final grid
5. Filtering
 - a. Apply 3×3 cell block filter to reduce noise and smooth the grid. This is the predictor grid.

6. Quality check for Internal Consistency (IC)

- a. Check if the duration-based IC is maintained by making sure that the next lower duration grid at the same frequency is smaller (e.g., $P_{2y6h} < P_{2y24h}$). For grid cells violating this rule, adjust the lower duration grid value by setting the grid cell equal to the next longer duration minus one percent.
- b. Check if the frequency-based IC is maintained by making sure that the next higher frequency grid of the same duration is smaller (e.g., $P_{100y24h} > P_{2y24h}$). For grid cells violating this rule, adjust the value by setting the grid cell equal to the next higher frequency plus one percent.

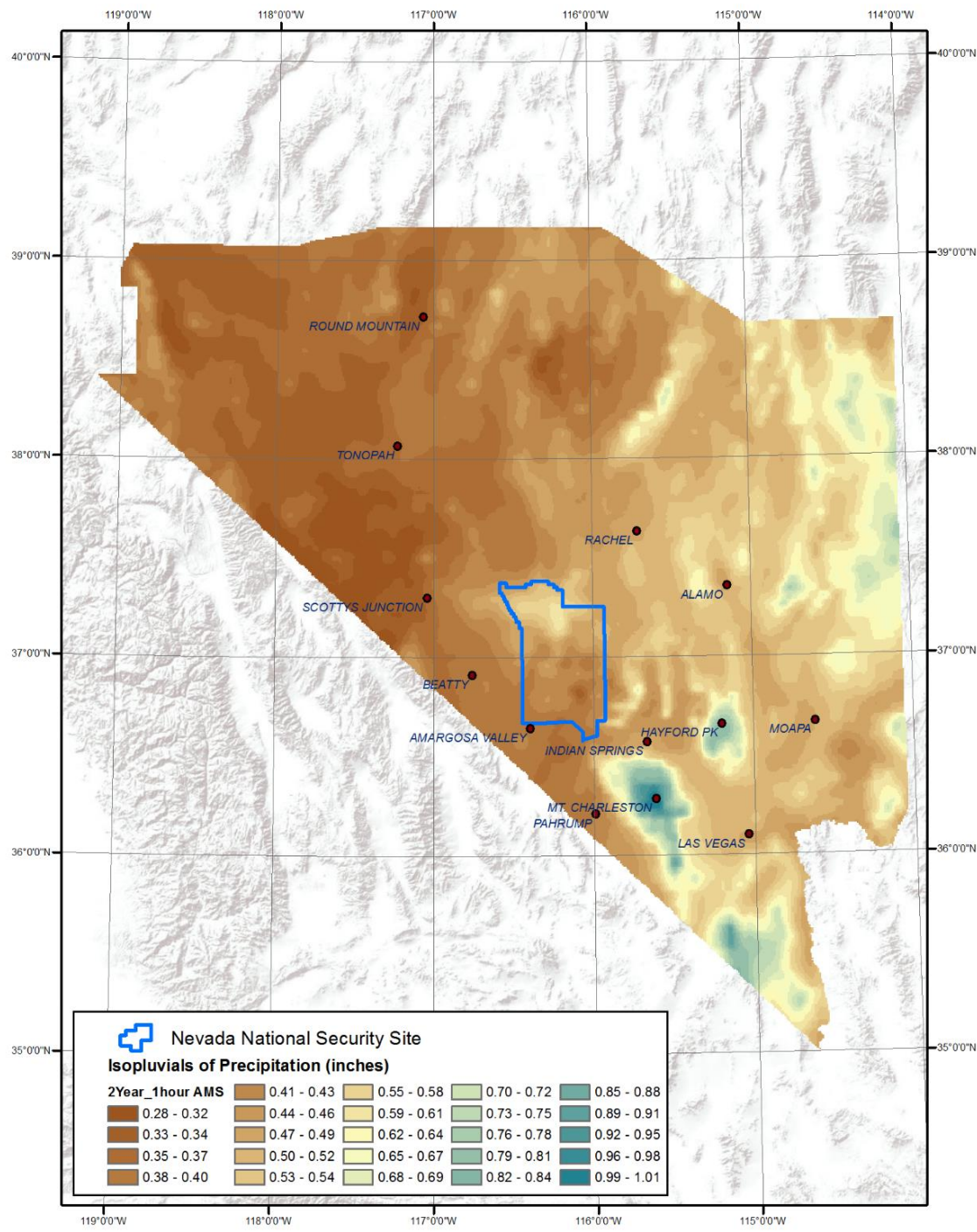


Figure A-8-1A. AMS-based NNSS Precipitation Depth-Duration-Frequency Grid: 2-yr, 1-hr.

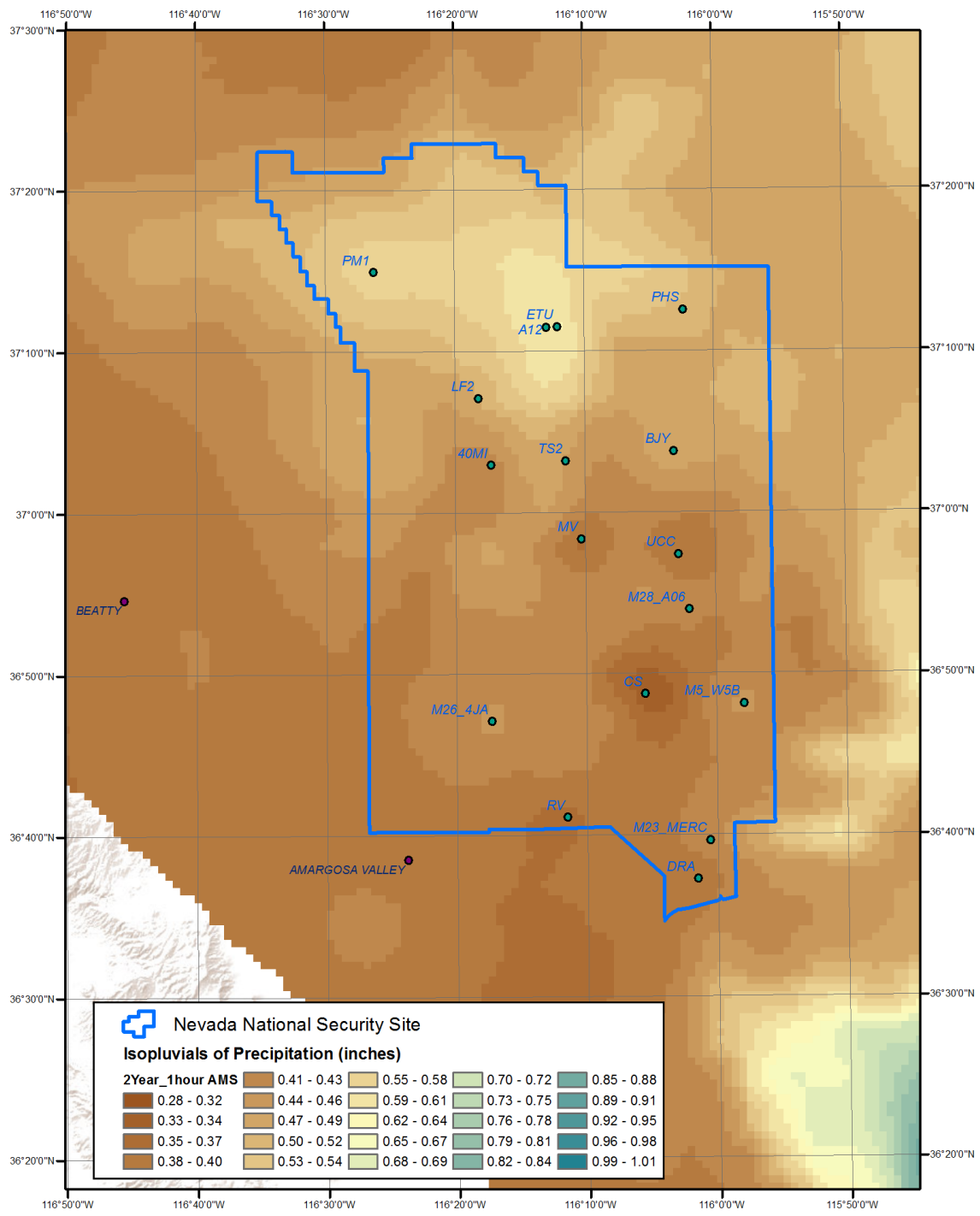


Figure A-8-1B. AMS-based NNSS Precipitation Depth-Duration-Frequency Grid for the focused area: 2-yr, 1-hr.

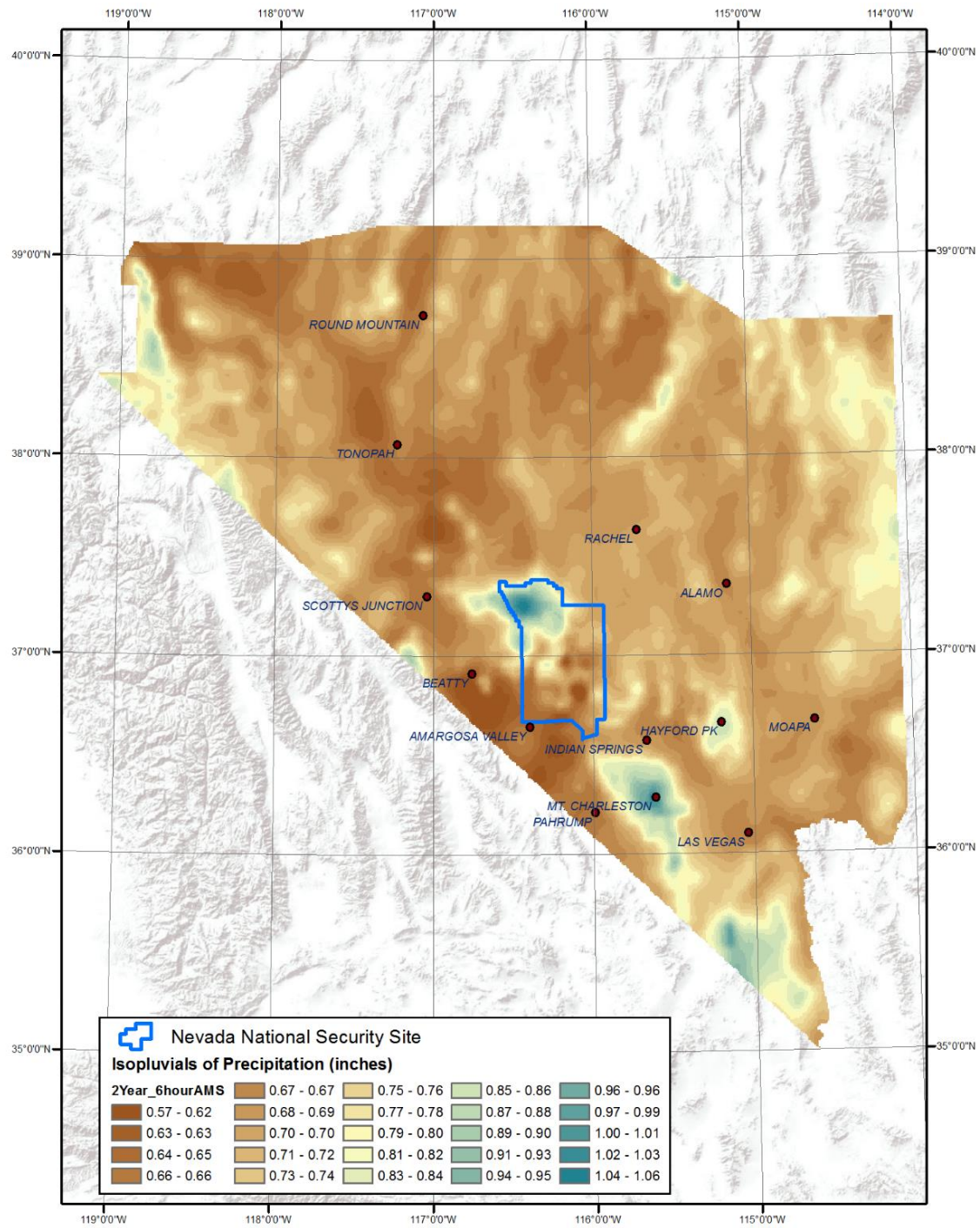


Figure A-8-2A. AMS-based NNSS Precipitation Depth-Duration-Frequency Grid: 2-yr, 6-hr.

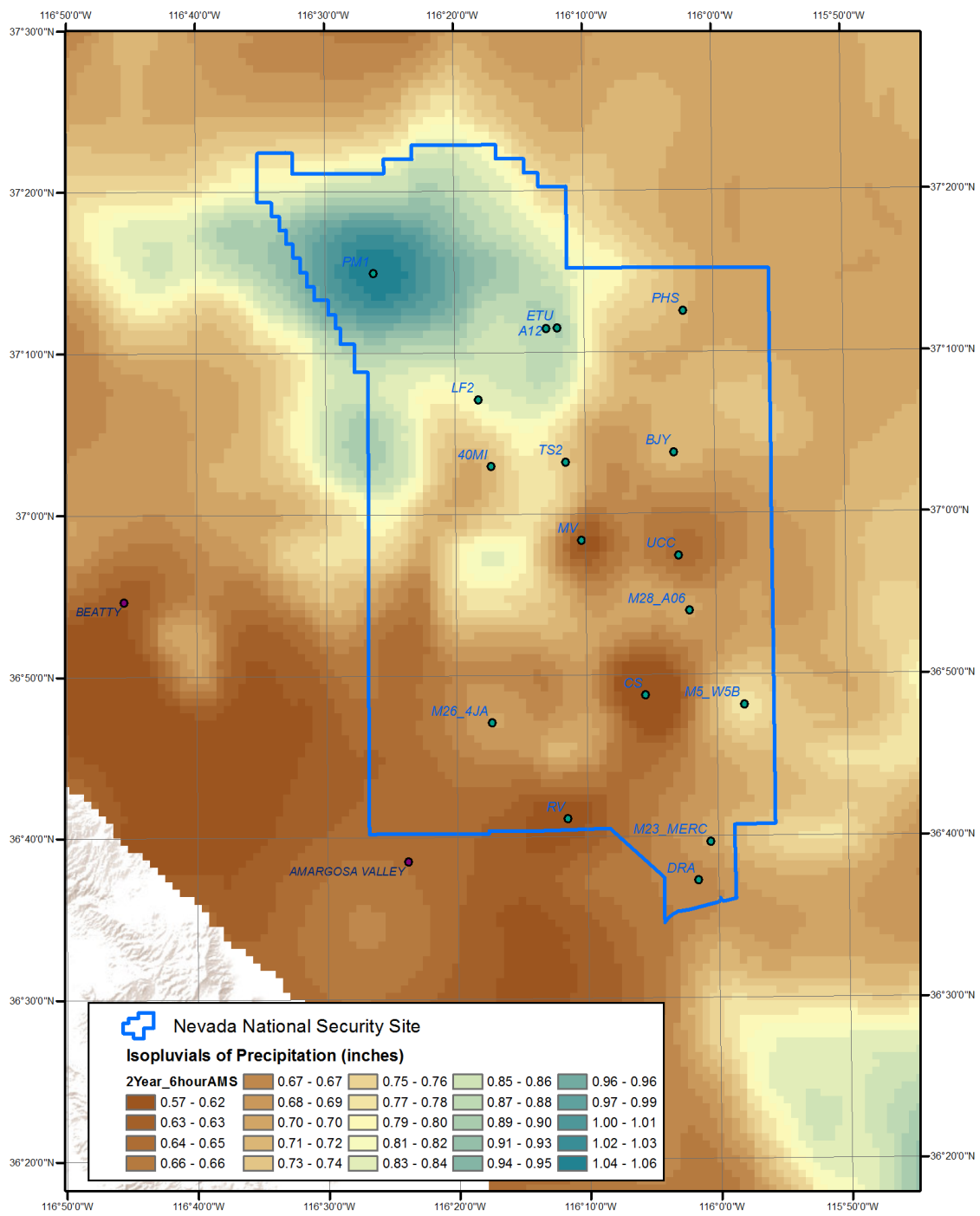


Figure A-8-2B. AMS-based NNSS Precipitation Depth-Duration-Frequency Grid for the focused area: 2-yr, 6-hr.

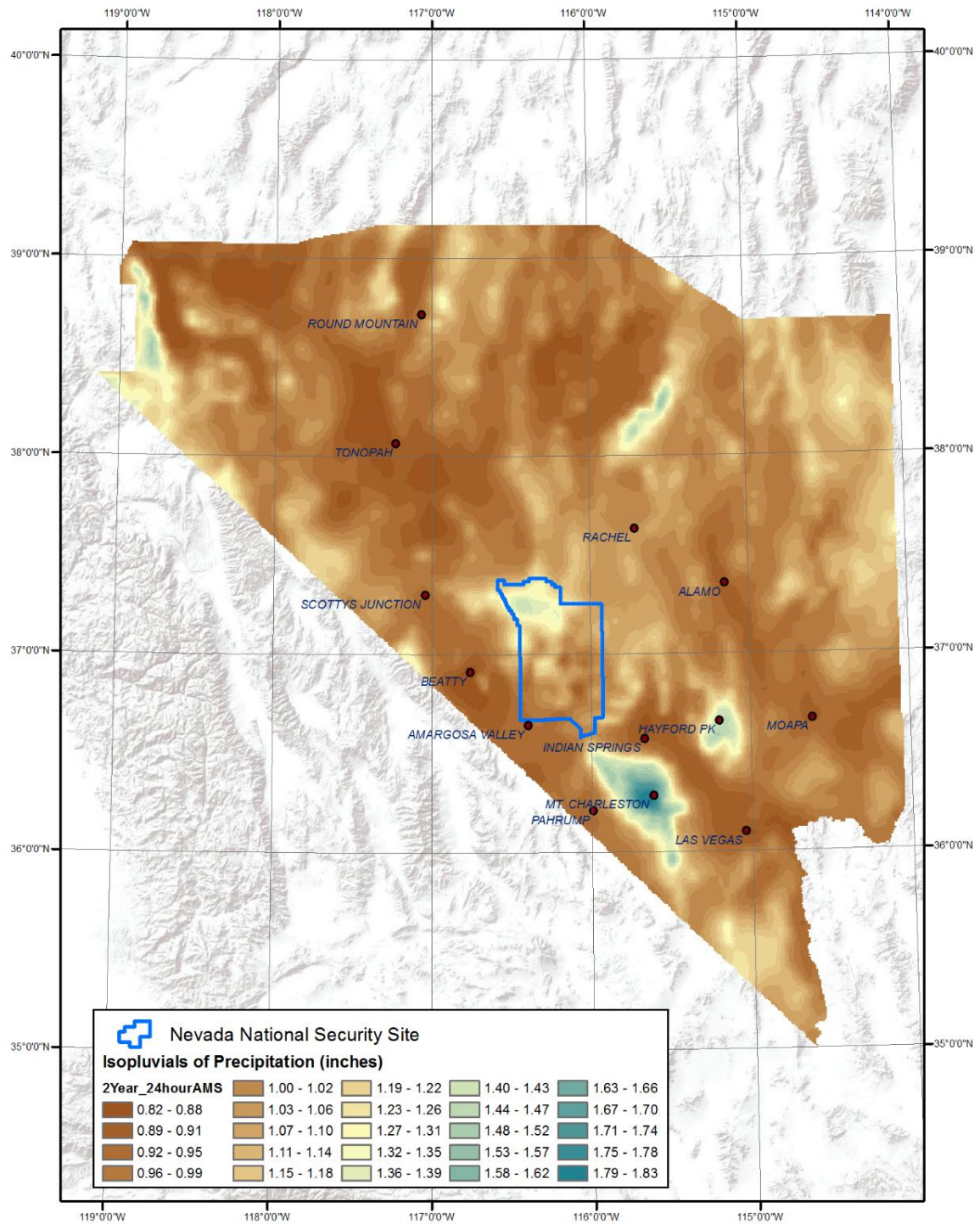


Figure A-8-3A. AMS-based NNSS Precipitation Depth-Duration-Frequency Grid: 2-yr, 24-hr.

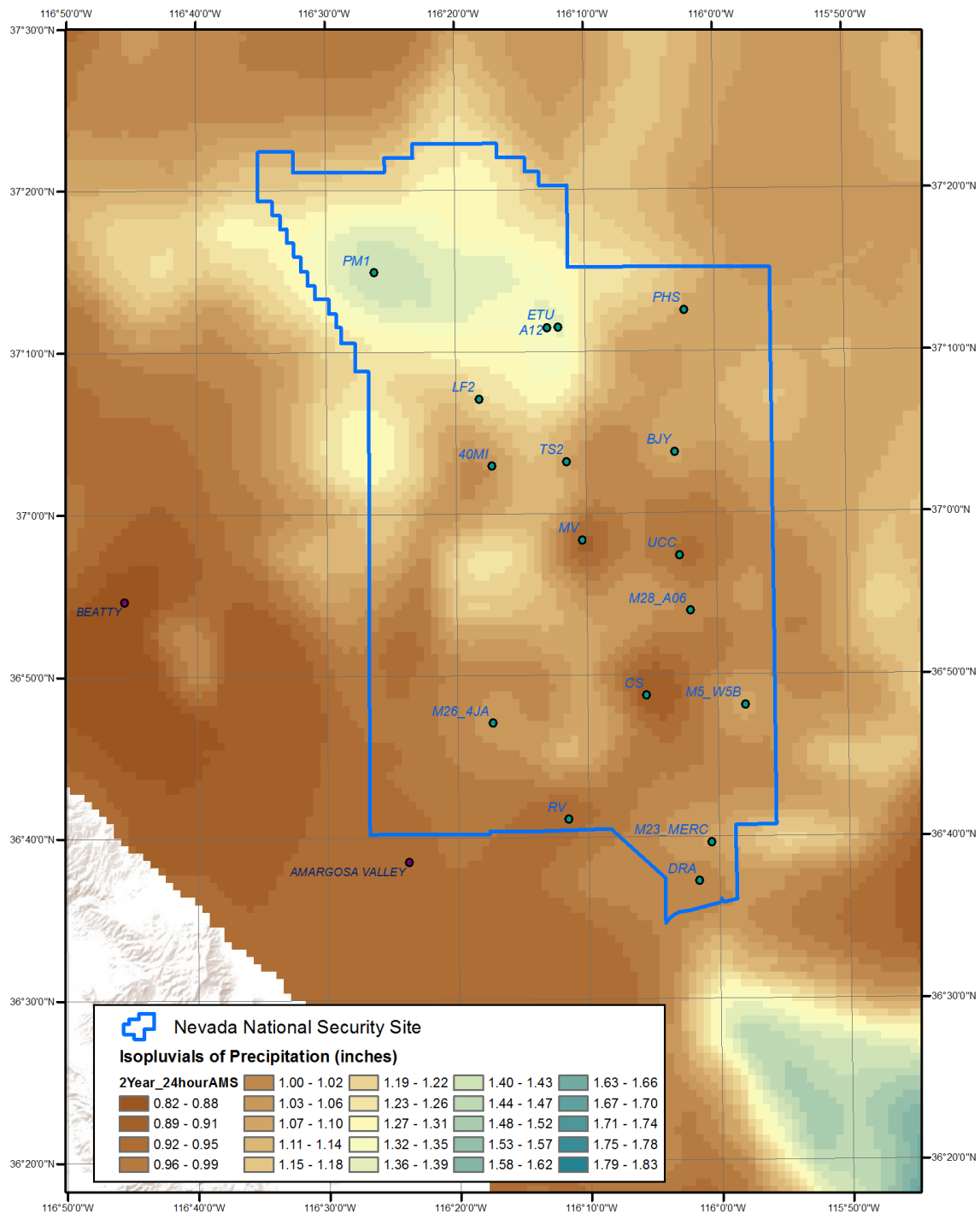


Figure A-8-3B. AMS-based NNSS Precipitation Depth-Duration-Frequency Grid for the focused area: 2-yr, 24-hr.

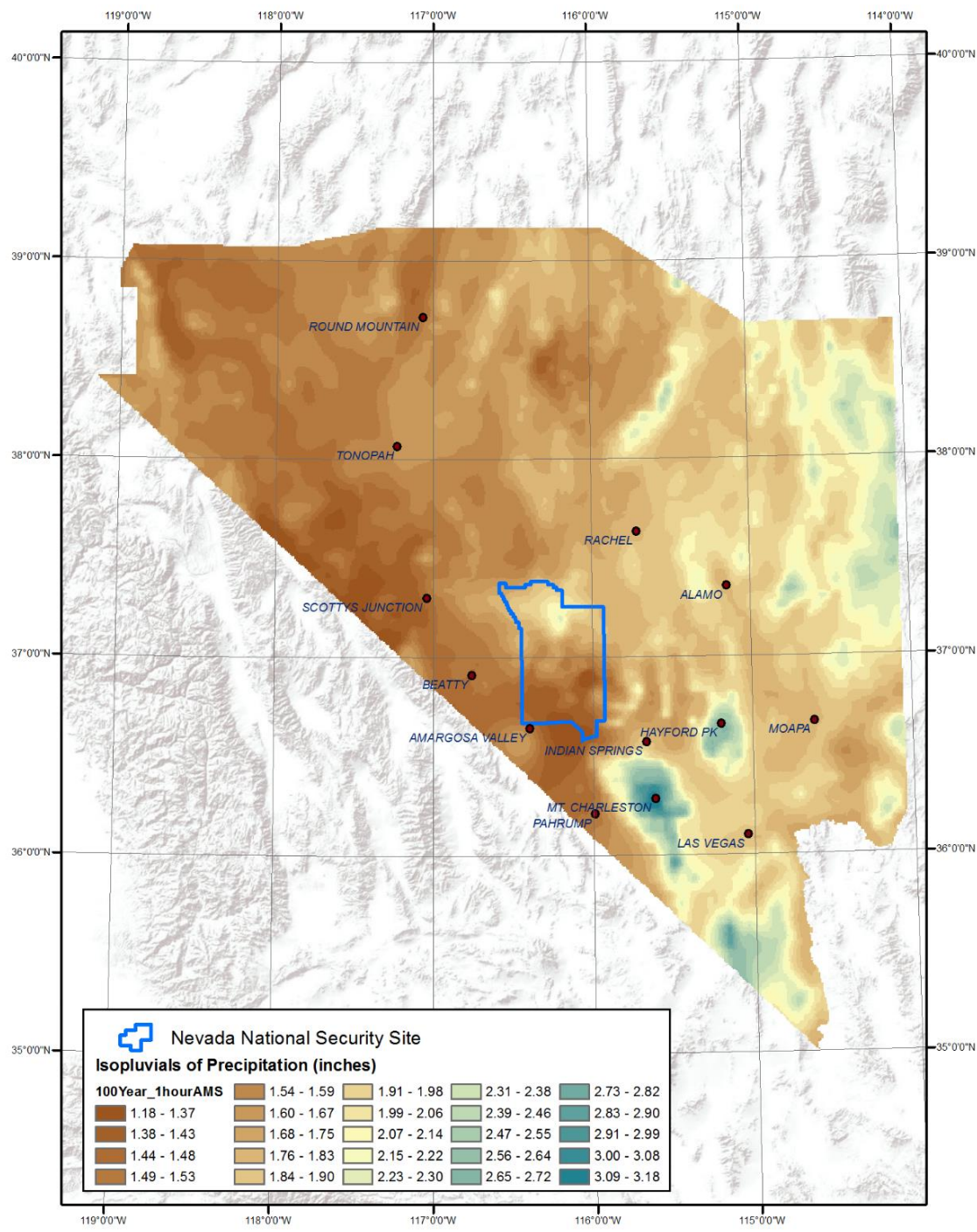


Figure A-8-4A. AMS-based NNSS Precipitation Depth-Duration-Frequency Grid: 100-yr, 1-hr.

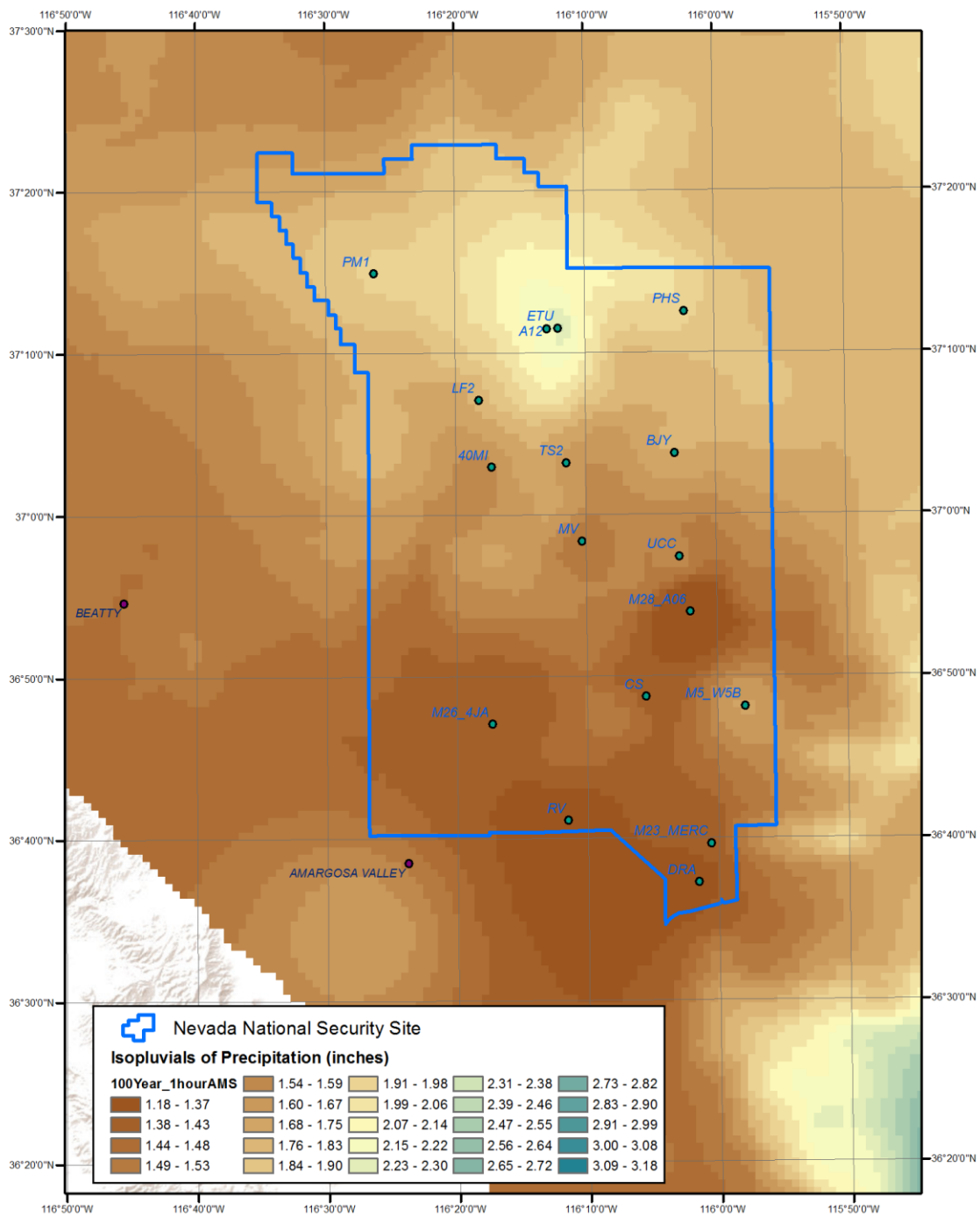


Figure A-8-4B. AMS-based NNSS Precipitation Depth-Duration-Frequency Grid for the focused area: 100-yr, 1-hr.

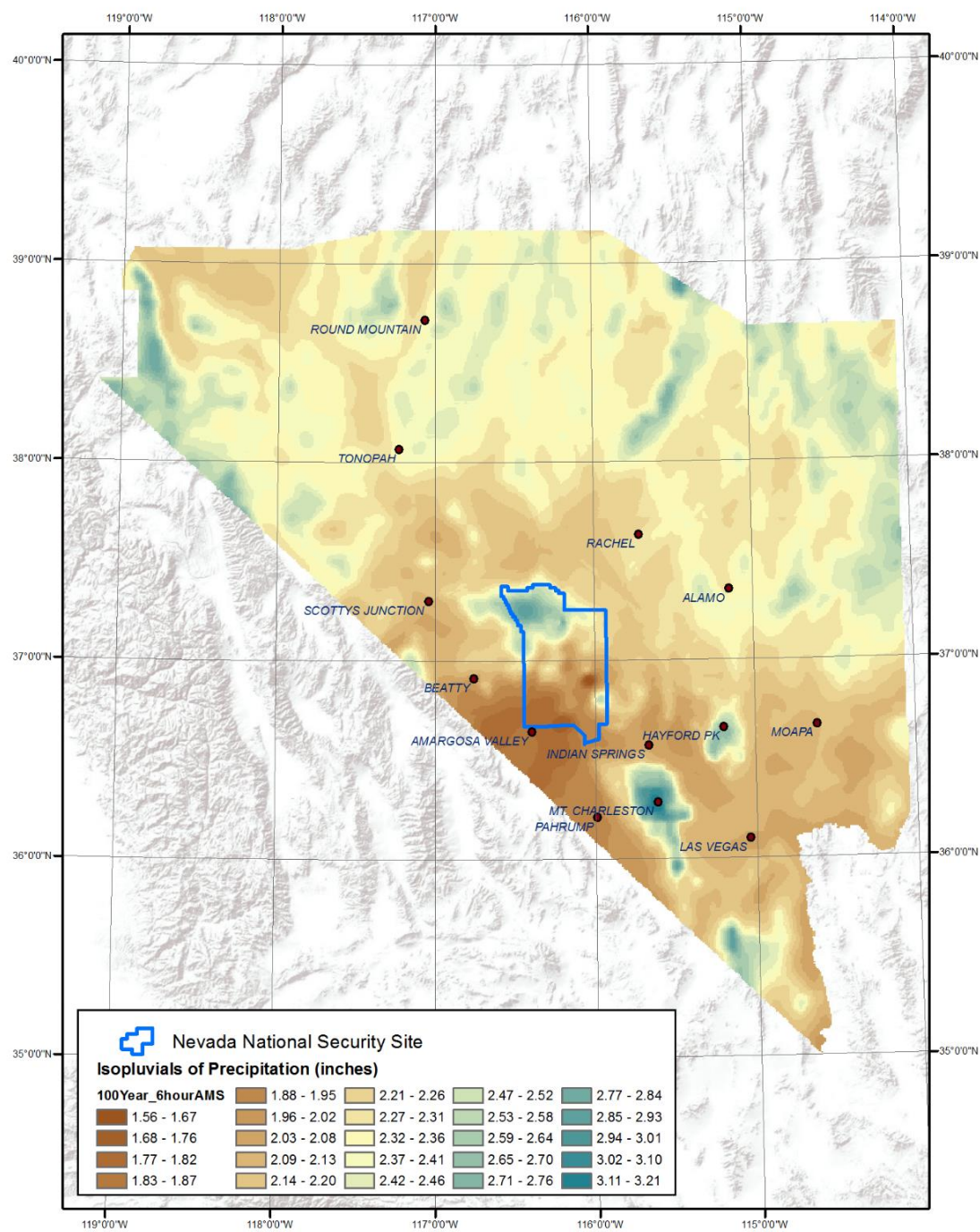


Figure A-8-5A. AMS-based NNSS Precipitation Depth-Duration-Frequency Grid: 100-yr, 6-hr.

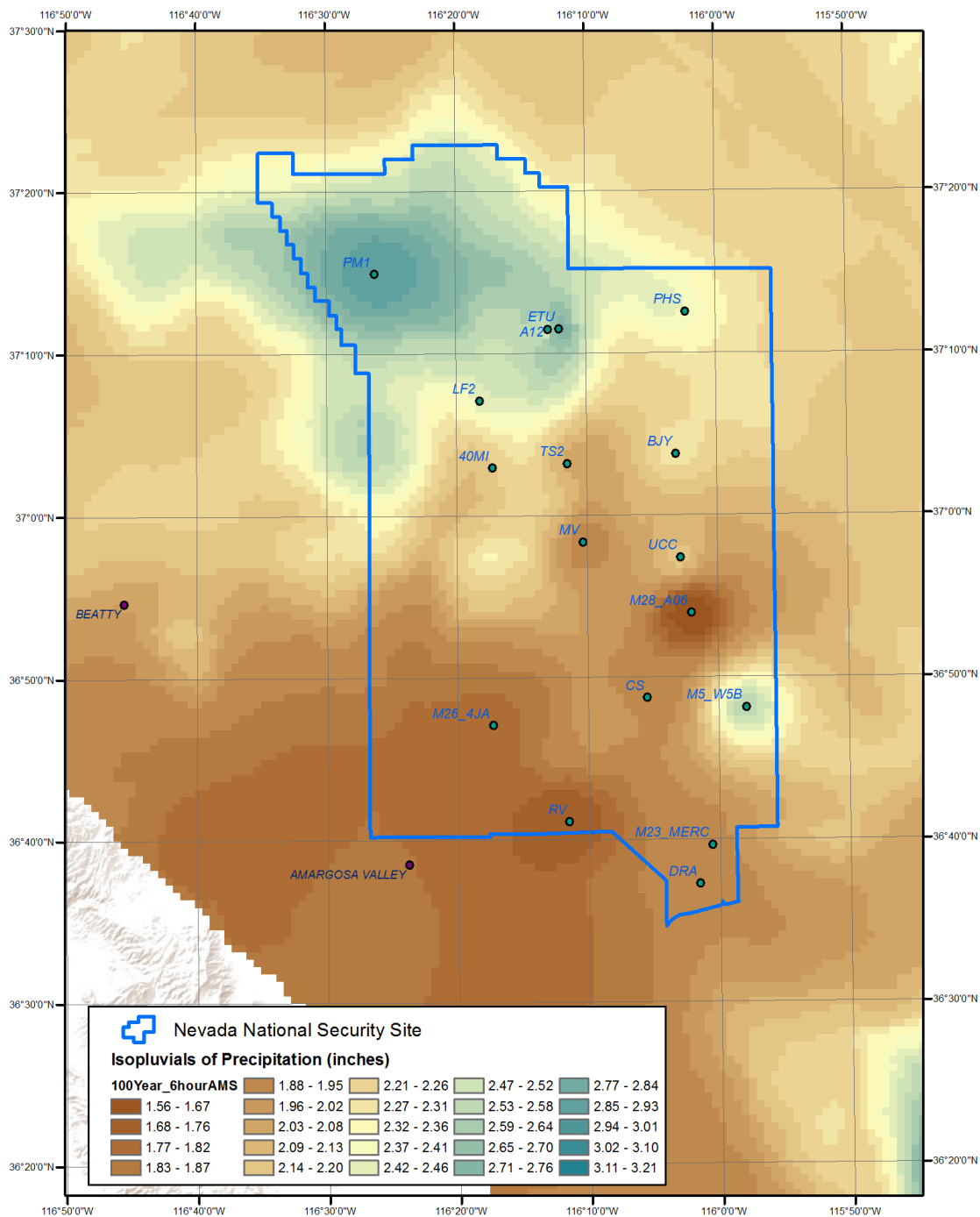


Figure A-8-5B. AMS-based NNSS Precipitation Depth-Duration-Frequency Grid for the focused area: 100-yr, 6-hr.

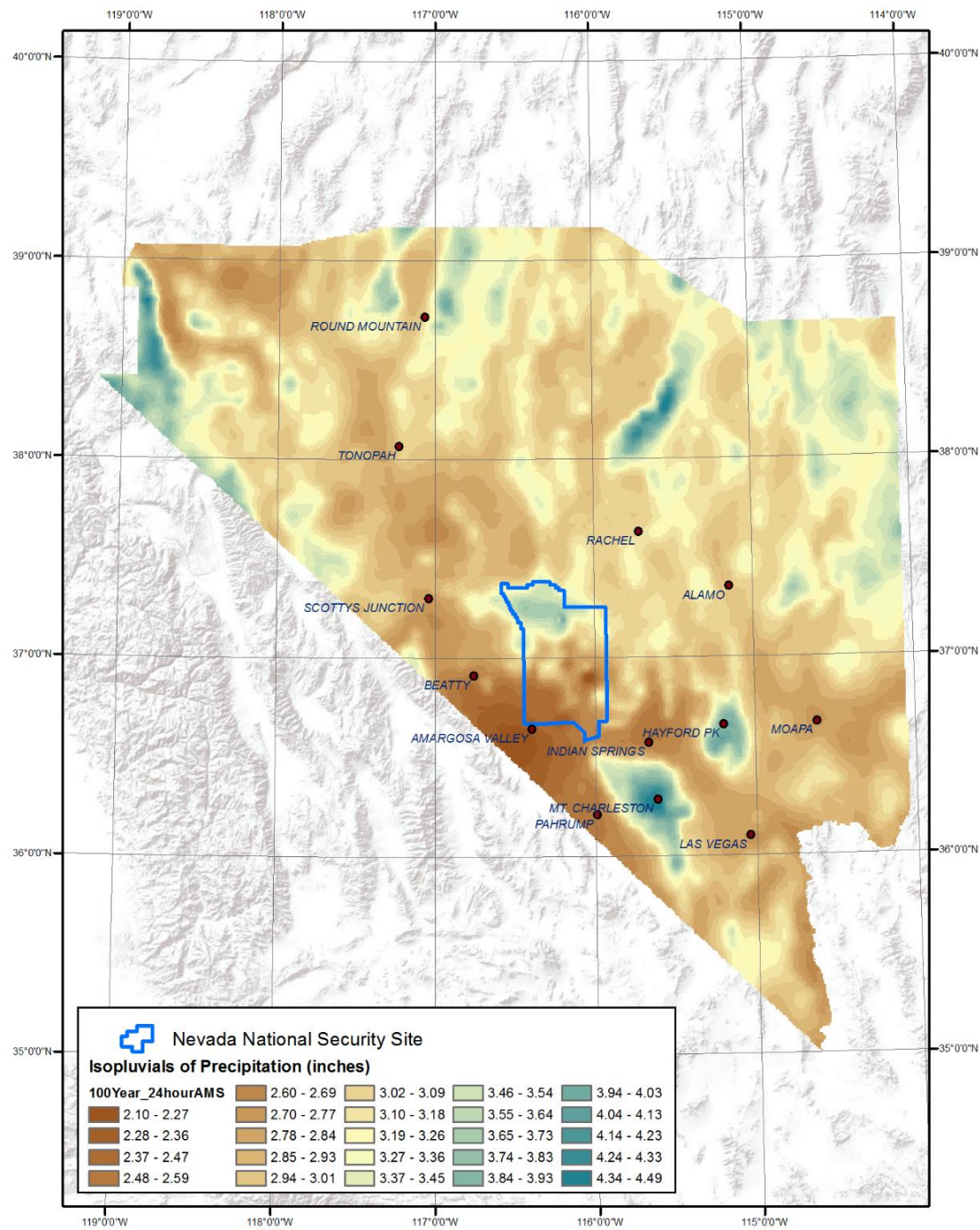


Figure A-8-6A. AMS-based NNSS Precipitation Depth-Duration-Frequency Grid: 100-yr, 24-hr.

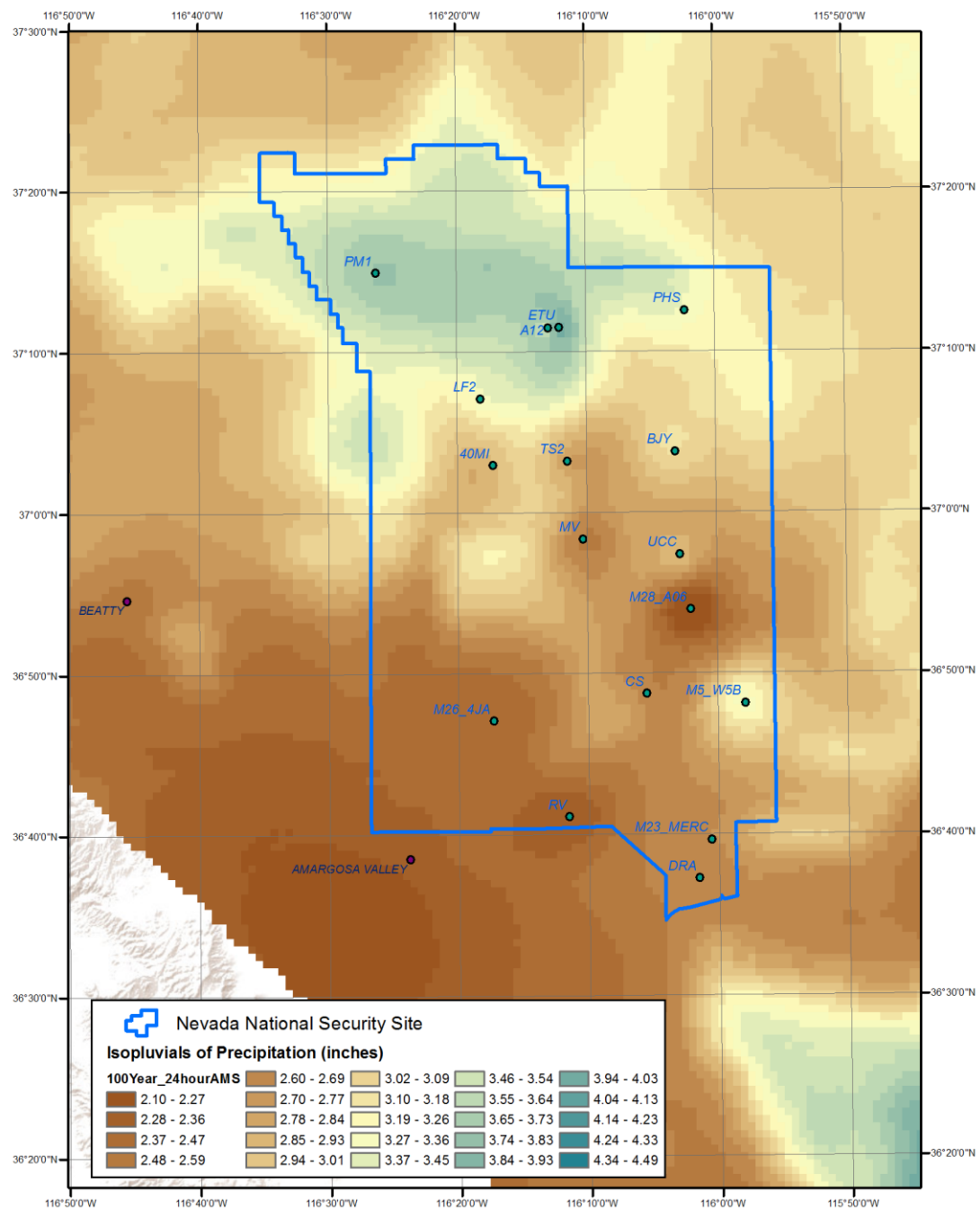


Figure A-8-6B. AMS-based NNSS Precipitation Depth-Duration-Frequency Grid for the focused area: 100-yr, 24-hr.

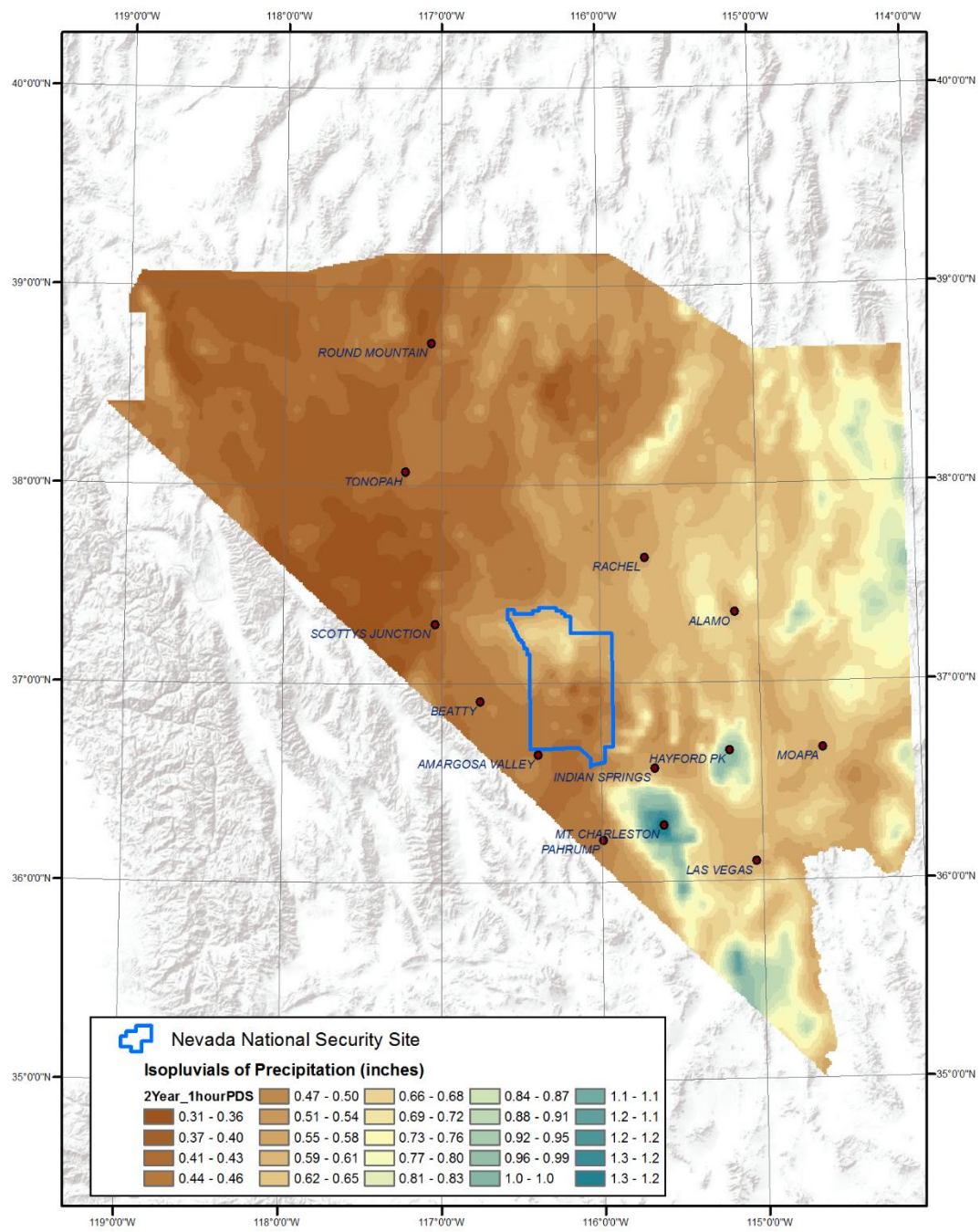


Figure A-8-7A. PDS-based NNSS Precipitation Depth-Duration-Frequency Grid: 2-yr, 1-hr.

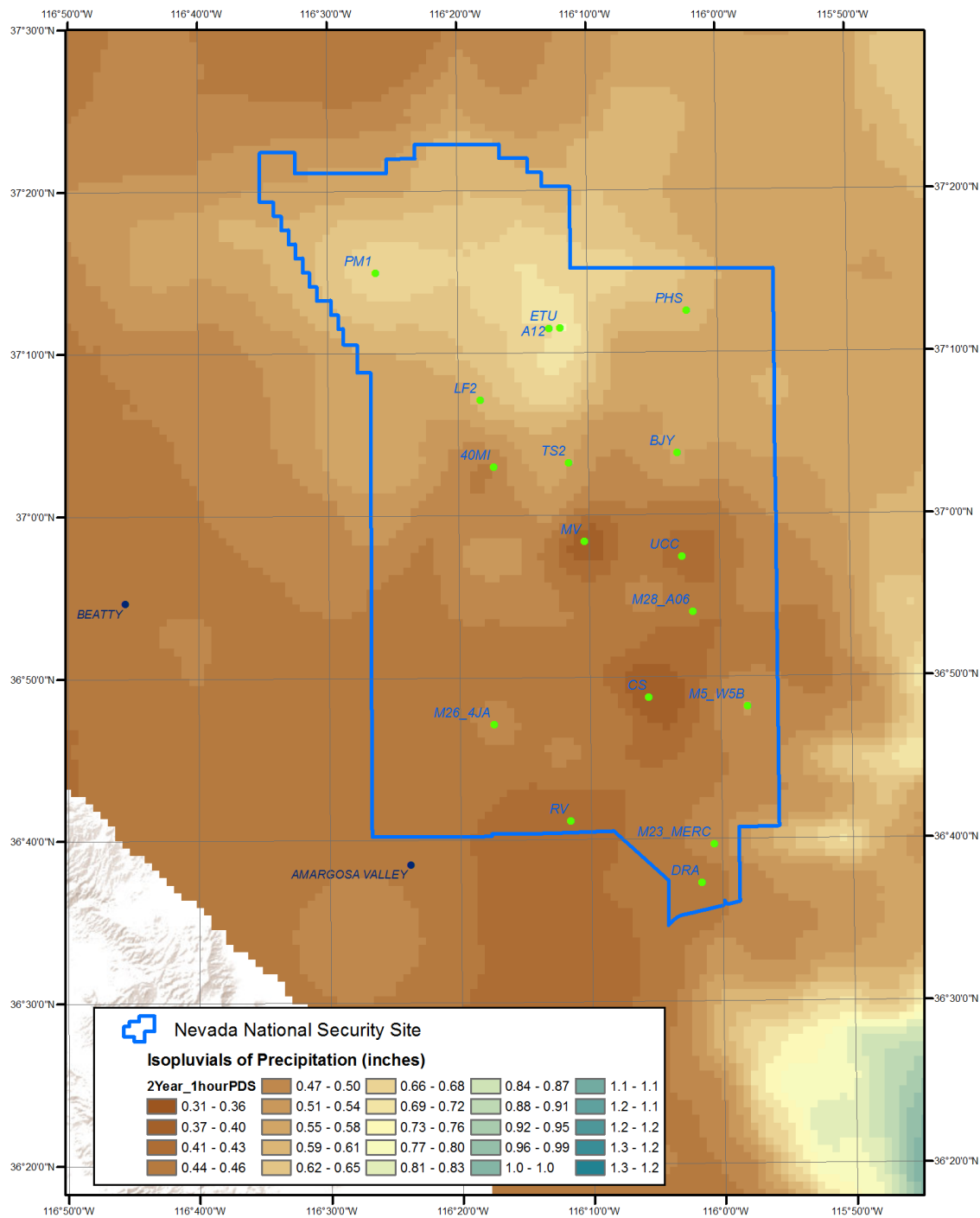


Figure A-8-7B. PDS-based NNSS Precipitation Depth-Duration-Frequency Grid for the focused area: 2-yr, 1-hr.

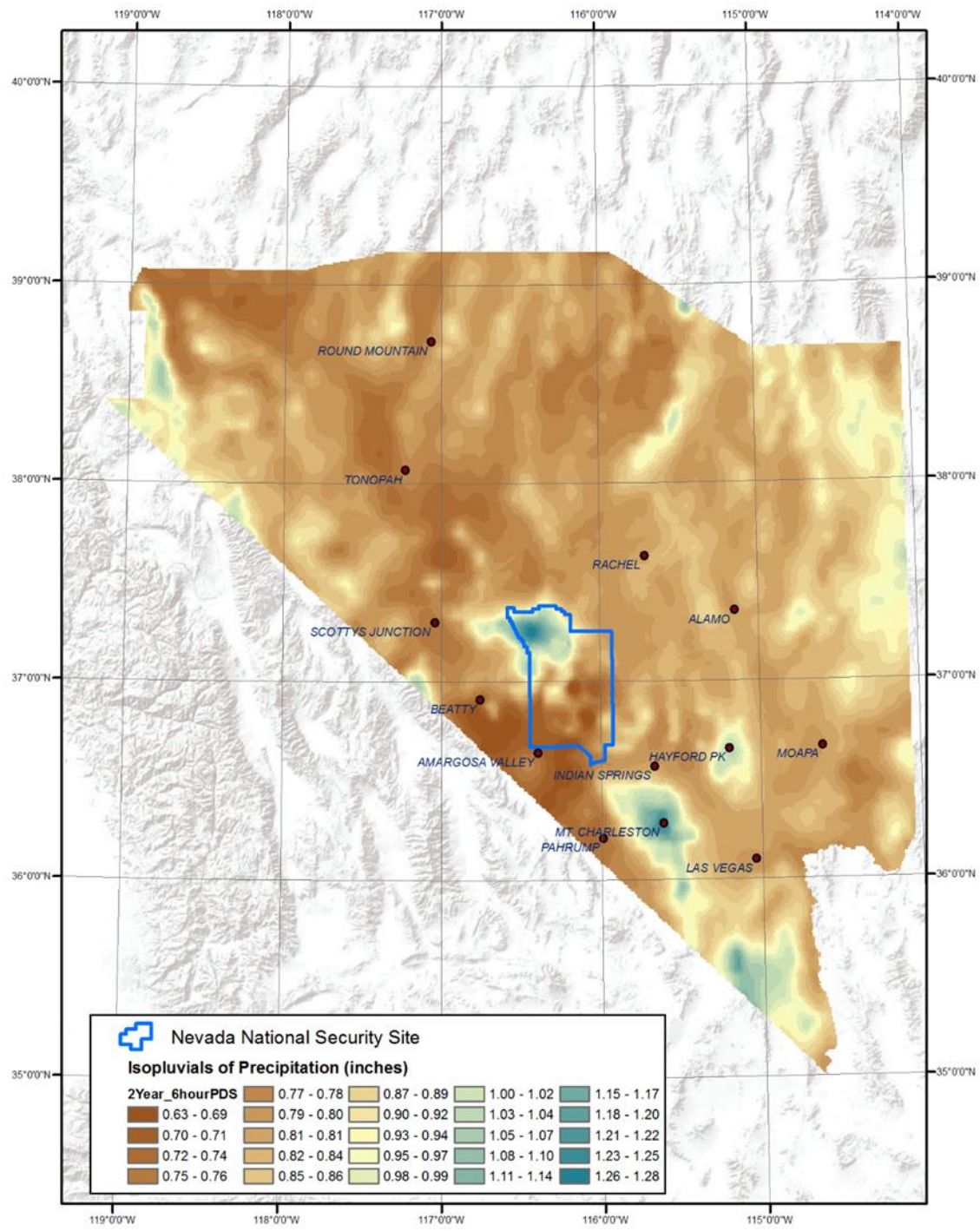


Figure A-8-8A. PDS-based NNSS Precipitation Depth-Duration-Frequency Grid: 2-yr, 6-hr.

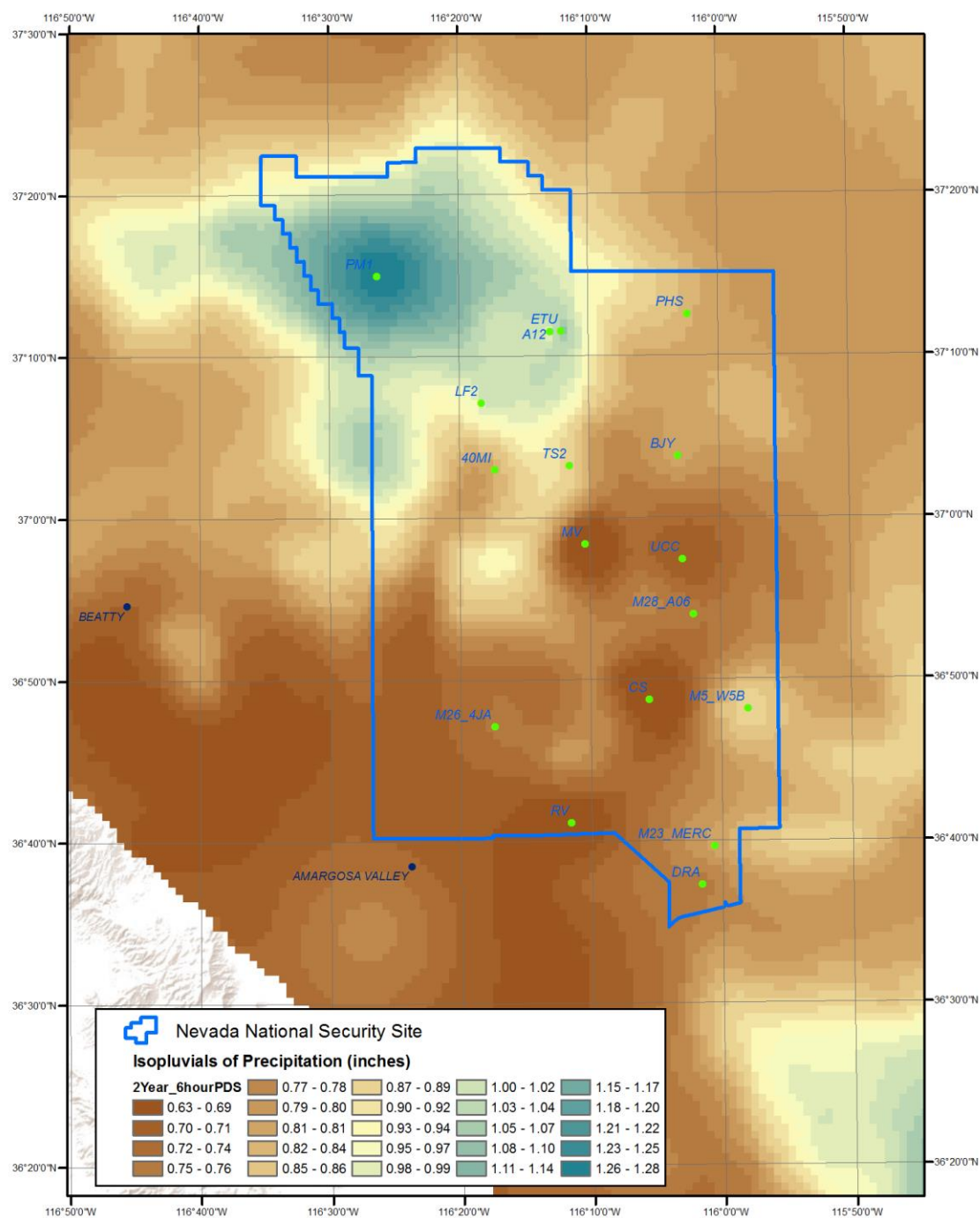


Figure A-8-8B. PDS-based NNSS Precipitation Depth-Duration-Frequency Grid for the focused area: 2-yr, 6-hr.

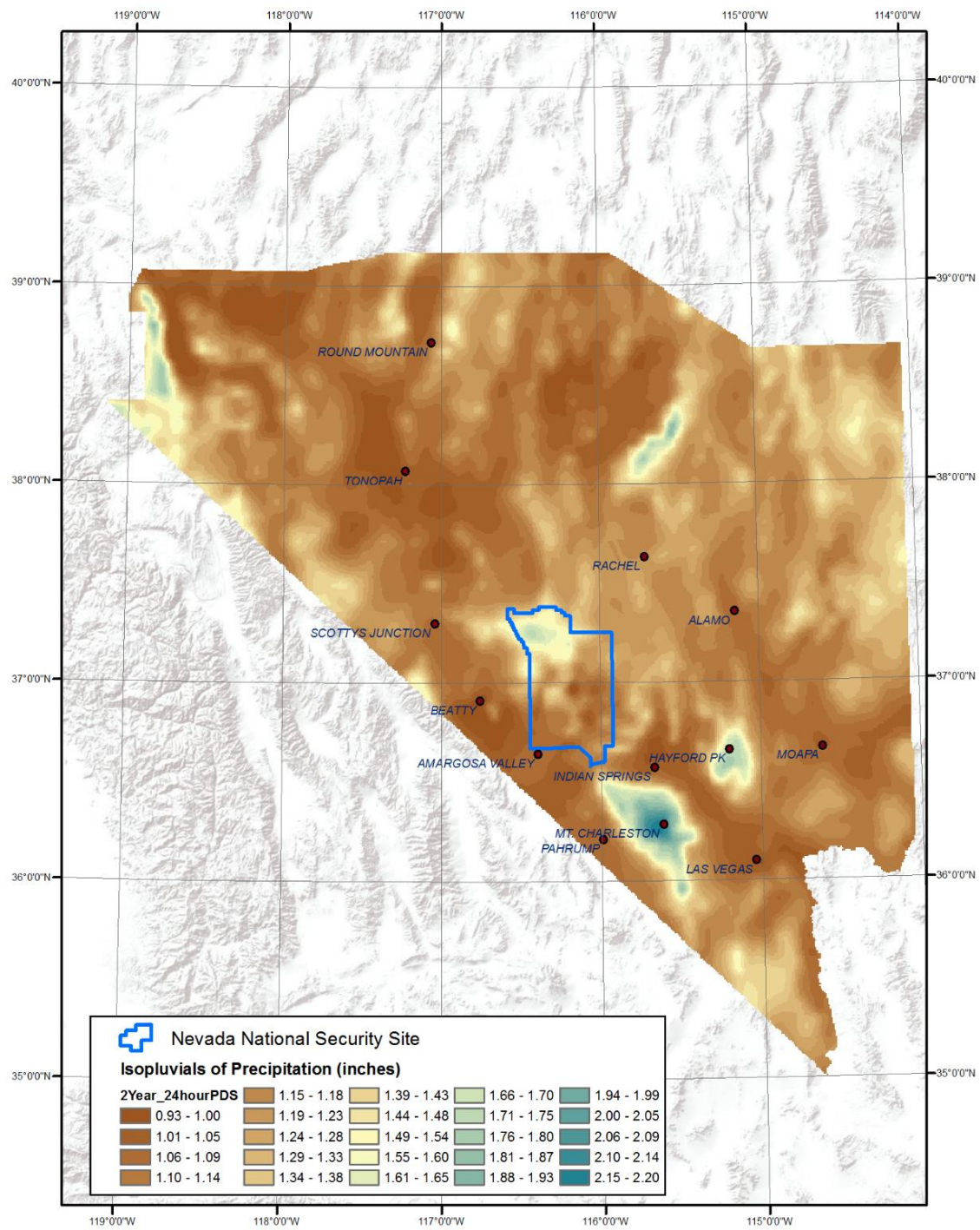


Figure A-8-9A. PDS-based NNSS Precipitation Depth-Duration-Frequency Grid: 2-yr, 24-hr.

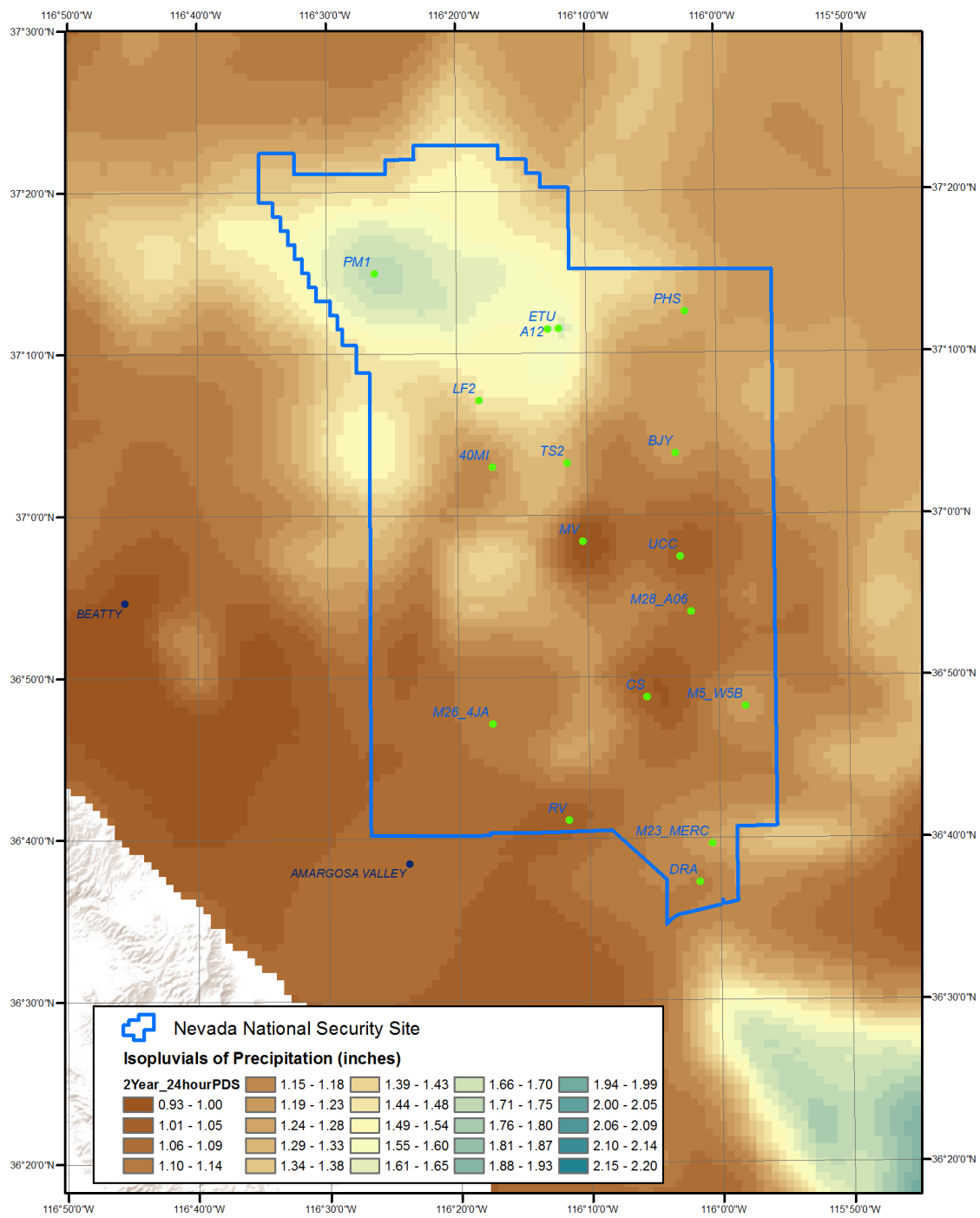


Figure A-8-9B. PDS-based NNSS Precipitation Depth-Duration-Frequency Grid for the focused area: 2-yr, 24-hr.

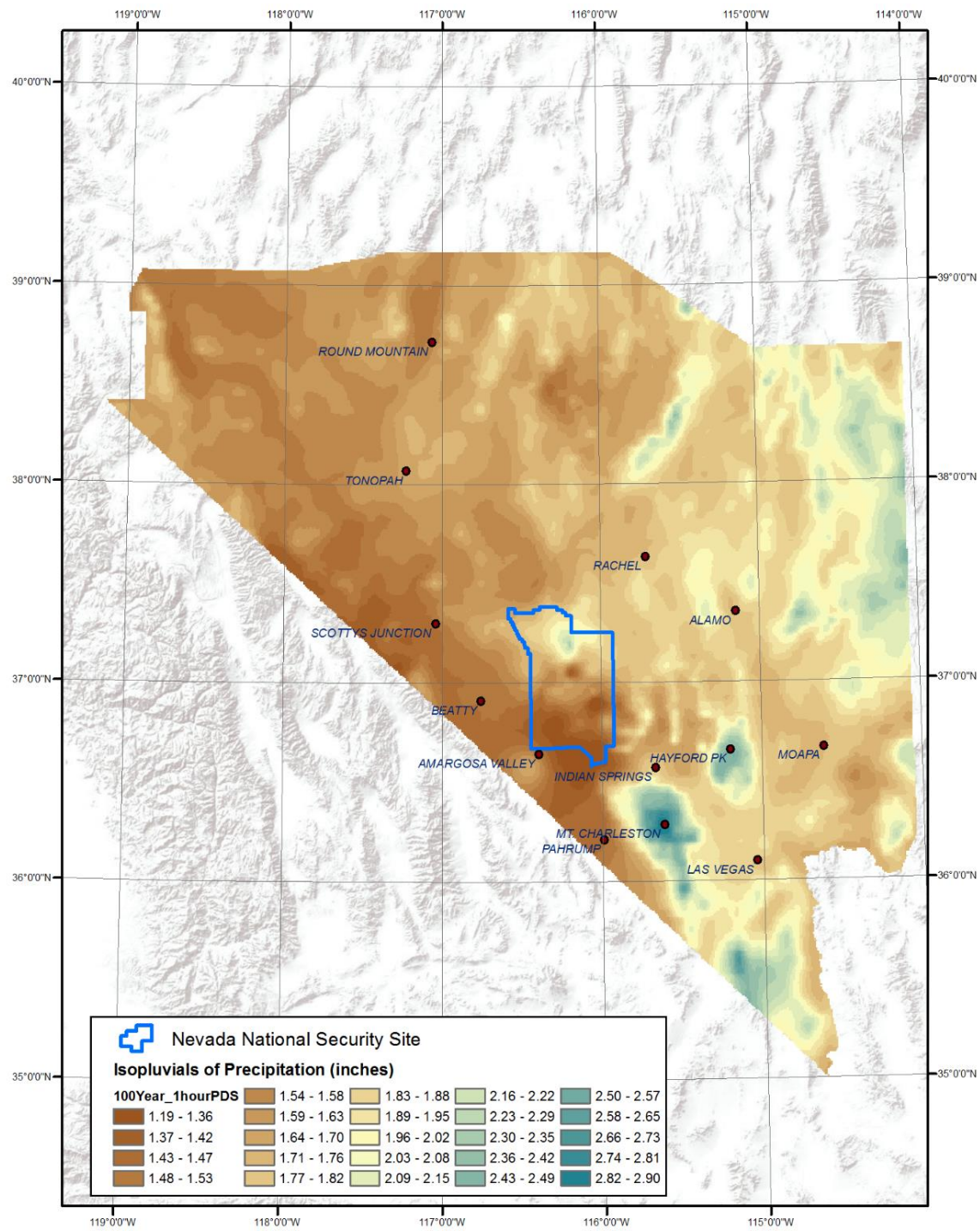


Figure A-8-10A. PDS-based NNSS Precipitation Depth-Duration-Frequency Grid: 100-yr, 1-hr.

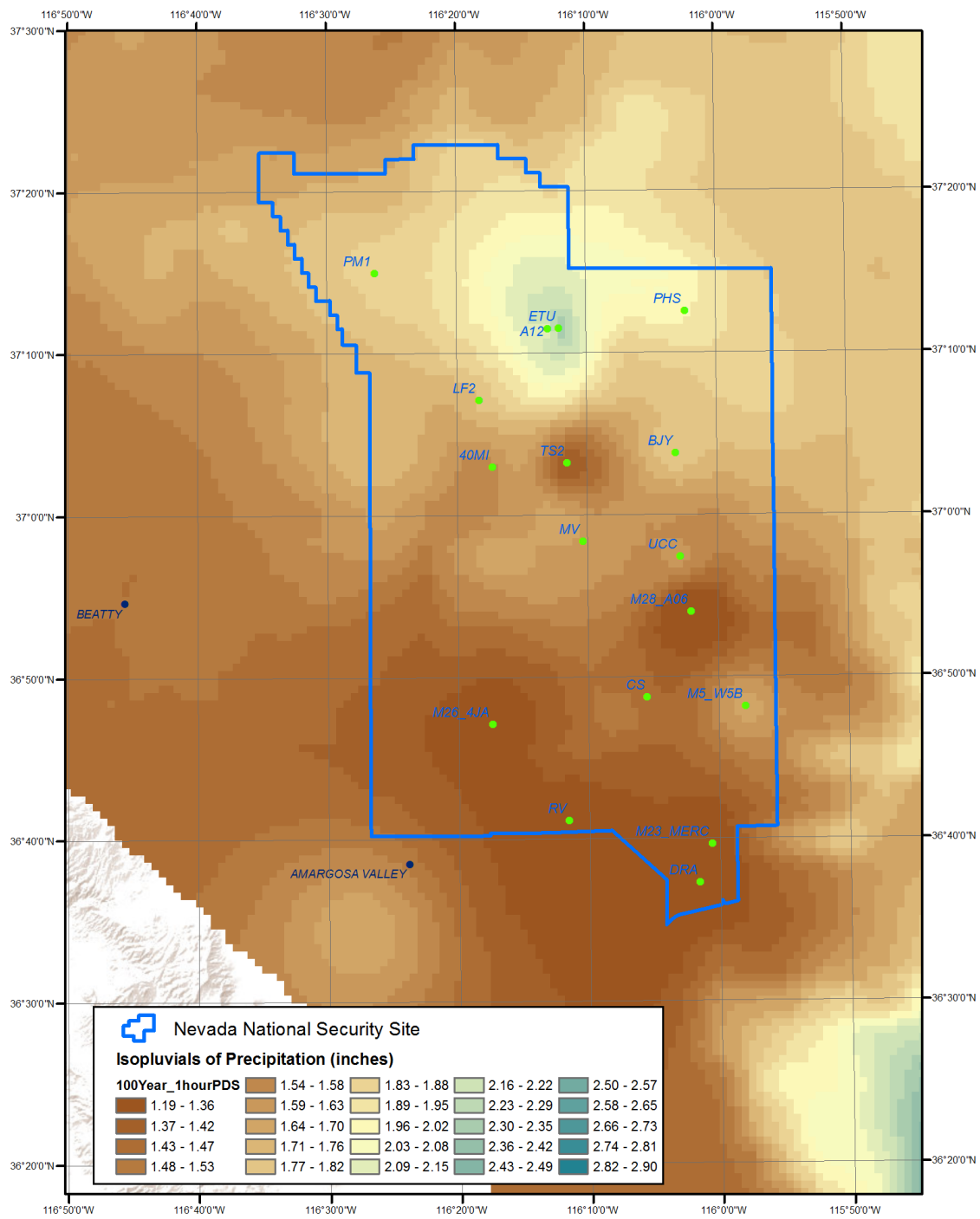


Figure A-8-10B. PDS-based NNSS Precipitation Depth-Duration-Frequency Grid for the focused area: 100-yr, 1-hr.

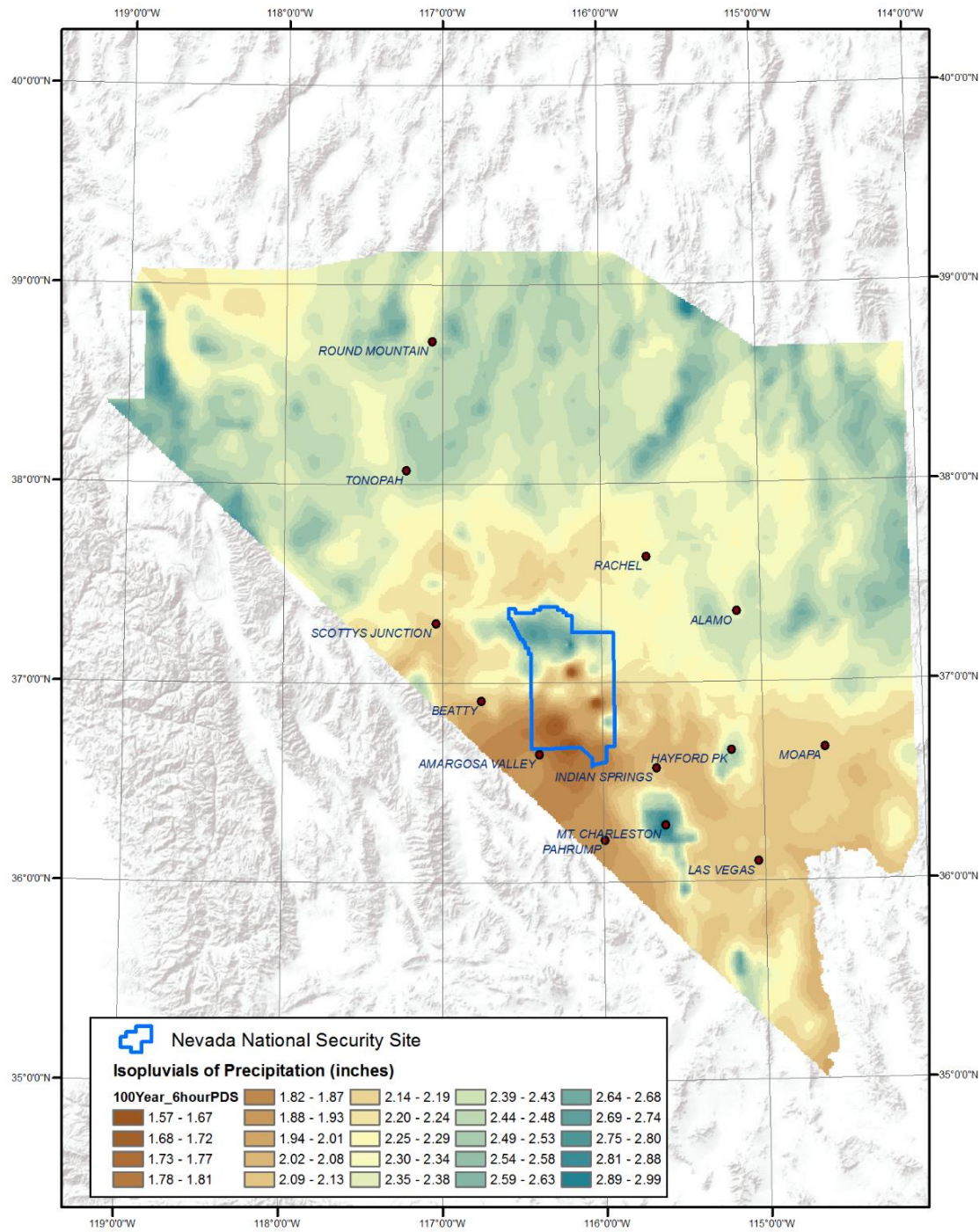


Figure A-8-11A. PDS-based NNSS Precipitation Depth-Duration-Frequency Grid: 100-yr, 6-hr.

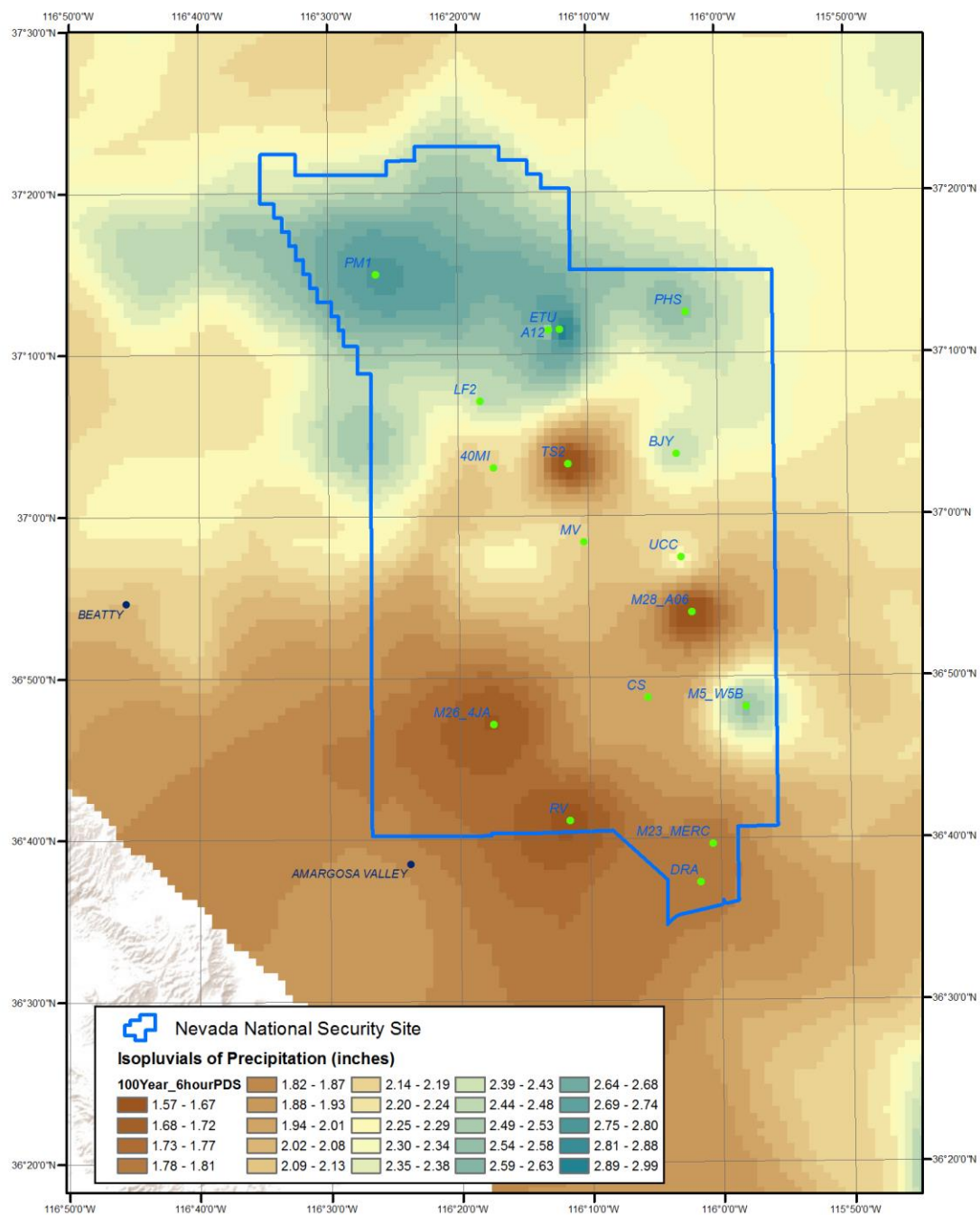


Figure A-8-11B. PDS-based NNSS Precipitation Depth-Duration-Frequency Grid for the focused area: 100-yr, 6-hr.

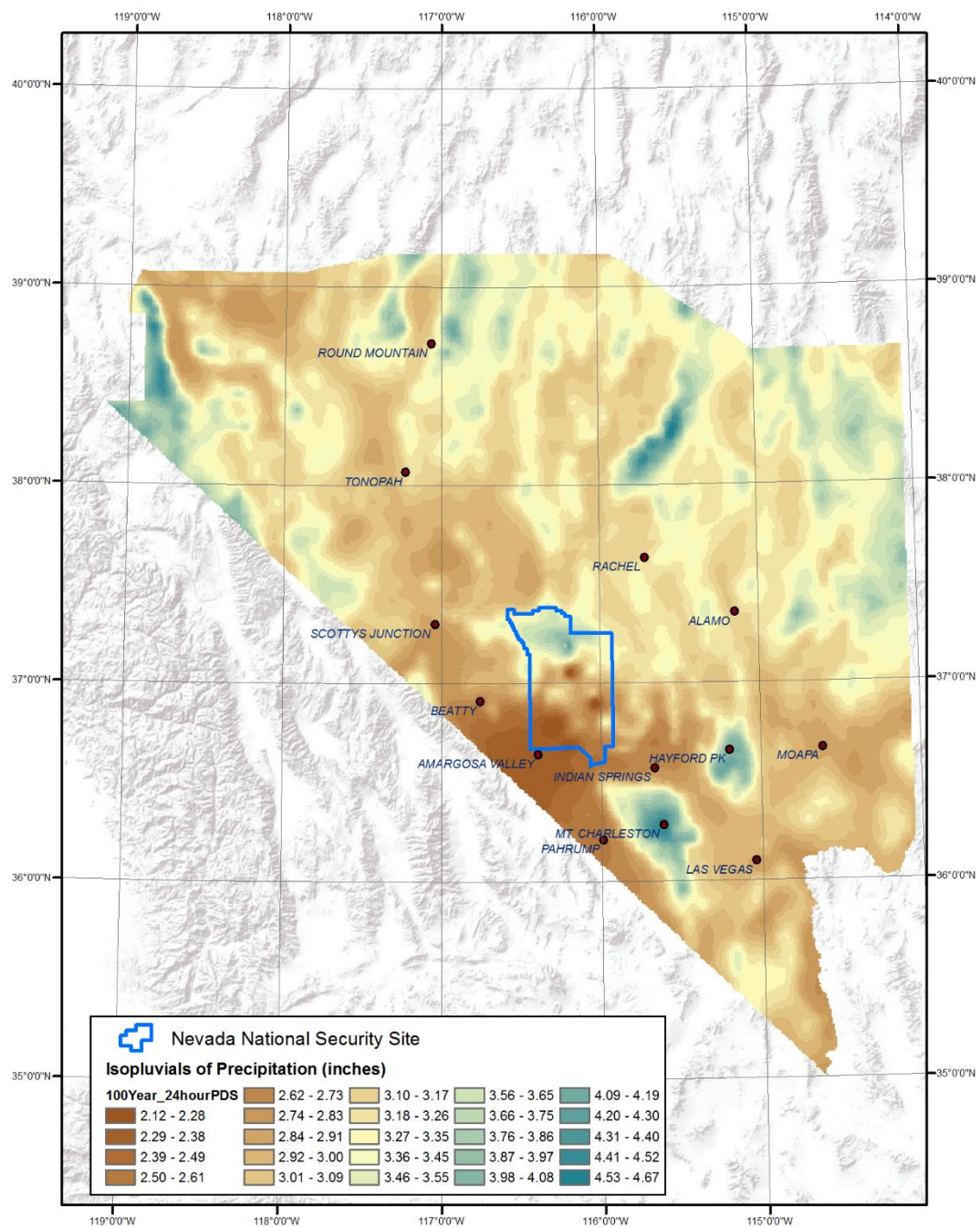


Figure A-8-12A. PDS-based NNSS Precipitation Depth-Duration-Frequency Grid: 100-yr, 24-hr.

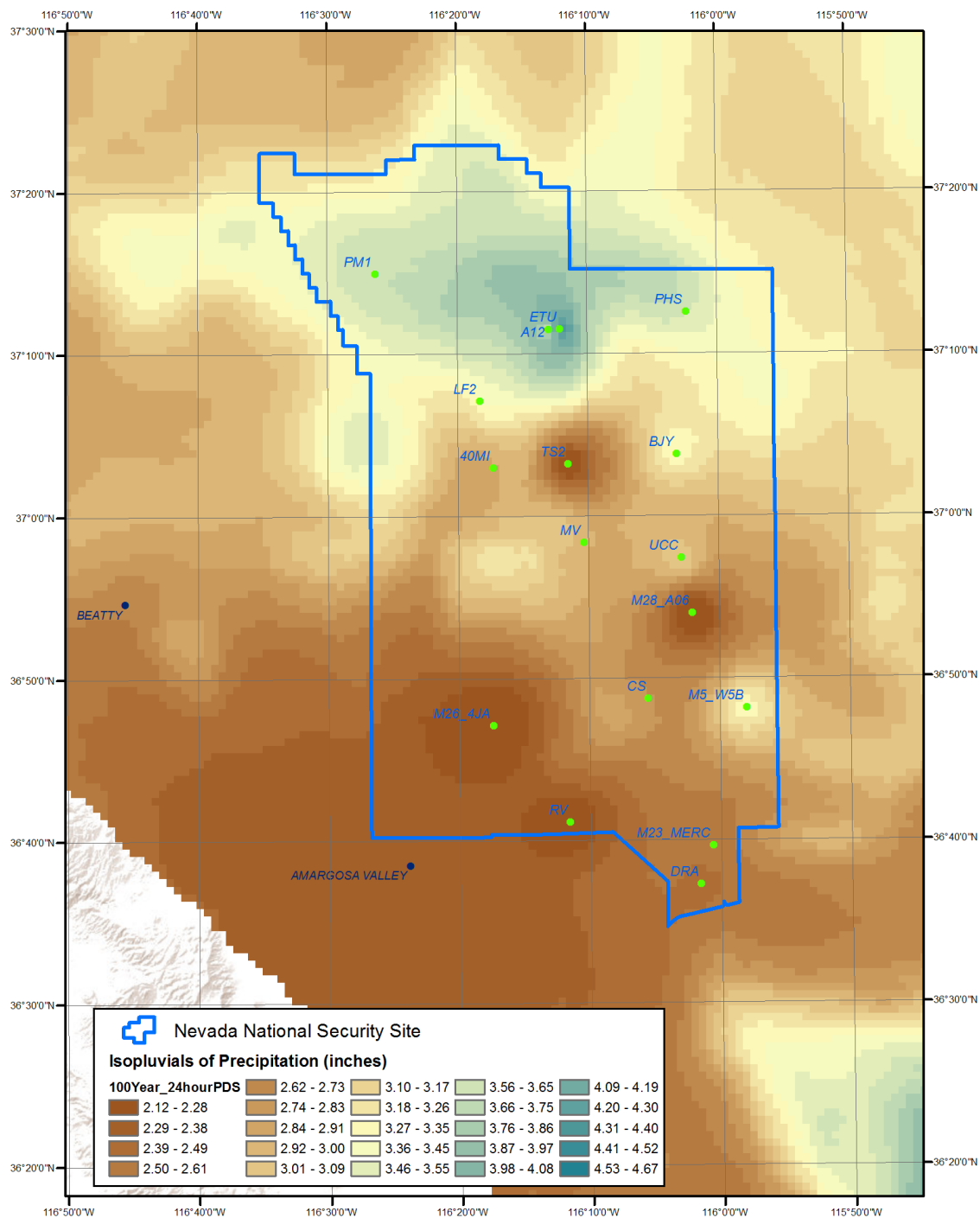


Figure A-8-12B. PDS-based NNSS Precipitation Depth-Duration-Frequency Grid for the focused area: 100-yr, 24-hr.

Result Validation

Five arbitrarily selected locations surrounding the NNSS (Figure A-9) were selected to validate the results of the precipitation frequency grid that include the NNSS precipitation gage records. These locations include one arbitrary location outside of each side (north, south, east, and west) of the NNSS, plus a high elevation location to the southeast of the NNSS. These are not locations of precipitation gages; rather they are locations that were arbitrarily selected from which NOAA Atlas 14 data were obtained for comparison with the revised NNSS precipitation gridded datasets. Both AMS and PDS precipitation values for these five arbitrarily selected locations obtained from both the NOAA Atlas 14 and from the study-generated precipitation grids (Figures A-8-1A through A-8-12B) were compared (Figures A-10a and A-10b).

In general, the results from the precipitation grids developed in this study agreed well with the NOAA Atlas 14 values for these five arbitrarily selected locations used for validation; thereby verifying that the two datasets had been adequately conjoined (Figures A-10a and A-10b). Only at the high elevation location to the southeast of the NNSS was there an outlier in both the AMS and PDS datasets. At this location, the 100-yr, 24-hour precipitation depth predicted by this study is significantly lower than the NOAA Atlas 14 reported value. This is likely because of the lower DDF values obtained from the actual observed precipitation gage data analyzed in this study than those values reported in the NOAA Atlas 14. The lower DDF values affected surrounding areas when calculating gridded data from point data. The comparison demonstrates the reliability of results in this study for the Off-Site area, which provides confidence for the reliability of the results on the NNSS.

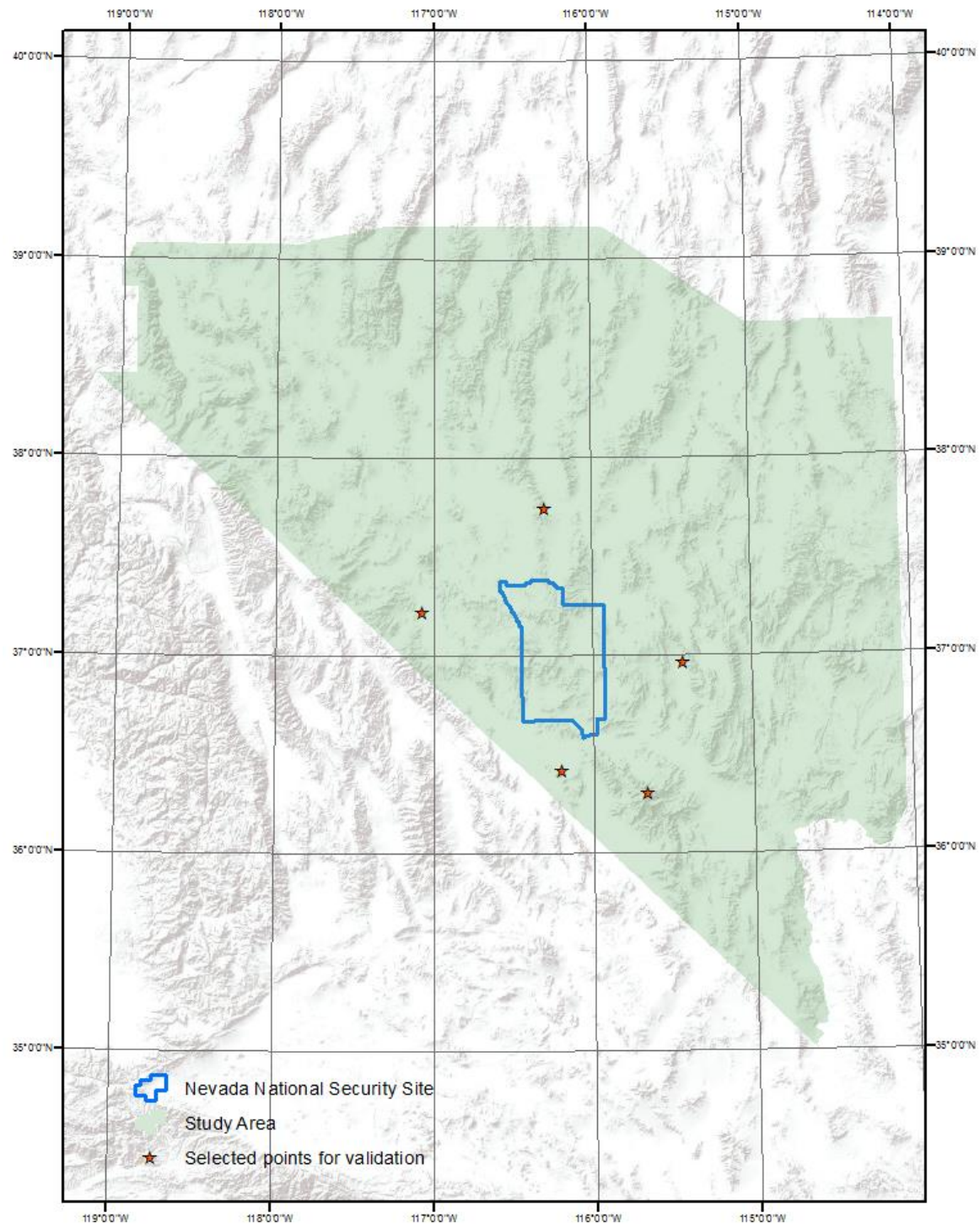


Figure A-9. Selected off-NNSS locations used for validation.

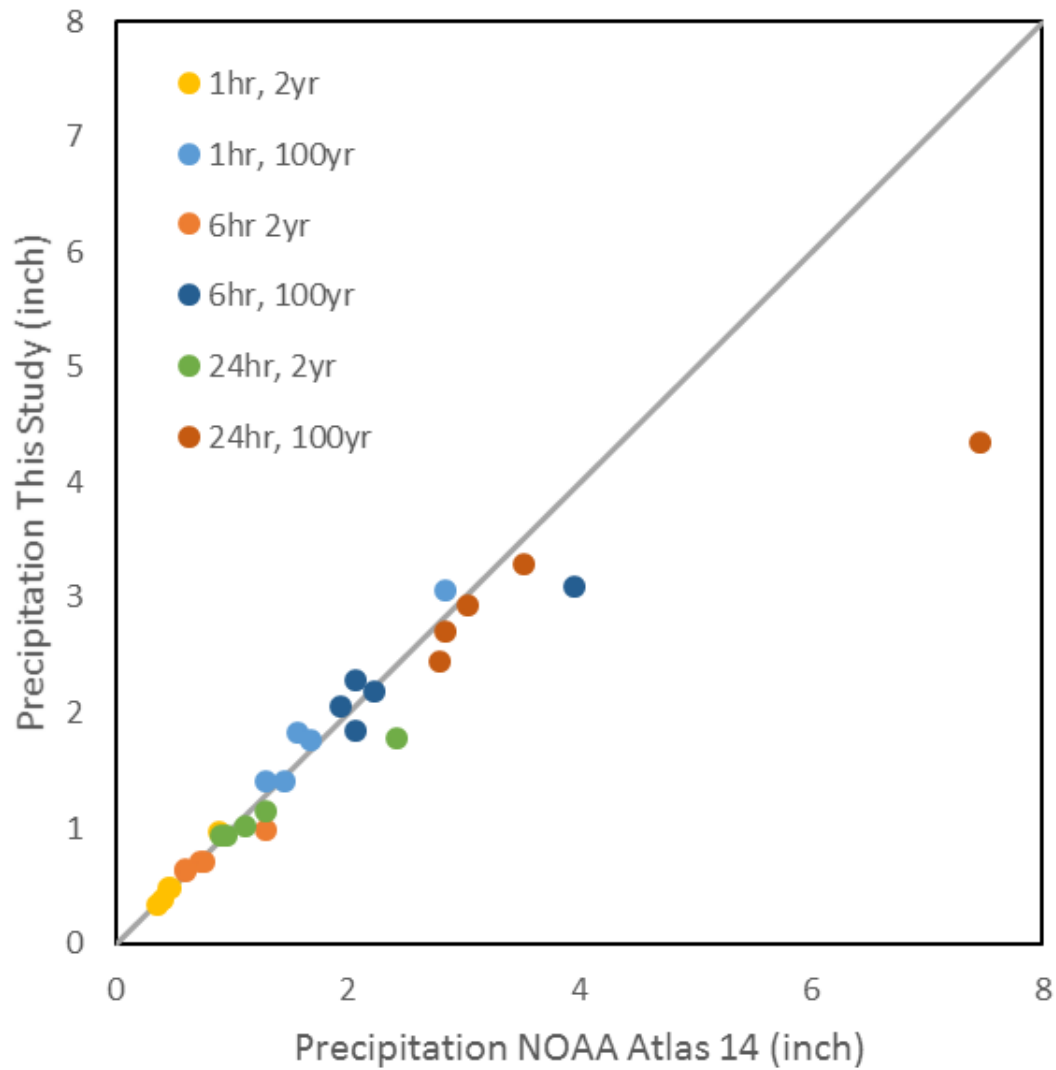


Figure A-10a. Comparison of NOAA Atlas 14 precipitation frequency and the precipitation grid values at five arbitrarily selected locations surrounding the NNSS: AMS results.

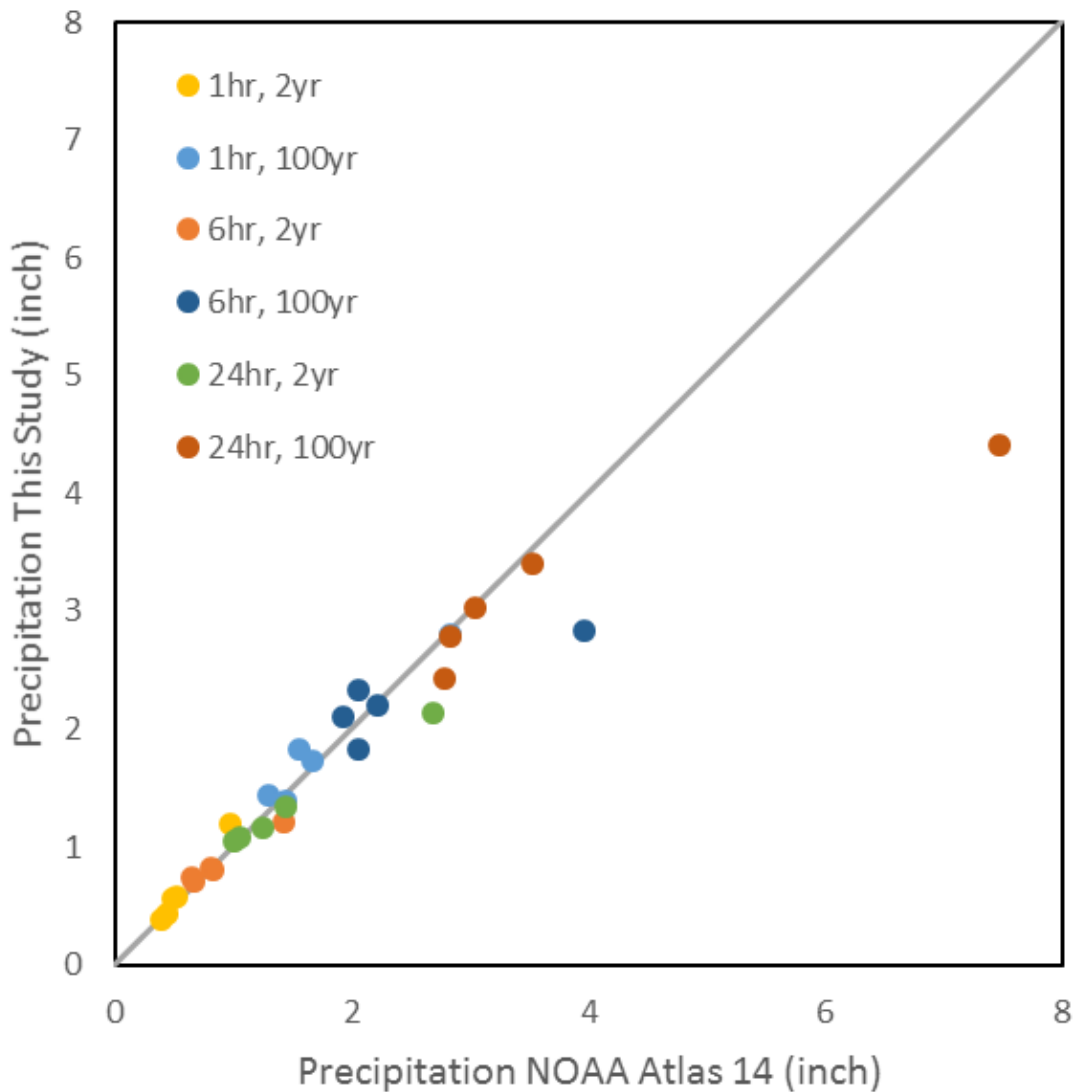


Figure A-10b. Comparison of NOAA Atlas 14 precipitation frequency and the precipitation grid values at five arbitrarily selected locations surrounding the NNSS: PDS results.

STANDING DISTRIBUTION LIST

Scott A. Wade
Assistant Manager for Environmental Mgmt
Nevada Field Office
National Nuclear Security Administration
U.S. Department of Energy
P.O. Box 98518
Las Vegas, NV 89193-8518
Scott.Wade@nnsa.doe.gov

Robert Boehlecke
Nevada Field Office
National Nuclear Security Administration
U.S. Department of Energy
P.O. Box 98518
Las Vegas, NV 89193-8518
Robert.Boehlecke@nnsa.doe.gov

Tiffany Lantow
Nevada Field Office
National Nuclear Security Administration
U.S. Department of Energy
P.O. Box 98518
Las Vegas, NV 89193-8518
Tiffany.Lantow@nnsa.doe.gov

Peter Sanders
Nevada Field Office
National Nuclear Security Administration
U.S. Department of Energy
P.O. Box 98518
Las Vegas, NV 89193-8518
Peter.Sanders@nnsa.doe.gov

Sarah Hammond, Contracting Officer
Office of Acquisition Management
NNSA Service Center
Pennsylvania and H Street, Bldg. 20388
P.O. Box 5400
Albuquerque, NM 87185-5400
Sarah.Hammond@nnsa.doe.gov

Jenny Chapman
DOE Program Manager
Division of Hydrologic Sciences
Desert Research Institute
755 E. Flamingo Road
Las Vegas, NV 89119-7363
Jenny.Chapman@dri.edu

Julianne Miller
DOE Soils Activity Manager
Division of Hydrologic Sciences
Desert Research Institute
755 E. Flamingo Road
Las Vegas, NV 89119-7363
Julie.Miller@dri.edu

Steve Mizell
Division of Hydrologic Sciences
Desert Research Institute
755 E. Flamingo Road
Las Vegas, NV 89119-7363
Steve.Mizell@dri.edu

Pat Matthews
Navarro, LLC
P.O. Box 98952
M/S NSF167
Las Vegas, NV 89193-8952
Patrick.Matthews@nv.doe.gov

Reed Poderis
National Security Technologies, LLC
P.O. Box 98521
M/S NLV082
Las Vegas, NV 89193-8521
poderirj@nv.doe.gov

*Nevada State Library and Archives
State Publications
100 North Stewart Street
Carson City, NV 89701-4285

Archives Getchell Library
University of Nevada, Reno
1664 N. Virginia St.
Reno, NV 89557
dcurtis@unr.edu

DeLaMare Library
262
University of Nevada, Reno
1664 N. Virginia St.
Reno, NV 89557
dcurtis@unr.edu

Document Section, Library
University of Nevada, Las Vegas
4505 Maryland Parkway
Las Vegas, NV 89154
sue.wainscott@unlv.edu

†Library
Southern Nevada Science Center
Desert Research Institute
755 E. Flamingo Road
Las Vegas, NV 89119-7363

‡Nuclear Testing Archive
ATTN: Martha DeMarre
National Security Technologies, LLC
Mail Stop 400
PO Box 98521
Las Vegas, NV 89193-8521
demarrme@nv.doe.gov
(2 CDs)

§Office of Scientific and Technical Information
U.S. Department of Energy
P.O. Box 62
Oak Ridge, TN 37831-9939

All on distribution list receive one electronic PDF copy, unless otherwise noted.

* 12 paper copies

† 3 paper copies; CD with pdf (from which to print)

‡ compact disc only

§ electronic copy (pdf) only